REEL-C 6803

A. T. I. 155704

UNCLASSIFIED

UNCLASSIFIED

ATI 155 704 (Copies obtainable from ASTIA-DSC)

University of Pennsylvania, Philadelphia (Tech Report No. 2)

Some Aspects of Photoconductivity in Zinc Oxide

Warschauer, Douglas 25 Jan'52 85pp. graphs, drwgs

USN Contr. No. N6onr-24914

Photoconductivity
Zinc oxide
Semiconductors

Physics (62)
Radiation (5)

UNCLASSIFIED

UNIVERSITY OF PENNSYLVANIA

Contract N6-onr-24914

Technical Report #2

January 25, 1952

Some Aspects of Photoconductivity in Zinc Oxide

Prepared by:

Douglas Warschauer*

* This report contains the essential portion of a thesis in partial fulfillment of the requirements for the Ph.D. degree, University of Pennsylvania.

Contents

Abstract

Measurements have been performed on the photoconductivity of pressed and sintered samples of zinc-oxide powder at room and at liquid air temperature. The behavior of the illuminated material as a function of time, incident light intensity, and frequency of light modulation indicate the existence of several mechanisms simulataneously participating in the photoconductive process: a slow bimolecular process having a decay constant of 50 minutes, a monomolecular process having a decay constant of about 5 minutes, and a monomolecular process of 0.3 second decay constant. The existence of processes of time constants of the order of one minute and of several milliseconds is also suspected. The maximum of photoconductivity occurs at the fundamental absorption edge (3900 $\mathring{A}$) of the material. Photoconductive response in several impure crystals is also reported.

The theory of the photoconductive process is developed and two calculations are described. The first is a method of determining the incremental response in a large dark-current semiconductor and indicates that the existence of an impurity or trap level in the forbidden band region can give rise to two exponential processes in the rise or decay of photoconduction. The second calculation uses a method of successive approximation to show that essentially the same model can give rise to a bimolecular and a monomolecular process simultaneously. Application of these models is made to the sintered-zinc-oxide data. The existence of an impurity level approximately 0.7 ev. below the conduction band is thought to be in agreement with the conductivity data of Hahn and Miller. It is suggested that this set of states may exist on the interfaces rather than in the bulk of the sintered material, and that the recombination of electrons from this level to the filled band region or to activators lying at the edge of the forbidden band may be responsible for the observed long-wave length (5100 $\mathring{A}$) luminescent band.

I. Properties of Zinc-Oxide Semiconductor

Zinc-oxide as commercially obtained is a white powder exhibiting negligible conductivity or visible luminescence. Hpwever, when the powder is baked in air or in a reducing atmosphere, or when layers are prepared by deposition from a flame, the material may be white or yellow or even black and exhibits typical semiconducting properties. This change in properties is thought to be due to driving-off oxygen from the lattice structure with the consequent formation of interstitial zinc in the wurzite structure.[1,2,3,5]

In measurements of the conductivity of sintered material two ranges are found in which a plot of $\ln \sigma$ versus $1/T$ is roughly linear, the lower range for T $25^{\circ}C$ in which an activation energy of .02-.04 ev. is measured,[4] and the higher range for $300^{\circ}K \leq T \leq 1040^{\circ}K$ in which an activation energy of from 1.4 to 2.4 ev. is measured.[5] The Hall effect and Seebeck e.m.f. indicate n type behavior with negligible hole conduction.[5]

Measurements of the optical transmission in the baked material[6] and in impure single[7] crystals indicates an ultra-violet absorption edge at about 3900 $\AA$ with a shift to larger wavelengths with increasing temperature of about 1 $\AA$ per degree Centigrade at room temperature. Measurements on evaporated layers[2,8] indicates an absorption edge at 3850 $\AA$.

Sintered zinc-oxide exhibits a luminescent emission in a narrow ultra-violet band peaked at the absorption edge.[9] Zinc-oxide prepared with additional interstitial zinc exhibits in addition a broad emission band peaked at about 5100 $\AA$.[10,11] The shift of the ultra-violet band as a function of temperature is the same as that for the absorption edge.[10]

The photoconductivity as observed by Mollwo[2] on evaporated layers and in the present paper on sintered and crystalline bulk material also indicates a peak of response at the absorption edge. Thus there is general agreement that the width of the forbidden gap is about 3 ev.[2,5,13] although Seitz's[12] theoretical

estimate was about 16 ev. The problem of the nature and distribution of the impurity levels is however completely unsettled as yet.[2,3,5,13]

The samples used in the present investigation were prepared by compressing Merck C.P. or spectroscopically pure* zinc-oxide powder into briquets 1½" long x ¼" wide x 1/16" thick at between 1000 and 1500 p.s.i. The briquets were then baked at temperatures ranging from 1000°C to 1200°C from 70 minutes to 6½ hours. Typical baking cycles are shown in Figure 1. It was found experimentally that significant increases in forming pressure did not noticeably increase the sample density but did cause an increase in cracks and shearing stresses in the sample because of uneven packing of the powder. Samples baked within the time and temperature schedule given ranged in room temperature resistance between 10^3 and 10^6 ohms, the resistance decreasing with increasing temperature or time. Samples baked for short times or at low temperatures did not sinter into the typical china-like material and do exhibit room temperature resistances above the megohm range. Samples baked in excess of 1200°C possessed extremely high conductivity because of the large amount of interstitial zinc formed and tended to react with the usually inert furnace support, which consisted of an alumdum plate. Neither type of sample exhibited measurable photoconductivity.

After baking, the samples were polished into rectangular parallelepipeds and were dipped into nitric acid to remove the yellow surface layer formed by polishing.[5,14] After washing and drying, the ends of the sample were electroplated with nickel contacts. Leads were soldered to the nickel contacts with Wood's metal alloy to avoid changing the sample characteristics by local heating during the soldering process.

Several impure but colorless single crystals which had been obtained from accidental growths in commercial furnaces used for the production of zinc-oxide were electroplated, from a cyanide solution, with copper contacts to which

* Obtained from New Jersey Zinc Company, Palmerton, Pennsylvania.

conductivity leads were soldered in the manner described above. All samples showed less than 1% change in resistance upon reversing the polarity of an applied voltage.

The samples were then cemented* to a thin layer of mica attached to the copper block of the system shown in Figure 2 to insure good thermal contact. The sample temperature was determined by a chromel-alumel thermocouple attached to a dummy sample as shown. An external heater which fitted into the air reservoir was used to obtain temperatures intermediate to room and liquid air temperature. A fore-vacuum was maintained to prevent condensation on the sample.

Several samples showed an increase in resistance during cycling between room and liquid air temperature. (See Figure 3) A tentative explanation for this effect is that cracks or deformations were produced in the sample by the thermal strains induced.

Another interesting phenomenon was a slow increase of resistance of the samples of the order of 8 to 15 minutes half-life after the thermocouple had indicated that the samples had come to thermal equilibrium with liquid air temperature in the dark. (See Figure 4) An interpretation of this effect will be given in a later section.

With suitable precautions to minimize the effect shown in Figure 3 and to ensure complete equilibrium, the conductivity was measured as a function of the temperature by cooling the samples to liquid air temperatures and then measuring the conductivity in the dark during the slow return to room temperature. A typical set of curves for sintered material is shown in Figure 5. These curves parallel those found by Hahn[5] on sintered zinc-oxide. We are thus reasonably certain that we are dealing with an n-type semiconductor of forbidden gap width about 3 ev.

* Bakelite Rubber Cement BC 6052, Bakelite Corp., proved very satisfactory for the room to liquid air temperature range.

II. Photoconductivity of Zinc-Oxide:

Photoconductivity occurs in a material when incident radiant energy liberates charge carriers which are free to move in an externally applied electric field. Experimentally, photoconductivity manifests itself whenever the application of radiant energy to a material causes the passage of charge (or additional charge) in an external circuit applying an electric field to the material.

Understanding of the internal processes of various insulators, e.g. NaCl, KCl, AgCl, and semiconductors, e.g. CuO, Si, Ge, PbS, has been furthered by the study of the photoconductive effect in these substances. Particular success in interpretation has been achieved in the study of alkali-halides which was initiated by Gudden and Pohl.[15,17] Less success has been attained in the investigation of other photoconductors, e.g. PbS, CdS.[16]

The existence of a photoconductive effect in zinc-oxide was first mentioned by Gudden and Pohl[17] in 1923. Later mention of the effect was made by de Boer and Verwey[18] in 1937, but the first quantitative interpretation was published by Mollwo and Stockmann[2] in 1948.

The latter investigated the photoconductive properties of thin (.01 mm. to .1 μ thick) white and yellow layers of zinc-oxide produced by deposition of the oxide from a blast flame into which zinc was evaporated. They found a process of photoconductive rise and decay in which the half life was of the order of seconds and in which the response peaked at 3900 $\mathring{A}$ for white and, 4200 $\mathring{A}$ for yellow layers. Their measurements indicated that the following laws were obeyed:

1. For the current after equilibrium with light had been attained (saturation current):

$$i_L^3 = \text{const.}\ i_o^2\, B \qquad (1)$$

2. For the initial rise upon turning on the light:

$$\left(\frac{di}{dt}\right)_1 = \text{const.}\ i_o\, B \qquad (2)$$

3. For the initial decay upon turning off the light:

$$\left(\frac{di}{dt}\right)_2 = \text{const.} \quad i_L^2 / i_o^{2/3} \qquad (3)$$

where i_L is the photoconductive current, i_o is the dark current and B is the incident light intensity. As will be demonstrated later, a dependence of i_L on $B^{1/3}$ does not fall within the framework of any of the usual theories, but Mollwo resorts to a catalyzer in his rate reactions to give this result theoretically.

Mollwo and Stockmann cite three reasons for using thermodynamical calculations rather than quantum mechanical calculations. They are:

1. the photoconductive theory is concerned with carrier concentration and not with energy considerations,
2. the disorder levels are identified chemically and thus qualitative, i.e., band-model, demonstrations are not necessary,
3. since the first approximation gives a sufficiently accurate picture, there is no need to resort to wave-mechanics.

Their fundamental process is thermal ionization of interstitial zinc atoms to provide electrons for the dark current according to the reaction

$$Zn \quad \overset{\text{thermally}}{\rightleftharpoons} \quad Zn^+ + e.$$

The incident light then causes the reaction

$$Zn^+ \quad \overset{\text{optically}}{\rightleftharpoons} \quad Zn^{++} + e.$$

This reaction is assumed to occur only at certain favorable positions, such as at the layer surface, so that the observed effect is cut down by the ratio of "effective" to "actual" cross section. Further, the speed of the thermal reaction is assumed to be large compared to that of the optical reaction so that the former is always an equilibrium reaction.

A catalyzer of concentration X is assumed to be produced which can affect the speed of the optical reaction in either direction. X is proportional to $i_c^{-2/3}$ and is independent of the illumination B. Thus

$$Zn^+ + X \quad \overset{\text{optically}}{\rightleftharpoons} \quad Zn^{++} + e + X$$

where it is assumed that the production of catalyzer is so fast that X is important even before the current has reached a stationary value. Mass reactions are then used to obtain expressions for the current and slopes.

It is claimed that the catalyzer might be able to be replaced by a proper selection of constants or by assuming that electron diffusion is important during illumination. The agreement of the thermodynamically derived equations with the rise and decay curves is excellent.

The experiments to be discussed in this paper were mainly performed on compressed sintered zinc-oxide prepared in the manner described in the section on the properties of zinc-oxide. For convenience the data will be divided into two sections, the first on rise and decay curves due to single light pulses, and the second on measurements taken with modulated light.

III. Single Pulse Measurements

The measurements to be described in this section are similar to those taken by Mollwo, but cover a wider range of time variable since it has been found that several processes having time constants of different orders of magnitude occur concomitantly.

Figure 6 shows the experimental arrangement for measuring the slowest of these processes. A Wheatstone bridge having a 1½ volt working battery is used to measure the resistance of the sample. A tungsten filament is imaged on the sample in such a way as to fill completely the surface of the sample with light in order to avoid space-charge and diffusion effects which might be caused by an electron concentration gradient in the field direction. The intensity of illumination in the image is determined by means of a Farrand Radiation Thermocouple. The possibility of an effect at the metal-semiconductor interface on account of light on the contact has been excluded by performing experiments in which the contacts were specifically shielded from light; it was found that the response was independent of the contact illumination.

In operation, the sample is allowed to come to dark equilibrium for a time of the order of days. The shutter is then opened, allowing white light to fall on the sample. Resistance measurements are taken at regular intervals of time. When the sample resistance has approached a saturation value (in a time of the order of a day), the shutter is closed and the decay is measured as a function of time.

The incident light is then calibrated by replacing the sample with the radiation thermocouple and the shutter with a rotating-sector disk which chops the light at ten cycles per second. The thermocouple output voltage is then read from a 10 cycle narrow band pass amplifier* with low input impedance. The thermocouple

* High-Gain Ten-Cycle Amplifier, Model 33B, Electro-Mechanical Research, Inc., Ridgefield, Conn., A full-scale deflection is obtained with 10^{-8} volts in series with a 20 ohm input circuit. Band width: 1 cycle at half power points.

has a calibrated response of 4.3 volts/watt. In this way the incident intensity may be determined.

Measurements were made at room and at liquid air temperatures, the latter being carried out in a system as shown in Figure 2. A typical curve is shown in Figure 7. In this plot the sample was initially at a dark conductance indicated by the point A. After 30 minutes of illumination, the conductance had risen to a value indicated by B, at which time the light was turned off. The path of decay for the following 30 minutes is indicated by the curve B-C.

The slow rise curve of a sample at liquid air temperature is shown in Figure 8. The half-life here is about 25 minutes, as closely as can be determined from the scattering of the final points.

Simple considerations, as will be shown later, lead to the conclusion that the rise curve should be exponential for a monomolecular process, i.e., one in which the recombination rate of free charge is proportional to the free charge concentration, and hyperbolic tangent in form for a bimolecular process, i.e., one in which the recombination rate is proportional to the square of the free charge concentration. In like manner, the decay curve is expected to be exponential for a monomolecular process and hyperbolic for a bimolecular process.

Repeated attempts to fit these curves with such functions have failed. An examination of the rise and decay in more detail, however, indicates that a combination of processes is occurring rather than a single process.

Let us examine the rise curve of a sample (11B). Figure 9 shows a section of the rise curve of this sample plotted to 50 minutes. As mentioned above, attempts to fit this curve with either an exponential or hyperbolic tangent have failed. Let us assume that two processes are involved, a long time one and one of much shorter time constant. A hyperbolic tangent is linear for small arguments, hence it would seem justifiable to approximate the contribution of the slower process to the observed current by a straight line. The actual determination of this linear

approximation is an art conditioned by trial and error. Such an approximation is shown by the straight line in Figure 9 which separates the early part of the rise from the later.

Figure 10 shows the complete rise curve of sample 11B with the linear approximation replacing the experimental points in the first 50 minutes. We note that a hyperbolic tangent curve with a half-life of about 38 minutes fits the curve to the order of accuracy of the experimental points. Thus a slow bimolecular process of 38 minutes half-life seems to exist in the rise curve of this sample.

What about the earlier part of the curve? Figure 11 shows the residue in Figure 9 in a semi-logarithmic plot as a function of time. The closest fit to the experimental points is a straight line representing an exponential having a time constant equal to 4.6 minutes. The fit on a linear plot is shown in Figure 12. Thus a monomolecular rise having a time constant of about 4.6 minutes seems to share concomitantly with the bimolecular 38 minute process in the rise curve of this sample. It is not certain whether a process occurring in the order of a minute is also effective here. The effect of heating of the sample by the light source may be the cause of the divergence of the experimental and fitted curve in the first minutes of Figure 12, since it is estimated that about a minute would be necessary for the sample to come to equilibrium, or another process may exist. Experimental facilities to record the response more accurately in this time range were not available at the time of the experiment.

It is now of interest to determine whether such a resolution can be effected on the decay, since if two mechanisms occur during the rise of photoconductivity the decay should also show such processes. Figure 13 shows the decay of sample 11B plotted as resistance vs. time counted from zero at the instant of turning off the light. Neglecting short times, the straight line fits to the experimental data a curve linear in resistance or hyperbolic in conductance. Figure 14 shows the decay plotted as conductance versus time. The half-life here is 51.7

minutes as compared to the 38 minute half-life of the bimolecular part of the rise process. Why the decay half-life should be longer will be indicated in a later section.

In fitting the curve of Figure 13, the early part of the decay was neglected. This section should now be examined for evidence of a shorter monomolecular process.

Figure 15 shows the shorter part of the decay on a semilogarithmic plot. The straight line represents an exponential having a time constant of 5.5 minutes. Figure 16 shows the match of the experimental and fitted curves on a linear plot. Again we note a divergence of the fitted and experimental curves which again raises the question of the possibility of a process of the order of a minute.

Thus we can conclude that for this sample two processes of the order of minutes are observed: a bimolecular rise and decay of half-lives 38 minutes and 51.7 minutes, respectively, and monomecular rise and decay with time constants 4.6 minutes and 5.5 minutes, respectively. The possibility of a rise and decay process of time constant of about 1 minute is not excluded.

By way of further illustration, Figure 17 shows a rise curve for sample 8D to which both an exponential and a hyperbolic tangent has been fitted. In this case, the experimental curve did not cover a sufficient number of half-lives to make the difference apparent. The proper curve, of course, should be the hyperbolic tangent one, but here there is no significant difference. The half-life here is about 20 minutes, but this value is doubtful since the curve never achieved saturation.

Figure 18 shows a plot of the difference between the actual and fitted curves on semi-logarithmic paper. The straight line represents an exponential of time constant 3.6 minutes. Figure 19 shows a plot of these curves on linear paper.

Thus again we see here two processes, a slow one with a possible half-life of 20 minutes and a faster exponential one of time constant 3.6 minutes.

The difference between the fitted exponential and the experimental curves of the rise in Figure 19 was plotted in Figure 20 and 21. It is seen here that if a still faster process exists, it would seem to be exponential with a time constant of the order of 0.74 minutes or 45 seconds. The fact that Mollwo and Stockmann[2] made their observations on a process occurring in the order of seconds in evaporated layers of zinc-oxide implies that such a process might exist here also, in addition to the others already described.

It might be pointed out here in this connection that Mollwo[2] mentions in his first paper that long time changes in the photoconductivity were observed in the evaporated layers. In the third paper of the series a guess is made that this effect might be explainable by photo-chemical dissociation of the zinc-oxide lattice.

The phenomenon of long time effects in the photoconductivity of many materials, incidentally, is a long known but poorly understood effect. See, for example, the discussion of Mott and Gurney[19] on the possible effects of space charge on contact potential barriers in insulating crystals, the discussion by Rose[20] on the effects of trapping and small capture cross section in hindering recombination, and the recent work of Chasmar and Gibson[21] on explaining long time effects in lead-sulphide cells by oxygen or sulfur barrier layer models.

It would be of considerable interest to determine the response that is due to each of these processes using as parameters, temperature and incident radiation wavelength. Because of the overlapping of the effects in the photoconductivity curves, the large amount of labor that needs be expended in resolving those processes precludes making such a study at this time.

Figure 22 shows the response in sample 11B as a function of time plotted for three different bands in the visible. Since the sample was not allowed to return to complete dark equilibrium (a matter taking days, at least), the abcissaes of the curves are shifted from horizontal. The important points however, are that

the time constants retain at least the same order of time, but the overall response, which is dominated by the slowest process, is about 100 times larger in the blue than in the red.

In order to determine whether processes of the order of a second or less existed, an apparatus such as is shown in Figure 23 was employed. The light source was a General Electric Street Lamp 1M/66 run at an overvoltage in order to obtain a filament temperature of 3200°K. A system of lenses was arranged to obtain the best possible aperture and to focus the filament image on the sample in order to obtain the maximum amount of light. In the first experiments a constant voltage source was used in conjuction with a matching resistor in the sample circuit. The voltage from the matching resistor was amplified by a wide band Howlett-Packard Model 40A amplifier. The amplified signal was then projected on an oscilloscope and the resultant traces were photographed. Figure 23 compares such traces with the output of a photocell replacing the sample-matching resistor circuit and also shows the linearization of response with decreasing illumination intensity. (The traces are not to scale.)

Figure 24 shows a reproduction of a curve taken when a constant current was passed through the sample and no matching resistor was used. The constant current method was effected by using the sample as the plate load in a pentode circuit. The duration of the flash in this figure was 2.5×10^{-2} sec. It is to be noted that the rise curve approached saturation, although this is not definite because of noise. In like manner, Figure 25 represents a photograph of the response taken when the flash duration was 1.72×10^{-3} sec.

It should be mentioned here that this method of taking the response with a rotating shutter did not allow the sample to return to a dark equilibrium between flashes. An arrangement was later devised, as depicted in Figure 26, which allowed a wider spacing of flashes. The flash time of 10^{-3} sec. was about the shortest that could be produced with our mechanical system of a high speed motor and a

shutter of twenty holes. In order to retain a good aperture a shutter with many more openings would have been of very large size -- 2 feet or more in diameter. Some consideration was given to using a Kerr Cell, but again, because of the need for high illumination, and because of the light losses involved in making a suitable arrangement, this project was abandoned.

The fact that the curves of Figure 24 and 25 show curvature indicates that a process of 10^{-3} seconds or faster occurs, i.e., if the curves shown were due to tracing a small part of the characteristic of a process involving time constants long in comparison to a millisecond, a sawtooth wave-shape would be expected to be observed since both monomolecular and bimolecular characteristics are linear for short times. On the other hand, processes with very much shorter time constants should yield a square wave as shown for the photocell output of Figure 23.

The arrangement shown in Figure 26 allowed a longer time to elapse between flashes of light on the sample. A tungsten source operating at about 3200°K was imaged onto an adjustable slit. The image of this slit was then focussed on the sample with a rotating mirror interposed in the light path. Rotation of the mirror then swept the rectangular light image across the sample once in each revolution of the mirror. Since the sample subtended only about 1° at the mirror, the light flash occupied only 1/360 of the whole cycle, allowing time for the sample to return to dark equilibrium. Further, since the width of the sample was about $1/10^{th}$ the width of the light image, only about $1/10^{th}$ of the initial rise or decay was involved in having the leading -- or trailing -- edge of the image traverse the sample; thus quite square pulses of light were effected.

The motor was controlled in rate of rotation by a variable-speed thyratron control circuit. Single sweeps were used in observing and photographing the curves and triggering was effected by reflecting part of the image back to a photocell whose output was amplified and fed to the triggering circuit of the oscilloscope.

Curves could also be taken from a complete light-on or light-off position by use of a hand-operated shutter in the beam when the mirror was left in the stationary position which allowed the image to fall on the sample.

The observed curves were quite similar to those shown in Figure 24 and 25. Unfortunately, the intensity of the light was not sufficient to cause saturation, i.e., pronounced flattening of the later portion of the photoconductive rise. These curves were for this reason not easily adapted to analysis and resort was made to obtaining rise and decay curves in which the curve was taken from a full dark or full light equilibrium position.

In order to obtain sufficient detail in the decay curve, for example, the following arrangement was used. A type 304H Dumont cathode-ray oscilloscope was employed. The sample circuit was connected to the D.C. amplifier section of the oscilloscope in series with a suitable bucking voltage circuit. A recurrent sweep was used with square-wave Z-axis modulation to provide a time base. See Figure 27.

After the sample had been illuminated for some time, the shutter was rapidly closed. A trace of the type shown in Figure 28 was thus obtained, where in this case the time between pips is $1/100^{th}$ of a second. This curve was then replotted in a linear fashion as shown in Figure 29, and could be analyzed in a manner analogous to that used for the slower decay; fluctuations at the tail of the curve are caused by distortion on account of CR tube curvature. Voltage calibration was obtained by photographing a sine wave of known voltage under the same amplification conditions.

Figure 29 shows the separation of a faster process from a slower one which is assumed linear in this range. Figure 30 shows the fit of the part of the curve due to the faster process, while Figure 31 shows the match of the experimental and fitted curve of Figure 30 on linear paper. We see that the fast decay here is fitted by a monomolecular decay of time constant 0.8 second.

Figure 32 illustrates the difficulties encountered in picking the proper linear approximation for the slow part of the decay in Figure 29. The crosses, circles and triangles each represent an attempt to linearize the fast process on a semi-logarithmic plot. Straight lines which approximate the best fit for each set of points are shown in the figure. The set of circles was chosen to give the best fit as shown in Figure 31.

Figures 33 to 35 indicate the existence of an exponential decay of time constant 0.26 seconds.

As was mentioned previously, attempts to fit the experimental curves directly without resort to the process of resolution discussed here always ended in failure. Thus several processes seem to be occurring concomitantly in the photoconductive effect. We have shown for sample 8D processes having time constants of decay of 0.8 seconds, about 1 minute(?), 3.6 minutes, and a bimolecular one of the order of twenty or more minutes.

In like manner in sample 11B we have shown decays of 0.26 seconds, possibly one of the order of a minute, 5.5 minutes, and a bimolecular process of the order of 52 minutes half-life.

In addition the photographs of Figures 24 and 25 indicate the possible existence of even faster processes. Since the observed luminescence transitions occur in 10^{-6} to 10^{-7} seconds,[6] faster transitions must exist, though it is not known whether photoconductivity is involved, i.e., whether the electrons spend any time in the conduction band.

A considerable amount of work can be outlined for pursuing the investigation of these processes further. (1) The scope of the investigation should be widened to examine time intervals between 10^{-3} and 10^{-7} seconds on the one hand, and intervals of the order of weeks or months on the other hand. (2) The effect of the wavelength of the incident radiation should be determined in more detail. (See Figure 22) (3) The effect of sample temperature on the individual processes

should be investigated. (4) The luminescence should be examined in an attempt to correlate the luminescent transitions with the photoconductive recombination. The indications at the present time are that the above program would take a considerable amount of time to carry out, so that no further experimental work on this topic will be reported in this paper. We now turn to the data observed with ten cycle shuttering and finally to a theoretical consideration of all the observed data on photoconduction in zinc-oxide.

IV. Modulated-Light Measurements

The response of photoconductors to chopped or modulated light has been determined for several reasons, one of which is that photoconductors with fast response are desirable for various practical applications. Second, the use of modulated light allows the application of methods in which D.C. drift and backgrounds are eliminated, and third, the high amplification easily obtainable in A.C. methods can be employed. Fourth, the modulated light may provide an easier method for examining the kinetics of a photoconductive process. For example, Lashkarev[22] has employed an alternating-current bridge similar to those employed in examining barrier layer properties in the hope of determining the number of impurity levels involved in the photoconductive process. Fassbender[23] attempted to use the A.C. response in cadmium sulphide to determine the mobility of the conduction electrons.

The experiments on zinc-oxide to be described here were derived originally in the hope of eliminating the drift on account of the slower processes while examining the faster response of the material and in the hope of being able to obtain data which would be easily interpretable.

The first experiments of this type were those shown in Figure 23 with the results shown in Figures 24 and 25. Later experiments were performed with the refined apparatus of Figure 26.

Figures 36 and 37 show plots of the relative response measured on a Ballantine V.T.V.M. as a function of flash duration and flash frequency, respectively, where the flash duration was equal to the time between flashes. A discussion of the significance of these curves will be given in a later section; it will be shown that these curves imply the existence of processes with time constants of the order of milliseconds.

The bulk of the work performed under this heading was done at ten c.p.s. primarily because excellent ten c.p.s. narrow-band-pass amplifiers were available.*

The arrangement of the apparatus is indicated schematically in Figure 38. The light from a tungsten source* was rendered parallel by a lens system and then passed through one of a series of interference filters,** which approximately monochromatized the light. The monochromatic light was then focussed on the sample by additional lenses. The sample was connected in series with a dry cell and a matching resistor. The output of the matching resistor was fed to the high-impedance 10-cycle amplifier. Calibration of the incident light intensity was effected by means of the radiation thermocouple and low-impedance 10-cycle amplifier previously described. Due to the narrow band-pass of the amplifier ($\pm$ 1 cycle at half-power points) thermal, contact, and pickup noise was largely avoided.

For measurements outside the visible range of illumination a quartz monochromator*** was employed. Attempts to observe photoconductive response in the infra-red using a Nernst glower or filtered light from a carbon arc did not succeed. Occasionally a constant-current circuit was used as the source of sample current, obviating the need for a matching resistor, but since the curves obtained using constant voltage always have the current directly proportional to the conduction-band electron concentration the constant current method was abandoned.

Figure 39 illustrates the validity of Ohm's law in the samples at room and liquid air temperature. Figure 40 shows that the shuttered response at either temperature is a linear function of the impressed D.C. current (or voltage). Figure 41 indicates that the 10 c.p.s. shuttered response is an approximately linear function of the illumination intensity. (This experiment was done by employing the inverse-square law, although other methods of using neutral filters of wire screen were devised.)

---

* G.E. IM/66 Street lamp operated at an overvoltage.

** Farrand Interference Filters, Farrand Optical Company, Bronx Blvd. and East 238th St., N.Y. 66, N.Y. Peak value $\pm$ 5 mμ nominal value. Half band-width 10 mμ to 20 mμ. Peak transmission of 20% to 35%. A series of 8 filters covering the visible was used.

*** Bausch and Lomb Quartz Prism Monochromator #2814.

Figure 42 shows a typical response as a function of incident wavelength in the visible region at both room and liquid air temperature. We note that the response increases by three orders of magnitude in the region between 8000 Å and 4000 Å. (The bump around 6900 Å is thought to be caused by leakage of shorter wavelength radiation through the edges of the filter concerned.) It is also of interest to note that the response is not significantly different at the two temperatures, and that the response is still not negligible at wavelengths as long as 7000 Å.

Figure 43 shows a typical response curve extending into the ultra-violet. The region of wavelengths shorter than 3500 Å is suspect; the plotted values may be due to fundamental (lattice) absorption or due to noise because of the insensitivity of the thermocouple used for calibration in this region. The important thing is the peak at 3900 Å with a tailing-off of the response into the visible. Figure 44 shows among other things, the shuttered response compared to that observed by Mollwo statically (not to scale). It is to be noted that both peaks lie at 3900 Å, the position of the absorption edge.

For the sake of completeness, a curve of the response at liquid helium temperature is included here (Figure 45), although the experimental conditions were not such that much faith can be put in this measurement. The sample was immersed in liquid helium in a double-Dewar system. The light was passed in through unsilvered slits on the Dewars. Unfortunately, the bubbling of the outer liquid air, by interrupting the light beam, caused the measurements to be noisy and it is not certain that the power dissipation in the sample did not exceed what is considered to be the maximum allowable for this sample to remain at helium temperature. A helium cryostat for making better measurements was built but has not been put in working order as yet. In any case, a response was observed which again increased toward the absorption edge, but the relative height of the peak with respect to the tail region was less.

Shuttered experiments were also performed on colorless, impure, single crystals* of zinc-oxide. Long-time photoconductive effects could not be observed in these crystals, since light intensities sufficient to cause a conductivity change in the crystals also warmed them appreciably. Noise, presumably at the contacts, was also present at a much higher level than that observed in the sintered specimens. Figures 46, 47 and 48 show respectively: verication of Ohm's law, response to blue light as a function of impressed constant D.C. current, and response per volt as a function of impressed current. The last curves are close to being flat. Figure 49 shows the crystal response per volt as a function of incident wavelength, the response increasing toward the absorption edge. For comparison, the absorption curves of Mollwo[2] on sintered material and of Melnick[7] on these crystals are included.

* See Hahn, reference 5, page 857, especially note 18.

V. Experimental Conclusions

Before summarizing, one more experiment should be cited here. Russell[24] found that illumination of a sintered sample during Hall measurements changed the conductivity by the expected amount, but the Hall coefficient was unaltered. This can be interpreted in two ways. Since $R\sigma \sim \mu$, where R is the Hall constant, σ is the conductivity, and μ is the mobility, μ increased proportionately to σ; or, since the Hall effect measures the bulk properties of the material, whereas the conductivity may measure surface or barrier layer properties in an inhomogeneous material, the photoconductive effect may be a surface or barrier phenomenon. This point will be discussed in more detail later.

In conclusion then, three processes definitely coexist in the photoconductive effect, of the order of a second, 5 minutes, and 40 minutes. Evidence is also given for the possible existence of a 1 minute process, and it is thought that processes may exist with time constants of 10^{-3} or 10^{-4} seconds and 10^{-6} or 10^{-7} seconds. (The latter would explain the luminescence transitions.) Both single pulse and shuttered measurements indicate an enhanced sensitivity toward the absorption peak. Shuttered response is not significantly dependent on temperature.

We shall now attempt to give a theoretical interpretation of the observed data.

VI. Theoretical Models of Photoconductivity

In a typical insulator or semiconductor one has a band-model energy diagram which in its simplest form is as shown in Figure 50. The model contains a filled band consisting of states which are non-conducting because they are filled, a conduction band consisting of unfilled states, and a forbidden energy region between the bands in which no energy levels exist in the case of an insulator or which contains only states associated with impurity atoms in the case of an extrinsic semiconductor. Electrons which by some means attain energies associated with the states in the conduction band are free to move through the crystal by a process of being associated with the energy configuration of different lattice atoms successively. In a similar manner, a deficiency of an electron in the filled band can move by the successive filling of the deficiency with electrons from other states in the band. Such a deficiency is known simply as a "hole", and the process above described is the motion of a hole through the filled band.

At sufficiently high temperatures, corresponding to an energy of the order of the width of the forbidden region, electrons can be excited from the states of the filled band by thermal phonon* collision into the empty states of the conduction band. The electrons are then effectively free to move and the holes may or may not be free to move. The directed motion of either type of carrier is manifested as the passage of charge through the material.

In a manner almost but not quite analogous to the phonon process, an incident photon may excite an electron to the conduction band. The electron, and possibly also the hole remaining in the filled band, is then free to move in the direction of an applied field until such time as the electron (and/or hole) is trapped by an impurity level or some other center, or until recombination of the electron with a hole occurs. Should recombination occur before the carriers have reached the contacts, the total charge measured in the external circuit will be

* A phonon is a quantum of lattice vibrational energy. A more explicit definition may be found in the work of reference 35.

equal to the charge of the free carriers times the ratio of the average distance moved in the conduction band during their free time to the length of the sample. Should the drift distance of the carriers exceed the sample dimensions, the charge measured externally is determined by whether replenishment occurs at the contacts, i.e. whether it is possible for the charge carriers to tunnel through the potential barriers at the contacts.

Further, should either type of charge carrier be easily trapped while the other type is free to move, or should the geometry be such that large concentration gradients of charge of one sign can occur, the observed currents will be conditioned by the space charges set up within the material. An excellent discussion of many such cases is given by Rose,[20] who also derives a general but as yet qualitative means of discussing photoconductivity in terms of the motion of a quasi-Fermi level through various impurity distributions. It is our intention to describe much the same type of observed phenomena through a different approach by examining the kinetics of the processes involved in photoconductivity.

It might be mentioned here that a similar attempt to describe the photoconductivity and luminescence in cadmium sulfide has been made by Broser and Warminsky[25] and in simpler fashion by Gildart and Ewald[26] on the same material.

Let us assume the process shown in Figure 50 of an incident radiation quantum exciting an electron from the filled to the conduction band.

For simplicity, and since it is our final aim to describe zinc-oxide here, we assume that the holes left in the filled band are not free to move for one reason or another. (The argument can easily be generalized for free holes.) The rate at which electrons are excited to the conduction band is assumed proportional to the incident light intensity, L. The rate of recombination of conduction electrons and holes should be proportional to the product of the hole and electron concentrations, which are here equal, n. We can then write for the time rate of change of the concentration of electrons in the conduction band,

$$\frac{dn}{dt} = A L - B n^2 \qquad (1)$$

where A and B are dependent at least on temperature, but will here be assumed constant for simplicity.

Equation (1) illustrates the typical bimolecular recombination process in which the recombination is proportional to the square of two concentrations. In equilibrium with light, the derivative is equal to zero, hence

$$n = \left(\frac{A}{B} L \right)^{\frac{1}{2}} \qquad (2)$$

or, since the conduction band concentration is related to the conductivity by the relation

$$\sigma = n e \mu \qquad (3)$$

where σ is the conductivity, e is the electronic charge, and μ is the carrier mobility (velocity/unit field), we see that the equilibrium conductivity varies as the square root of the incident light intensity for constant mobility.

Integration of (1) for the rise when the light is initially turned on yields

$$n = \sqrt{\frac{AL}{B}} \tanh \left\{ \sqrt{\frac{AL}{B}} (Bt + \text{const.}) \right\} \qquad (4)$$

where the constant can be evaluated from the initial conduction concentration.

For the decay $L = 0$; counting $t = 0$ from the moment the light is turned off, one obtains

$$n = (Bt + \text{const.})^{-1} \qquad (5)$$

where the constant can be evaluated at $t = 0$.

Thus this simple bimolecular process is characterized by a hyperbolic tangent rise (4), a decay of hyperbolic form (5), and an equilibrium proportionality of the conductivity on the square root of the light intensity (2).

On the other hand, cases exist in which a monomolecular recombination can be postulated. For example, Figure 5la shows an n or donor type semiconductor in which N electrons/cm^3 are in the conduction band in the dark at some temperature, say room temperature. The addition of light then increases the conduction concen-

tration by an additional amount n, leaving n holes in the filled band. Or, in Figure 51b, acceptors or frozen-in lattice defect produce a dark concentration of holes N in the filled band. For the case of Figure 51a one obtains for the conduction band concentration,

$$\frac{d(N + n)}{dt} = A L - B'(N + n)n \qquad (6)$$

while for the case of Figure 51b,

$$\frac{dn}{dt} = A L - B'n(N + n) \qquad (7)$$

where again we neglect the temperature effect and assume large numbers of states involved compared to the concentrations involved in the photoconductive process alone, so that A and B' may be considered constant. If then in either (6) or (7) the conditions N = const. $\gg$ n are satisfied, we have

$$\frac{dn}{dt} = A L - B n \qquad (8)$$

where A and B are constants.

Equation (8) is of the monomolecular form since the recombination is proportional to the first power of the concentration. In equilibrium with light,

$$n = \frac{A}{B} L \qquad (9)$$

and by (3) it is seen that the light equilibrium conductivity will be linearly proportional to the incident radiation intensity.

For the rise upon turning-on the light,

$$n = \frac{AL}{B}(1 - e^{-Bt}) \qquad (10)$$

where n(0) = 0.

For the decay, L = 0, hence

$$n = \text{const. } e^{-Bt} \qquad (11)$$

where the constant can be evaluated from n(0) where t = 0 is the moment of shutting the light off.

Thus in the simple monomolecular case one obtains an exponential rise (10), an exponential decay (11), and a linear dependence of the conductivity on the

light intensity (9).

Attempts were made to fit either of these processes to the observed fast and slow responses of sintered zinc-oxide. For example, the photographs of Figures 24 and 25 looked as if they could be fitted with a single process until it was found that the lack of equilibrium with light, i.e., sufficient flattening of the rise curve, and the broad trace width precluded exact fitting by one type of curve to the exclusion of the other. A pulsed light method using a harmonic analyzer was then resorted to. We will now consider this method.

The monomolecular form (8) was solved for a square chopped-light input of the form shown in the inset of Figure 52, where τ is the pulse duration and 2τ the pulsing period. Using Laplace transforms, we define $\mathcal{L}\, n = y$. where $\mathcal{L}$ indicates the transform operation. Then

$$\frac{dn}{dt} = py - pn_o = py \tag{12}$$

where $n_o = n(0) = 0$.

From tables,[27] $\mathcal{L}\, L(t) = \dfrac{L_o}{e^{p\tau} + 1}$ (13)

Then substituting in (8) yields

$$py + B\,y = \frac{AL_o}{e^{p\tau} + 1}\ , \tag{14}$$

or

$$n = \mathcal{L}^{-1} \frac{AL_o}{(p+B)(e^{p\tau} + 1)} \tag{15}$$

Applying the definition of $\mathcal{L}$, we obtain

$$n(t) = \frac{AL_o}{2\pi i} \int_{c-i\infty}^{c+i\infty} \frac{e^{p\tau}\, dp}{p(p+B)(e^{p\tau}+1)} \tag{16}$$

Integration is effected around a contour consisting of a straight line parallel to the ordinate and c to the right of it in the p plane intercepted by a circular arc of radius R concentric to the origin.

There are poles at $p = -b$ and $p = 0$ and singularities at

$$p = \frac{(2n+1)\pi i}{T} = \xi_n$$

The integrand does not necessarily approach zero for $R \to \infty$, but Jordan's lemma applies except at a singularity. Thus we let $R \to \infty$ but between singularities in the limit. One then obtains

$$n(t) = AL_o\left\{\frac{1}{2B} - \frac{e^{-Bt}}{B(1+e^{-B\tau})} - \frac{2}{\tau}\sum_{n=0}^{\infty}\left[\frac{B\sin\omega_n t}{n(B^2+\omega_n{}^2)} - \frac{\cos\omega_n t}{(B^2+\omega_n{}^2)}\right]\right\} \qquad (17)$$

where $\xi = i\omega_n$. Rewriting (17),

$$n(t) = AL_o\left\{\frac{1}{2B} - \frac{e^{-Bt}}{B(1-e^{-B\tau})} - \frac{2}{\tau}\sum_{n=0}^{\infty}\frac{\sin(\omega_n t+\delta)}{\omega_n\sqrt{B^2+\omega_n{}^2}}\right\} \qquad (18)$$

where $\omega_n = \frac{(2n+1)\pi}{\tau}$.

After a long period of time we can neglect the transient term in (18) and write

$$n(t) = AL_o\left\{\frac{1}{2B} - \frac{2}{\tau}\sum_{n=0}^{\infty}\frac{\sin(\omega_n t+\delta)}{\omega_n\sqrt{B^2+\omega_n{}^2}}\right\} \qquad (19)$$

Using a circuit in which a constant voltage V is impressed on a sample in series with a matching resistance R and measuring the alternating voltage V' developed across the resistor we should obtain by (19)

$$V' = \frac{2AL_o e\mu V\alpha R}{\ell\tau}\sum_{n=0}^{\infty}\frac{\sin(\omega_n t+\delta)}{\omega_n\sqrt{B^2+\omega_n{}^2}} \qquad (20)$$

where α and ℓ are the sample cross section and length respectively, e is the electronic charge, and μ is the sample mobility.

Thus if we use a particular light intensity and shuttering speed, taking measurements of V' using a harmonic analyzer set to frequencies $\omega_n = \frac{(2n+1)\pi}{\tau}$ should give a response of the form

$$\text{const.} \times \frac{1}{\omega_n\sqrt{B^2+\omega_n{}^2}} \qquad (21)$$

Figure 52 shows a typical experimental curve with the most closely fitted curve of form (21). It is noted that the deviations are large, particularly for

larger values of ω_n. A closer investigation indicates that B is not a single time constant, which is not in accord with the original assumptions, but which is in agreement with the fact that several processes of differing time constants occur simultaneously.

The same technique was considered for a model of bimolecular form as exemplified by (1). The Laplace transform method is not easily applicable here because the differential equation is not linear. Fassbender[23] obtains an approximate solution for the equation

$$\frac{dn}{dt} = \mu e^{-uZ} - \alpha n^2 \qquad (22)$$

where μ here is the absorption coefficient at the incident wavelength. The solutions are obtained for two cases, one in which α is a function n and constant mobility is assumed, the other in which α is assumed constant and the concentration is related to the current through a mobility which is dependent on the concentration n, which stem from the experimental fact that n is not proportional to $L^{\frac{1}{2}}$ in light equilibrium, as might be expected from (22). The shuttered light is assumed to be of the form $L = L_0(1+\cos(\omega)t)$.

Unfortunately, his solution is done by approximating by the first two terms of a Fourier expansion the coefficients which were determined exactly in the monomolecular case, so the harmonic analysis experiment which depends on determining the higher order harmonics could not be performed. The conclusions reached by Fassbender will be compared with those to be obtained from the monomolecular solution (18).

The monomolecular model and Fassbender's model demand the observed response be a linear function of the incident light intensity in the long wavelength region. Slopes ranging from 0.87 to 1.03 were obtained by the author on zinc-oxide for the response as a function of light intensity in this region.

In the short wavelength region, i.e., that beyond absorption edge, Fassbender's model demands linearity for constant mobility and that the response be proportional to $L^{1/\beta + \frac{1}{2}}$ for constant recombination, where β is the recombination

coefficient, i.e., the power to which the concentration is raised. Our measurements, as exemplified in Figure 41, yielded slopes from 1.01 to 1.35, which would make $\beta \sim 1.5$, or somewhere between monomolecular and bimolecular. (Rose[20] points out that a simple combination of monomolecular and bimolecular processes cannot be used to get a process which give a response proportional to L^{δ} where $\frac{1}{2} < \delta < 1$ over a significant range.)

Both models demand that the response be inversely proportional to the shuttering frequency, Fassbender's model requiring this at high shuttering speed at least. (That the monomolecular model requires this can be seen from (20) in which the summation for small B and τ is simplified to

$$\frac{\tau^2}{\pi^2} \sum \frac{1}{(2n+1)^2} \approx 1.2 \frac{\tau^2}{\pi^2}$$

so that $V_{RMS} \propto L_o \tau$.)

Figures 36 and 37 indicate that such inverse proportionality was never achieved, even at the highest attainable shutter speeds, the response being approximately proportional to $\omega^{-0.6}$. One might expect, incidentally, any slow process which is linear for times short compared to the process lifetime to give rise to a sawtooth waveform whose response would vary as $1/\omega$. Thus the dependence on $\omega^{-0.6}$ is considered evidence for the existence of faster processes in sintered zinc-oxide.

A feature of Fassbender's equation (22) which is not shared by the monomolecular equation cited is the inclusion of the absorption constant in the activation term. This is based on the assumption that one has activation from both the filled band and from a set of levels lying above or overlapping the filled band. Excitation in the filled band (short-wave side of the fundamental absorption edge) does not give a strong photoconductive effect because the activation is confined to a small surface layer, leading either to fast recombination due to the high pair concentration or to low carrier mobility because of the non-uniform and defective nature of practical surfaces. On the other hand, irradiation on the long wavelength

side yields low photoconductivity merely because of the low number of impurity levels. The overlap region gives rise to a photoconductive peak such as is observed in cadmium sulfide[23] and in zinc oxide. (See reference[2] and Figures 42 and 43.) A comparison of the expected and observed responses is shown in Figure 44, where it is seen that the observed responses agree quite well in this respect with Fassbender's model.

Rose[20] points out that this argument can be put into more general terms. If the equilibrium current as a function of light intensity is of the form $I \sim L^{\gamma}$ where $\gamma < 1$, it is easy to show from γ and $d\mu/d\lambda$ that a peak is expected at the absorption edge. For $\gamma = 1$ no peak is expected.

As is also pointed out by Rose, the presence of additional states between the filled and conduction bands causes three first order effects:

1. The photosensitivity is reduced by the ratio n_c/n_t where n_c is the concentration of states effective for trapping electrons.

2. The observed decay lifetime may be unaffected or increased by the inverse of the above ratio, depending on the trap distribution.

3. Response proportional to L^{γ} yields $\gamma = 0.5$ for no traps (strict bimolecular process) but γ approaches unity with increasing trapping.

The next step then was to devise a model which perhaps would not be a strict physical picture of the band structure of zinc-oxide but would be at least a fair approximation of the physical reality. It was also hoped that a sufficient number of experiments could be devised to avoid the numerous assumptions which have previously had to be introduced in constructing a model*

With these aims, a technical report was prepared by the author[28] in which the models of Figure 53 were discussed. It was shown in this report that all the parameters of the illustrated and similar models could be determined by measuring the equilibrium photocurrent and the initial slopes of the rise and decay. It was

* See, for example, reference[25].

felt though that the initial slopes may occur in times of the order of atomic transition times (10^{-13} seconds) and that the physically measurable slopes may for this reason be considerably different from the true initial slopes. Computations were then undertaken to examine the processes in detail for a longer period of time. The incremental method to be described in the following section leads directly into a consideration of the proposed mechanism for zinc-oxide.

VII. Incremental Calculation of the Photoconductive Process

The differential equation which represents a bimolecular photoconductive process, as exemplified by equation (1), is not linear, which adds to the difficulty of solving the equations involved in any but the simplest processes. A method of using small increments will be used to effect solution in one case of interest. Other cases may be solved in a similar manner.

A matter of considerable interest is the effect of traps or additional impurity levels on the simple photoconductive process as described in the previous section. The approach to be taken here will be to consider a simple n-type semiconductor which exhibits dark current at normal operating temperatures. All the possible transitions between the conduction and filled bands and the impurity level will be examined and a simple but physically possible case will be computed. Some other cases follow directly from this case; other situations will require additional and more complicated analysis.

Figure 54 shows the model concerned with the possible transitions. It is assumed that the temperature is such that n_{cd} electrons are in the conduction band in the dark, leaving n_{td} of the N total impurity donor levels filled, while intrinsic thermal excitation of electrons from the filled to the conduction band will be taken as negligible.

Transition A is an optically stimulated excitation of an electron from the filled to the conduction band, leaving a hole in the filled band which for simplicity will be assumed immobile.* Transitions B and C are effective between the conduction band and the impurity level and in the dark cause equilibrium between the two. D and E are the recombination transitions between conduction band or impurity level and the filled band, respectively. For simplicity one of these transitions, E, will be assumed negligibly small in probability. The solution assuming the other transition, D, small and the first large follows in exactly

* The hole could be trapped, for example, in an impurity level immediately above the filled band.

the same manner as the solution to be presented. To include both D and E simultaneously would complicate the solution considerably.

The fundamental equation for the time rate of change of the conduction band electron concentration can then be written as:

$$\frac{dn_c}{dt} = AL - Bn_c(N-n_t) + Cn_t - Dn_c n_h \qquad (23)$$

where L is the incident light intensity, assuming uniform bulk excitation. The temperature is assumed to be held constant so that A, B, C, and D are constants.

In dark equilibrium $L = 0$ and $dn_c/dt = 0$, therefore,

$$-Bn_{cd}(N-n_{td}) + Cn_{td} = 0$$

But $N = n_{td} + n_{cd}$ $\therefore$

$$Bn_{cd}^2 = Cn_{td} \qquad (24)$$

We now assume that the concentrations with the light on are

$$n_c = n_{cd} + \epsilon \qquad n_t = n_{td} + \varphi \qquad \text{where} \quad \epsilon + \varphi = n_h \qquad (25)$$

Substituting (24) and (25) in (23), where ϵ and φ are small, yields

$$\frac{d\epsilon}{dt} = AL + \varphi(Bn_{cd} - Dn_{cd} + C) - \epsilon(B+D)n_{cd} \qquad (26)$$

In like manner, writing the balance for the impurity level,

$$\frac{dn_t}{dt} = Bn_c(N-n_t) - Cn_t$$

or,

$$\frac{d\varphi}{dt} = -\varphi(Bn_{cd} + C) + \epsilon Bn_{cd} \qquad (27)$$

Adding (26) and (27) gives

$$\frac{d(\epsilon+\varphi)}{dt} = \frac{dn_h}{dt} = AL - Dn_{cd}(\epsilon+\varphi) = AL - Dn_{cd}n_h$$

as is intuitively expected.

It is easily seen that without the impurity level the intrinsic decay is exponential with a time constant $1/Dn_{cd}$ and that the equilibrium value of this portion of the photocurrent is AL/Dn_{cd}. We let $\alpha_1 = Dn_{cd}$. We also define $\alpha_2 = Bn_{cd}$.

Assuming the light impulse is a square pulse $L \rightarrow LF(t)$, (26) and (27) become

$$\frac{d\epsilon}{dt} = AL\,F(t) + \phi\,(\alpha_2 - \alpha_1 + c) - \epsilon\,(\alpha_1 + \alpha_2) \tag{28}$$

and

$$\frac{d\phi}{dt} = \epsilon\alpha_2 - \phi\,(\alpha_2 + c) \tag{29}$$

Solving (29) for ϵ and substituting in (28),

$$\frac{d^2\phi}{dt^2} + (\alpha_1 + 2\alpha_2 + c)\frac{d\phi}{dt} + \alpha_1(2\alpha_2 + c)\phi = AL\alpha_2 F(t) \tag{30}$$

The Laplace transform method can now be applied to our equation. The transform of the right side of (30) with the pulse illustrated in Figure 55 is given by*

$$f(s) = \int_0^\infty e^{-st} F(t)dt = \int_0^\tau AL\alpha_2\, e^{-st}\, dt = \frac{AL\alpha_2}{s}\,(1-e^{-s\tau}) \tag{31}$$

We let $\phi(0) = 0 \quad \epsilon(0) = 0 \quad \therefore \quad \phi'(0) = 0$ by (27), thus

$$\mathcal{L}\frac{d^2\phi}{dt^2} = s^2 f \qquad \mathcal{L}\frac{d\phi}{dt} = sf \qquad \text{where} \quad \mathcal{L}\,\phi = f \tag{32}$$

Substituting (31) and (32) in (30),

$$f = \frac{AL\alpha_2\,(1-e^{-s\tau})}{s(s+\alpha_1)(s+2\alpha_2+c)} \tag{33}$$

By use of Doetsch[29] 1, 17, (33) can be transformed to yield the solution

$$\phi(t) = \frac{AL\alpha_2}{\alpha_1(2\alpha_2+c)(2\alpha_2+c-\alpha_1)}\left[-(2\alpha_2+c)e^{-\alpha_1 t} + \alpha_1\, e^{-(2\alpha_2+c)t} + 2\alpha_2 + c - \alpha_1\right]$$

$$\text{for} \quad t < \tau \tag{34}$$

and

$$\phi(t) = \frac{AL\alpha_2}{\alpha_1(2\alpha_2+c)(2\alpha_2+c-\alpha_1)}\left[-(2\alpha_2+c)e^{-\alpha_1 t}(1-e^{\alpha_1\tau}) + \alpha_1 e^{-(2\alpha_2+c)t} \cdot (1-e^{2\alpha_2+c)\tau})\right] \quad \text{for} \quad t > \tau \tag{35}$$

Solving (29) for ϵ and substituting (34) and (35) for $t < \tau$ and $t > \tau$ respectively, give

$$\epsilon = \frac{AL}{\alpha_1(2\alpha_2+c)(2\alpha_2+c-\alpha_1)}\left\{(2\alpha_2+c)(\alpha_1-\alpha_2-c)e^{-\alpha_1 t} - \alpha_1\alpha_2\, e^{-(2\alpha_2+c)t}\right.$$

$$\left. + (-\alpha_1+2\alpha_2+c)(\alpha_2+c)\right\} \qquad \text{for} \quad t < \tau \tag{36}$$

and

---

* Using Doetsch's[29] notation.

$$\epsilon = \frac{AL}{\alpha_1(2\alpha_2+C)(2\alpha_2+C-\alpha_1)}\left\{(2\alpha_2+C)(\alpha_1-\alpha_2-C)(1-e^{\alpha_1\tau})e^{-\alpha_1 t}\right.$$

$$\left.-\alpha_1\alpha_2(1-e^{(2\alpha_2+C)\tau})e^{-(2\alpha_2+C)t}\right\} \quad \text{for} \quad t>\tau \qquad (37)$$

From (36) or (37)

$$\epsilon(\tau) = \frac{AL}{\alpha_1(2\alpha_2+C)(2\alpha_2+C-\alpha_1)}\left\{(2\alpha_2+C)(\alpha_1-\alpha_2-C)e^{-\alpha_1\tau}\right.$$

$$\left.-\alpha_1\alpha_2 e^{-(2\alpha_2+C)\tau} + (-\alpha_1+2\alpha_2+C)(\alpha_2+C)\right\} \qquad (38)$$

For $\tau\to\infty$, $\epsilon(\tau)\to\frac{AL(\alpha_2+C)}{\alpha_1(2\alpha_2+C)}$. In like manner, from (34) or (35) for $\tau\to\infty$, $\phi(\tau)\to\frac{AL\alpha_2}{\alpha_1(2\alpha_2+C)}$ so that $(\phi+\epsilon)(\tau)\to\frac{AL}{\alpha_1}$ as is intuitively expected.

We shall now attempt to interpret these equations physically. Equation (28) shows that electrons are added to the conduction band by two processes: by the light (AL F(t)) and by the C transition, the latter proportionally to ϕ, the incremental charge in the impurity level.

Electrons are being lost from the conduction band by two processes: by the D recombination proportionally to ϵ and by the B transition proportionally to the difference $(\epsilon - \phi)$.

Examination of equation (29) shows that electrons are being lost due to the C transition proportionally to the surplus ϕ and are being gained in the B transition proportionally to the difference $(\epsilon - \phi)$. Figure 56 shows the functional dependence of each transition.

Thus what is happening is that electrons are being raised optically and B and C attempt to effect a readjustment between the impurity level and conduction band. At the same time electrons are decaying to the filled band via D. The two exponential factors in (35) or (36) reflect these two simultaneous effects.

The interdependence of ϵ and ϕ as illustrated in Figure 56 complicates the interpretation of the overall process. Let us, however, examine the readjust-

ment process by assuming D small.

Letting $\alpha_1 = 0$ and $F(t) = 0$ in equations (28) and (29) we get a decay readjustment due to B and C alone represented by

$$\frac{d\epsilon}{dt} = \phi(\alpha_2+C) - \epsilon\alpha_2$$

and

$$\frac{d\phi}{dt} = \epsilon\alpha_2 - \phi(\alpha_2+C)$$

Solving for ϵ alone we obtain

$$\frac{d^2\epsilon}{dt^2} + (2\alpha_2+C)\frac{d\epsilon}{dt} = 0.$$

This equation readily integrates giving

$$\epsilon = \text{const.}\ e^{-(2\alpha_2+C)t}$$

for the decay. Thus we see that the time constant associated with the decay of electrons from the conduction band into the impurity levels is $1/2\alpha_2+C$. This value is understandable in view of the ratio of B to C as illustrated in (24) and the functional dependence of B and C as shown in Figure 56. In this model, B operates to a limited number of available states while C is a transition to a nearly empty band. The time constant for the adjustment process contains the factor 2 because it is the reciprocal of the sum of C plus the ϵ part of

$B(n_{cd}+\epsilon)^2 \approx Bn_{cd} + 2\,Bn_{cd}\epsilon$, where the Bn_{cd} term is part of the normal dark equilibrium.

A better understanding of the meaning of the equations derived can be obtained from examination of (36) or (37). For simplicity we shall consider the decay above in two cases, the first when the thermal readjustment is fast compared with the intrinsic recombination, and the second when the thermal readjustment is slow compared to the intrinsic decay.

Let $t' = t - \tau$ in (37) and let τ approach infinity. Then t' is the time after turning off the light after equilibrium has been achieved. The expression for ϵ in this case is

$$\epsilon = \frac{AL}{\alpha_1(2\alpha_2+C)(2\alpha_2+C-\alpha_1)}\left\{\alpha_1\alpha_2 e^{-(2\alpha_2+C)t'} - (2\alpha_2+C)(\alpha_1-\alpha_2-C)e^{-\alpha_1 t'}\right\}$$

Where again, for $t' = 0$ we have the saturation value

$$\epsilon(\tau) = \epsilon_s = \frac{AL(\alpha_2+C)}{\alpha_1(2\alpha_2+C)} \ .$$

Consider now the first of the two cases:

1) $\underline{\alpha_2 \gg \alpha_1}$

$$\epsilon \approx \frac{AL\alpha_2}{(2\alpha_2+C)^2} e^{-(2\alpha_2+C)t'} + \epsilon_s e^{-\alpha_1 t'} \qquad (40)$$

Here the decay is separated into two understandable terms. The first term on the right is small in magnitude compared to the second, but rapid in time dependence. It represents the rapid readjustment with the impurity level. The second term on the right represents the slow process of intrinsic decay from the saturation value, which is the controlling effect here.

2) $\underline{\alpha_1 \gg \alpha_2}$

$$\epsilon \approx \frac{AL}{\alpha_1} e^{-\alpha_1 t'} - \frac{AL\alpha_2}{\alpha_1(2\alpha_2+C)} e^{-(2\alpha_2+C)t'} \qquad (41)$$

In this case, where the D transition is much more probable than the B transition, the first term on the right represents a fast intrinsic decay from an equilibrium value which would be obtained if no impurity level were present at all. On the other hand, the second term on the right is a slow emptying of the impurity level into the conduction band starting initially with the saturation value of ϕ (the coefficient of the exponential in the second term). In other words, in this case the conduction band is emptying rapidly by the intrinsic recombination of conduction electrons with filled-band holes while the impurity level is slowly releasing electrons into the conduction band.

Figure 55 shows the general shape of the response to be expected on this model with a light input as shown at the top of the figure. The dotted section of the curve indicates a case in which the light pulse was long enough to allow the rise to saturate. The initial slopes of the rise and decay for small times after

the shuttering are shown. It is to be noted that if saturation is achieved, the decay slope is the negative of the rise slope.* The value of ϵ_s is also indicated. If saturation be achieved, experimentally, it should be possible to determine the parameters of the model by fitting the slopes and saturation values of the experimental curves.

The conclusions that can be drawn on the effect of adding an impurity level of the type described are summarized as follows:

1) The effect of the additional levels is to reduce the equilibrium response by a factor $\frac{\alpha_2+C}{2\alpha_2+C}$, which ranges between $\frac{1}{2}$ and 1.

2) As was shown in equations (40) and (41), the decay always consists of a relatively fast exponential superimposed on a slower decay is either the controlling part of the process or adds a "tail" to the decay. Thus the observed decay constant may be longer than the intrinsic decay constant unless pains are taken to resolve the two processes.

The above conclusions are in agreement with Rose's statements cited in the previous section, where the decrease in sensitivity is at most $\frac{1}{2}$ in this model. The third effect mentioned by Rose does not apply here, since we have assumed an incremental process in a large dark-current material so that linearity of response with incident light intensity must result.

As mentioned previously the calculation can be applied to other cases, for example, the substitution of recombination according to E rather than D as shown in Figure 34. In this case one obtains the same type of equations involving

---

* The decay slope for a pulse of arbitrary length τ is more complicated, viz.

$$\frac{d\epsilon}{dt} = \frac{AL}{-\alpha_1+2\alpha_2+C}\left\{(-\alpha_1-\alpha_2+C)(1-\alpha_1 t')e^{-\alpha_1\tau+\alpha_2\tau}e^{-(2\alpha_2+C)\tau}\right.$$

$$\left.(1-(2\alpha_2+C)t')+(-\alpha_1+2\alpha_2+C)(\alpha_1+\alpha_2)t' - (-\alpha_1+2\alpha_2+C)\right\}.$$

time constants $(En_{td})^{-1}$ and $(2Bn_{cd}+C)^{-1}$ for the recombination and readjustment processes, respectively.* There is no general agreement as yet as to whether transition E or D is physically more realizable.

---

* In this case one obtains

$$\frac{dn_c}{dt} = AL - Bn_c(N-n_t) + Cn_t$$

and

$$\frac{dn_t}{dt} = Bn_c(N-n_t) - Cn_t - En_t n_h,$$

from which

$$\frac{d\epsilon}{dt} = AL\,F(t) - Bn_{cd}\epsilon + (Bn_{cd}+C)\,\phi \quad \text{and}$$

$$\frac{d\phi}{dt} = \epsilon\,(Bn_{cd} - En_{td}) - \phi(Bn_{cd} + C + En_{td}),$$

replacing (26) and (27) respectively. The remaining equations then take a somewhat different form, i.e., the intrinsic term now appears in the ϕ rather than the equation, but the method of solution remains the same.

VIII. Interpretation of the Photoconduction in Zinc-Oxide

The calculation of photoconduction in the previous section yields only processes of monomolecular forms, i.e., exponential rises and decays, because of the incremental nature of the solution. Unfortunately, the effect of largest magnitude in zinc-oxide is the slow bimolecular rise and decay illustrated in Figures 10 and 14. To explain this process we have to resort to a method of interpretation which is somewhat intuitive since the exact equations involved cannot be solved analytically.*

The model to be discussed is shown in Figure 57a. The similarity to the case of Figure 54 is evident except that the states in the forbidden region are now not donors but traps, i.e., normally uncharged sites which can accept an electron. Transition E is preferred here. In a manner analogous to that of the previous section we can then write for the time rate of change of conduction electrons,

$$\frac{dn_1}{dt} = AL - B'n_1(N-n_2) + Cn_2 \qquad (42)$$

and for the trap level,

$$\frac{dn_2}{dt} = B'n_1(N-n_2) - Cn_2 - En_2(n_1+n_2) \qquad (43)$$

Since $N >> n_2$ we can write

$$\frac{dn_1}{dt} = AL - Bn_1 + Cn_2 \qquad (44)$$

and

$$\frac{dn_2}{dt} = Bn_1 - Cn_2 - En_2(n_1+n_2) \qquad (45)$$

for the conduction and trap levels respectively, where $B = B'N$.

Equation (45) is quadratic in the E term which makes simple linear analysis impossible. We thus work with linear combinations of (44) and (45) which are easier to understand.

The sum $n_1 + n_2$ represents the total number of excited electrons (or

* This part of the theory was developed in conjunction with Mr. Donald A. Melnick of this laboratory.

holes) at any instant. From (44) and (45),

$$\frac{d(n_1+n_2)}{dt} = AL - En_2(n_1+n_2) \tag{46}$$

Now transitions B and C effect a quasi-equilibrium between the conduction band and the trap level. Assuming the recombination probability of E to be small, by (45) a quasi-equilibrium is obtained for

$$n_1 = \frac{C}{B} n_2 \tag{47}$$

for any (n_1+n_2) at any moment. $n_1 - \frac{C}{B} n_2$ then is a parameter measuring the departure from quasi-equilibrium at any moment.

From (44) and (45)

$$\frac{d}{dt}\left(n_1 - \frac{C}{B} n_2\right) = AL - (B+C)\left(n_1 - \frac{C}{B} n_2\right) + \frac{C}{B} En_2(n_1+n_2) \tag{48}$$

Since the term $\frac{C}{B} En_2 (n_1+n_2)$ has $\frac{C}{B}$ which will presently be seen to be somewhat smaller than one and since $En_2(n_1+n_2)$ varies between zero and AL in what we will see is a long period, this term is slowly varying compared to the other terms, hence we assume the E term of (48) to be relatively constant. The equation then is of the form,

$$\frac{dx}{dt} = \left[AL + \frac{C}{B} En_2 (n_1+n_2)\right] - (B+C)\, x \tag{49}$$

where $x = n_1 - \frac{C}{B} n_2$

The solution of (49) is

$$x = \text{const.} \cdot e^{-(B+C)t} + \frac{1}{B+C}\left[AL + \frac{C}{B} En_2(n_1+n_2)\right]$$

or since equilibrium must obtain at t = 0, i.e., before the light is turned on, $x(0) = 0$, implying

$$x = \frac{1}{B+C}\left[AL + \frac{C}{B} En_2(n_1+n_2)\right](1-e^{-(B+C)t}) \tag{50}$$

Thus for t approaching infinity the deviation from true equilibrium with light on approaches a constant.

Now, as discussed in Section III, the two slowest processes are a bi-molecular process of time constant about 50 minutes and a monomolecular process of

time constant about 5 minutes. We assume the 5 minute monomolecular process is the one associated with the readjustment process, i.e. we assume $\frac{1}{B+C}$ is of the order of 5 minutes. Then the fact that the longer time constant is of the order of ten times the shorter provides a justification for the assumption made earlier that the E term is slowly varying. We now assume the exponential is negligible in (50) after 5 minutes, i.e., quasi-equilibrium is rapidly attained.

Solving (50) for n_1,

$$n_1 = \frac{AL}{B+C} + \frac{C}{B} n_2 \tag{51}$$

where we neglect the E term in comparison to AL. (46) is now solved for n_2 with the aid of approximation (51):

$$\left(1+\frac{C}{B}\right) \frac{dn_2}{dt} = AL - En_2 \left(\frac{AL}{B+C} + \left(1 + \frac{C}{B}\right) n_2 \right) \tag{52}$$

Integration of (52) yields

$$n_2 = \sqrt{\frac{B^2A^2L^2}{4(B+C)^4} + \frac{BAL}{E(B+C)}} \tanh \left(\sqrt{\frac{B^2 A^2 L^2 E^2}{4(B+C)^4} + \frac{BALE}{B+C}} \; t + \text{const.} \right) - \frac{BAL}{2(B+C)^2} \tag{53}$$

where the constant is determined by $(n_1+n_2)(0) = 0$.

Examining the slow part of the process we have roughly the form

$$\frac{dn}{dt} = AL - En^2$$

which yields a saturation value $n_s = \sqrt{\frac{AL}{E}}$ and a decay $n = \frac{1}{Et + \text{const.}}$

But for decay $n(0) = n_s$, therefore $n = 1/ E\left(t + \sqrt{\frac{1}{ALE}}\right)$; thus, the half life of the process is $1/\sqrt{ALE}$ roughly. From our experimental results this is of the order of 10 times $\frac{1}{B+C}$. Thus in the square roots in (53) we can neglect the terms involving the squares, and

$$n_2 = \sqrt{\frac{BAL}{E(B+C)}} \tanh \left(\sqrt{\frac{BALE}{B+C}} \; t + \text{const.} \right) - \frac{BAL}{2(B+C)^2} \tag{54}$$

Equation (54) yields a half-life for the slow process of $\sqrt{\frac{1}{ALE}(1+\frac{C}{B})}$. This checks with the rough determination of the half-life as $\sqrt{\frac{1}{ALE}}$ above.

n_1 is now determined by the substitution of (54) in (50), where again the E-term is neglected in (50) as a small correction:

$$n_1 = \frac{AL}{B+C}(1-e^{-(B+C)t}) + \frac{C}{B}\sqrt{\frac{BAL}{E(B+C)}}\tanh\left(\sqrt{\frac{BALE}{B+C}}\,t + \text{const.}\right)$$

$$- \frac{CAL}{2(B+C)^2}$$

$$\frac{AL(2B+C)}{2(B+C)^2} - \frac{AL}{B+C}e^{-(B+C)t} + \frac{C}{B}\sqrt{\frac{BAL}{E(B+C)}}\tanh\left(\sqrt{\frac{BALE}{B+C}}\,t + \text{const.}\right) \quad (55)$$

Equation (55) determines n_1 which is proportional to the conductivity. The constant as evaluated makes $(n_1+n_2)(0)$ equal to zero. We see that two effects are observed according to (55): an exponential process and a bimolecular process, the time constants being $\frac{1}{B+C}$ and $\sqrt{\frac{1+C/B}{ALE}}$ respectively.

As mentioned before, $\frac{1}{B+C}$ and $\sqrt{\frac{1+C/B}{ALE}}$ were set equal to 4.6 minutes and 38 minutes. From the decay of Figure 14, $\frac{C}{B}$ was determined to be 0.4, which is in accord with the assumption that $\frac{C}{B} < 1$ made earlier. Computation of the parameters from the decay curve of Figure 14 then allowed prediction of the rise curve to within 1%, which is better than the experimental accuracy.

Figures 61 and 62 shows that the time constant for the bimolecular process is dependent on the square root of the light intensity. In Figure 61 two curves of the rise are shown, one for an incident light intensity 3.64 times that of the other. Since these curves, beyond 25 minutes at least, should be tanh in form, the time constants involved can be determined from the relation $\tanh kt \approx 1 - 2e^{-2kt}$ for large values of t. Thus asymptotic values have been chosen and the difference between the actual curve and the asymptotic value in each case has been plotted in Figure 62. Thus we see that the bimolecular time constants are 160 and 320 minutes which are in agreement with the fact that the ratio should be $\sqrt{3.64}=1.9$.

The amplitudes, however, although differing in the right direction, are not in the ratio of 2 to 1. It is thought that it is not the concentration n_1 that is at fault, because of the good agreement of the rest of the theory, but that the observed conductivity may be too low because of a functional dependence of the mobility on the conduction band electron concentration such as might be caused by space-charge formation or a concentration-dependent potential barrier.

The liquid-air temperature experiments illustrated in Figures 4 and 8 are also explained by this model. Transition C depends exponentially on temperature whereas B varies as $\sqrt{T}$. Thus at room temperature we have $\frac{1}{B+C} = \frac{1}{1.4B}$, but at liquid air temperature we have $\frac{1}{\frac{1}{2}B}$ since C is negligible at this low temperature. Thus a factor of about 3 in the time constant appears, and this is in agreement with the experiment as is shown in Figure 4.

It should also be mentioned here that the model shown in Figure 57a in which the impurity level consists of traps can be altered without changing the calculation to the model shown in Figure 57b.

Here a set of acceptors lying immediately above the filled band maintains electrical neutrality when a set of donors is substituted for the originally neutral traps. At normal and low temperatures the donor electrons will fill the acceptors, leaving the donors nearly empty, as is desired. Holes produced by optical excitation via A can then be captured by the acceptors, thus making physically understandable the reason why E is such a slow process, and also is the reason for negligible hole mobility. The overlap of acceptors and filled band then explains the peak of photoconductivity at the absorption edge and the "tailing-off" into the visible in accordance with Fassbender's[23] theory as mentioned earlier. The additional exponential processes described in Sections III and V can then be explained in pairs by adding a suitable trap level in the forbidden region for each pair of observed processes, properly picked. The situation is complicated by the apparent presence of barrier layers or surface states as will be discussed in the next section.

IX. Quantum Efficiency

Since no definite conclusions can be drawn from the experiments performed to date pertinent to this topic, only a brief outline will be presented here.

Two definitions for the quantum efficiency of a photoconductive process exist.[32] The first defines the quantum efficiency as the number of charge carriers produced per incident photon of light. The second definition defines the quantum efficiency as a response or sensitivity factor, viz., the total charge measured in the external circuit due to the incidence of one quantum. For several reasons we shall prefer the first definition: measurements on the basis of the second definition are best performed with sufficiently high field strength to collect all the liberated charge carriers at the electrodes if replenishment at the electrodes does not occur. If replenishment of charge does occur at the electrodes then the charged measured is proportional to the voltage applied and the quantum efficiency thus determined is of more technical than physical interest.

Secondly, the presence of dark current obscures the significance of a quantum efficiency based on charge passing in an external circuit. Third, unless high energy quanta (e.g., x-rays) which produce secondary ionization are being used, there is reason to expect a unit quantum efficiency on the basis of the first definition in most true resonant processes.

Let us then define the quantum efficiency χ as the number of free charge carriers produced per incident photon. In the case of immobile holes, this is equivalent to the number of conduction electrons produced per incident photon.

In a sample of zero dark current in equilibrium with light we must have

$$Q\chi = \frac{n}{T} \tag{56}$$

where Q = number of photons absorbed/unit area-sec

χ = number of conduction electrons/incident photon

n = concentration of conduction electrons

T = lifetime of a conduction electron (sec.)

If a dark concentration of conduction N, electrons exist we have

$$Q\chi = \frac{N + n}{T} \tag{57}$$

Now Mott and Gurney[30] show that

$$T = \frac{1}{N_h \sigma_c u} \tag{58}$$

where N_h is the number of available electron states having a capture cross-section σ_c. u is the thermal velocity of the conduction electrons. Then by (57) and (58)

$$\chi = \frac{N+n}{Q\,T} = \frac{(N+n)N_h\,\sigma_c u}{Q} \tag{59}$$

(N+n) is determined from the observed response assuming a value of the mobility derived from Hall measurements. σ_c is a capture cross-section determined to be of the order of 10^{-14} to 10^{-15} cm^2 for F centers[30], and $u = \sqrt{\frac{3kT}{m}}$. N_h is determined in terms of N and n by the particular model assumed, whether it be the simple model of Figure 50 in which N = 0, $N_h = n$ or the model Figure 54 in which $N = n_{cd}$, $N_h = \gamma$. Computations based on such a calculation always yielded χ of the order of 10^4 electrons/photon in zinc-oxide at the absorption edge. Thus either the computation was not correct, or the process is one in which multiplication can occur, such as the lowering of a barrier by an initial process.

A calculation was then done assuming Hahn's[5] model of cubes of highly conducting material (A) surrounded by a layer (B) of poorly conducting material. The model is shown in Figure 58. Since $\sigma_o << \sigma$ we have n_B upper traps thermally emptied in region B and n_A, in region A, where $n_A >> n_B$.

In the illuminated crystal N_A and N_B lower traps are excited optically to give $N_A + n_A$ and $N_B + n_B$ electrons in equilibrium in the respective conduction bands.

Now since $n_A >> n_B$ we expect that the excited lower states $N_B > N_a$ since electrons dropping from the conduction band are much more likely to fill

upper traps rather than lower traps in this region. We further assume $N_A < n_A$ and $N_B < n_B$, i.e., large dark current. Using this model it can be shown that $\chi = (\frac{b}{a})^2 \chi'$ where χ' is the quantum efficiency measured, χ is the actual quantum efficiency and $\frac{b}{a}$ is the ratio of barrier layer to cube dimensions.

As described in a paper on this topic,[31] measurements of $\frac{b}{a}$ by the method described by Hahn[5] indicate $\frac{b}{a}$ cannot be less than 10^{-2}. This reduces the quantum efficiency to the order of 1 to 10 in the fundamental region.

The value of σ_c used in the computation is open to doubt, the Mott and Gurney[30] value of $\sigma_c = 10^{-15}$ cm^2 being the one used. Rose[20] shows for two cases that γ / σ_c is approximately 10^{26} where $\gamma \doteq 10^8$ sec^{-1}.[33*] A more general argument for donors may be given as follows. Let N_p donors (or a slice of the filled band) be b_o in depth. Let the Fermi level be b in depth. Detailed balance in equilibrium yields

$$n_c N_p (1 - e^{-b/T}) u \sigma_c = N_p \gamma e^{-b_o/T}$$

where n_c = conduction band concentration of electrons having thermal velocity u. But it is well known that the product of hole and electron concentrations is

$$n_c N_p (1 - e^{-b/T}) = N_c N_p e^{-b_o/T}$$

where N_c = concentration of states in bottom slice, a few kT wide, of the conduction band $\doteq 10^{19} (\frac{T}{300})^{3/2}$ cm^{-3}. Thus $\gamma / \sigma_c = N_c u = 10^{26}$, yielding σ_c of the order of 10^{-18} cm^2.

Now a reduction of σ_c as assumed by a factor of 10 or 100 would bring the calculated quantum efficiency into the right order of magnitude, i.e., between 0.1 and unity. σ_c would then be 10^{-16} to 10^{-17} cm^2 which is a little smaller than is expected on the basis of atomic dimensions for the former value and is one or two orders of magnitude larger than predicted above. Rose[20] points out that values from 10^{-14} cm^2 to 10^{-22} cm^2 have been observed in other materials. It is suggested by him that small capture cross-section might be explained by shielding of the

---

* This is an experimental, not a theoretical value. See the reference cited.

capturing center by a potential barrier.

Although this is not explicitly indicated by the order of magnitude of the capture cross-section here it has been mentioned that the Hall effect exhibits no change with illumination, and this suggests that the photoconductivity is a surface effect which is not concerned with the bulk of the material.

In the previous section it was shown that $\frac{1}{B+C} \doteq 276$ seconds and $\frac{C}{B} = 0.4$. Thus $C = 1.04 \times 10^{-3}$ sec^{-1}.

Since the probability of escape from a trap as derived from thermoluminescence measurements[33] is

$$P = \nu e^{-\mathcal{E}/kT} \text{ sec}^{-1}$$

where $\nu = 10^{8\pm1}$ sec^{-1} and $\mathcal{E}$ is the trap depth, this indicates that the depth of the impurities in zinc-oxide should be between 0.57 and 0.69 ev. below the conduction band. Such a level has not been detected by Hall measurements to date.[5,24] Thermoluminoscence measurements now in progress[34] indicate the existence of a 0.3 volt deep level. On the other hand, a level at 0.04 ev. below the conduction band, which is detected by bulk measurements[4], would yield a transition probability of $10^{7\pm1}$ sec^{-1} at room temperature, which is considerably larger than the determined value of c.

The existence of states shielded by a surface potential as shown in Figure 59 would allow for the existence of a 0.7 volt deep level which would not be detected by bulk measurements such as the Hall measurements, since these levels would be on the surface of the neck between microcrystals in the material as shown in this figure. The 0.04 ev. levels however, are thought to exist in the bulk of the material. The conductivity measurements of Hahn[5] and Miller[4] indicate the presence of 0.7 ev. states if the slope gives the activation energy directly.*

The existence of 0.7 volt deep levels allows a possible explanation of the 5100 Å luminescent transition as the E transition mentioned previously, as shown in Figure 60. Since photoconductivity concerns itself with measurement of

* A technical report being prepared by Mr. S. Harrison of this laboratory will

electron concentration, while the luminescence depends on $\frac{dn}{dt}$ from the 0.7 volt states, the fact that fast decays have been measured is not inconsistent with the photoconductive measurements; it is entirely probable that a long time phosphorescence of low intensity exists. Attributing this transition to states on the surfaces is not necessarily in disagreement with the fact that the transition is observed in the impure single crystals previously described. Microscopic observations and a hysteresis effect in the conductivity determined as a function of temperature indicate the existence of flaws which might be the sites of these states in the single crystals.

X. Summary

It has been demonstrated that at least three processes occur simultaneously in the photoconduction of zinc-oxide. A slow bimolecular process with a decay constant of 50 minutes, a monomolecular process of 5 minute constant, and a monomolecular process of 0.3 seconds constant are observed. The existence of other processes of the order of a minute and of milliseconds is also suspected. The response with modulated light and with single pulses has been shown to reach a maximum at the fundamental absorption edge. The photoconduction in single crystals and at liquid air temperatures has also been examined.

The theory of photoconductivity has been briefly developed and two models have been constructed, one of which explains the coexistence of a monomolecular and bimolecular process in terms of transitions to an impurity level situated in the forbidden energy gap in the energy band picture of the material. Agreement with experiment is shown to be good. The additional monomolecular processes may be explained in pairs according to the results of an incremental method of calculation which was developed.

The peaking of the photoconductive response at the absorption edge and the low probability of the main recombination transition are thought to be caused by the presence of acceptors which act as hole traps. Determinations of the quantum efficiency, along with the cited lack of effect of light on the magnitude of the Hall coefficient, seem to indicate the presence of barriers layers and/or surface states in the sintered material. The presence of a level 0.7 ev. below the conduction band suggests a mechanism for the long wavelength fluorescence. The depth of this level agrees with measurements performed by Miller and Hahn.

Acknowledgements

The author expresses his appreciation to Prof. P. H. Miller, Jr., who supervised this investigation, for his constant encouragement and helpful advice; to Mr. Donald Melnick for his aid in formulating the monomolecular-bimolecular theory presented; to Prof. B. R. Russell and the author's fellow workers for discussion of many topics during the course of the investigation.

Many thanks are also due to Mr. Paul Miller for a critical reading of the final manuscript and to Mr. Herman Mohr for his excellent work in constructing much of the necessary apparatus.

Bibliography

1. Hahn, E. E. Technical Report No. 17 (October 31, 1949) Nobsr-42487 p.7 ff. cites previous work supporting this assumption.

2. Mollwo, E. and F. Stockmann, Ann. Phys. 3, 223, 240 (1948).

   Mollwo, E. Ann. Phys. 3, 230 (1948)

3. Stockmann, F. Zeits. f. Phys. 127, 563 (1950)

4. Miller, P. H., Phys. Rev. 60, 890 (1941)

5. Hahn, E. E., Jour. App. Phys. 22, 855 (1951)
   This is a revision and condensation of the technical report[1] above.

6. Leverenz, H. W. Luminescence of Solids, Wiley, New York (1950), Page 218

7. Bi-Monthly Progress Report, Bureau of Ships Contract Nobsr 42487, University of Pennsylvania, P. 12 b (June 1, 1950)

8. Mollwo, E. Reichsber. d. Phys. 1, 1 (1944)

9. Leverenz, Op. cit. p.74, 218

10. Leverenz, Op. cit. pp. 72, 74, 218

11. Progress Report #4, Contract N6onr-24914, University of Pennsylvania p.3 ff. (June 30, 1951)

12. Seitz, F. The Modern Theory of Solids, McGraw Hill, New York (1940) p. 448

13. Leverenz, Op. cit. p.201, 218

14. Leverenz, Op. cit. p. 385

15. See, for example, the review article by Nix, F. C. Rev. Mod. Phys. 4, 742 (1932) or

    Mott, N.F. and R. W. Gurney, Electronic Processes in Ionic Crystals, Oxford University Press, London (1948) Chapter IV

16. See, for example, the description of the mechanism of photoconductivity by Frerichs, R. and J. E. Jacobs, G.E. Review (Aug. 1951)

17. B. Gudden and R. W. Pohl, Zeits. Phys. 16, 42 (1923)

18. de Boer, J. H. and E.J.W. Verwey, Proc. Phys. Soc. 49, Extra part 59, (1937)

19. Mott, N.F. and R.W. Gurney, Op. Cit. pp. 117 ff., 185

20. Rose, A. R.C.A. Review XII, 362 (1951)

21. Chasmar, R. P. and A. F. Gibson, Proc. Phys. Soc. (B) 64, 595 (1951)
Gibson, A. F., Proc. Phys. Soc. (B) 64, 603 (1951)

22. Lashkarev, V. E., Jour. Exp. and Theor. Phys. 19, 876 (1949) (In Russian)

23. Fassbender, J. Ann. Phys. Lpz. 5, 33 (1949)
Fassbender, J. and H. Lehmann, Ann. Phys. Lpz. 6, 215 (1949)

24. Russell, B. R. Private communication to the author.

25. Broser, I. and R. Warminsky, Ann. Phys. Lpz. 7, 289 (1950)

26. Gildart, L. and A. W. Ewald, Phys. Rev. 83, 359 (1951)

27. Pipes, L. H., Applied Mathematics for Engineers and Physicists, p.577 McGraw Hill, New York (1946)

28. Warschauer, D., Technical Report #1, Contract N6onr-24914, University of Pennsylvania (August 7, 1951)

29. Doetsch, G. Tabellen zur Laplace-Transformation und Anleitung zum Gebrauch, Springer, Berlin (1947)

30. Mott, N. F. and R. W. Gurney, Op. cit. p. 131

31. Miller, P.H., D. M. Warschauer, and T.T. Reboul, Phys. Rev. 82, 330 (1951)

32. Smith, R. W. R.C.A. Review XII, 350 (1951) uses the second definition.

33. Fonda, G. R. and F. Seitz, Preparation and Characteristics of Solid Luminescent Materials, Wiley, New York (1948) p. 90 ff.

Garlick, G.F.J., Luminescent Materials, Oxford Press, London (1949) p.29 ff.

34. Reboul, T.T., University of Pennsylvania, Phila. Penna.

35. Seitz, F. Op. Cit. in reference[12] Chapter 3

Also, Seitz, F. "Imperfections in Almost Perfect Crystals: A Synthesis" Department of Physics, University of Illinois, Urbana, Ill. Oct. 1950. A discussion of phonons is given on p.14 ff.

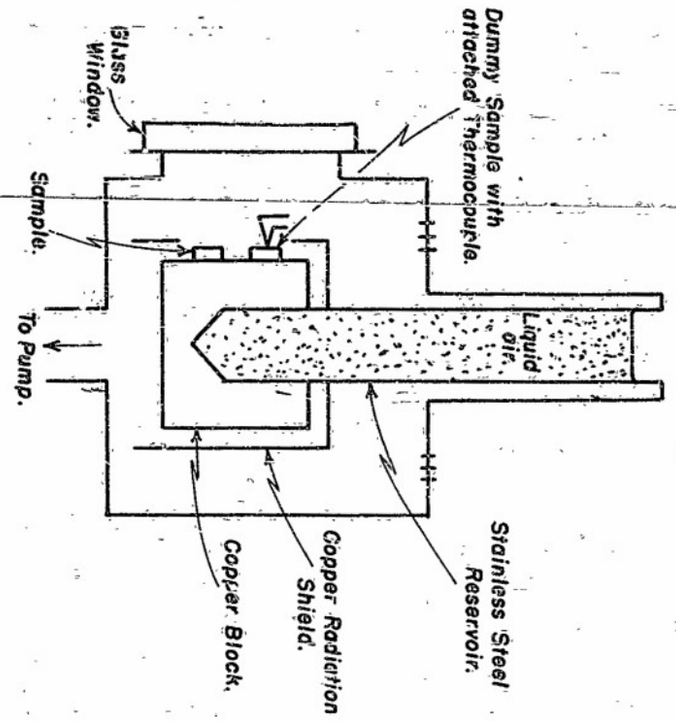

Fig. 2

Apparatus for Low Temperature Measurements.

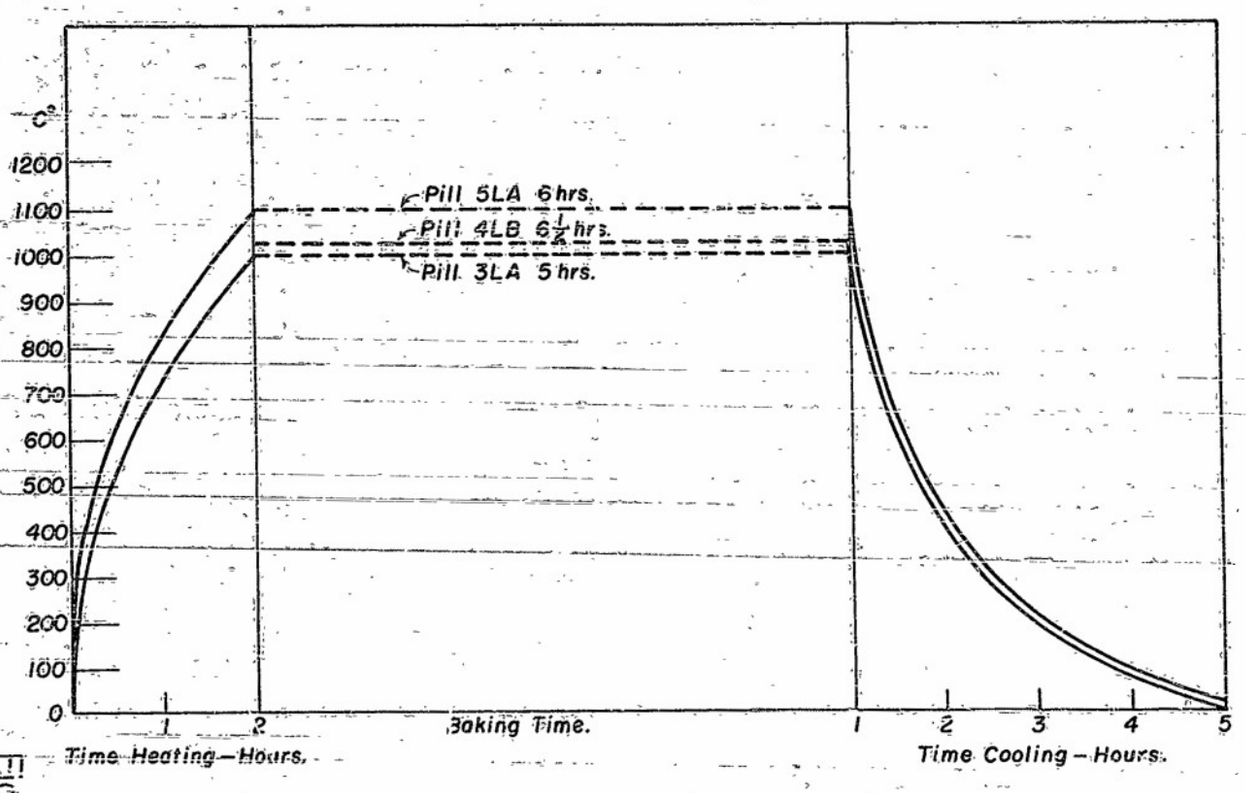

Fig. 1

Typical Baking Cycles for Sintered Samples.

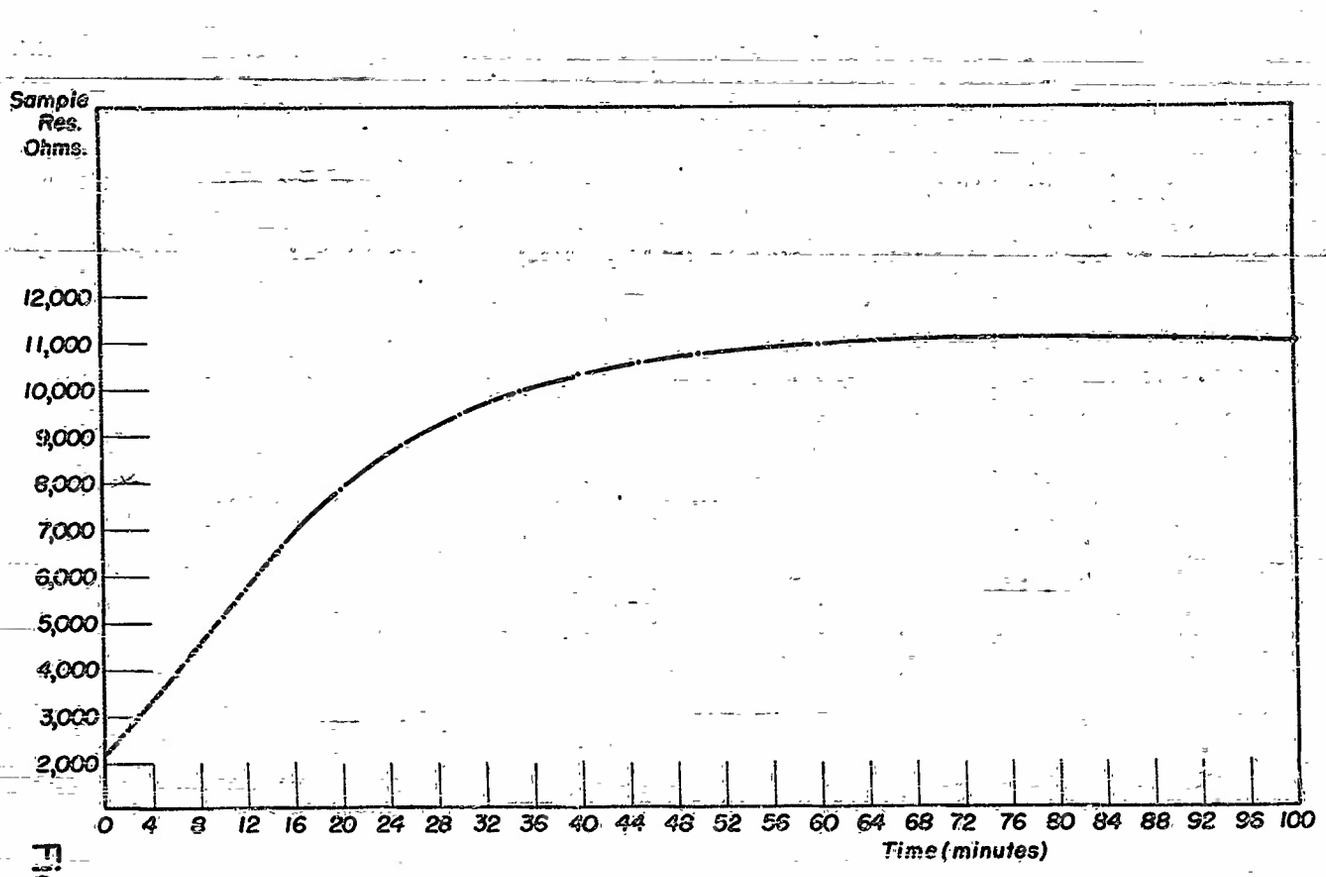

Fig. 4

Sample Resistance vs Time After Cooling to Liquid Air Temperature.

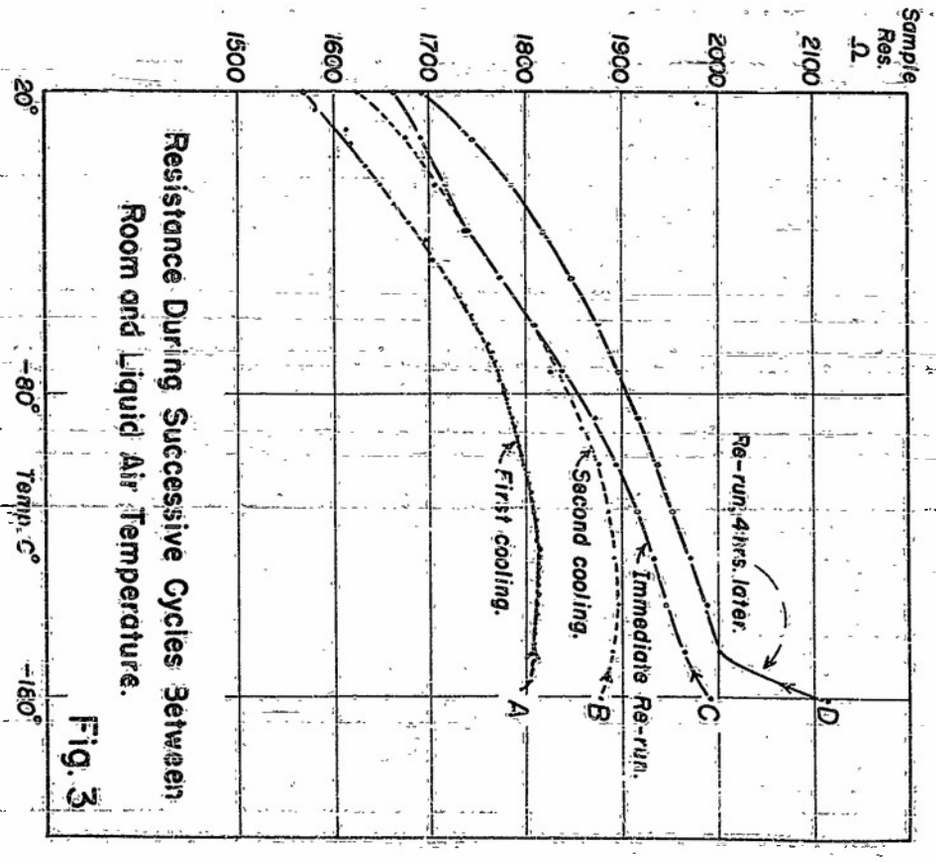

Resistance During Successive Cycles Between Room and Liquid Air Temperature.

Fig. 3

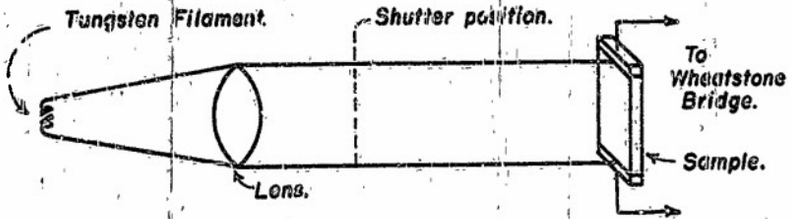

Measurement Arrangement.

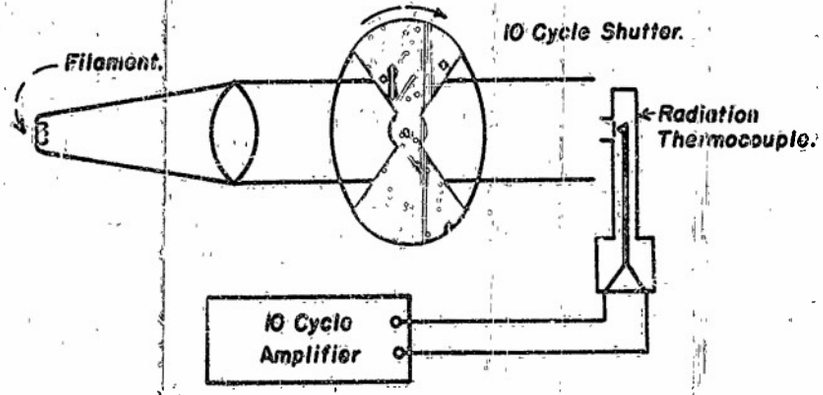

Calibration Arrangement.

Single Pulse Apparatus.

Fig. 6

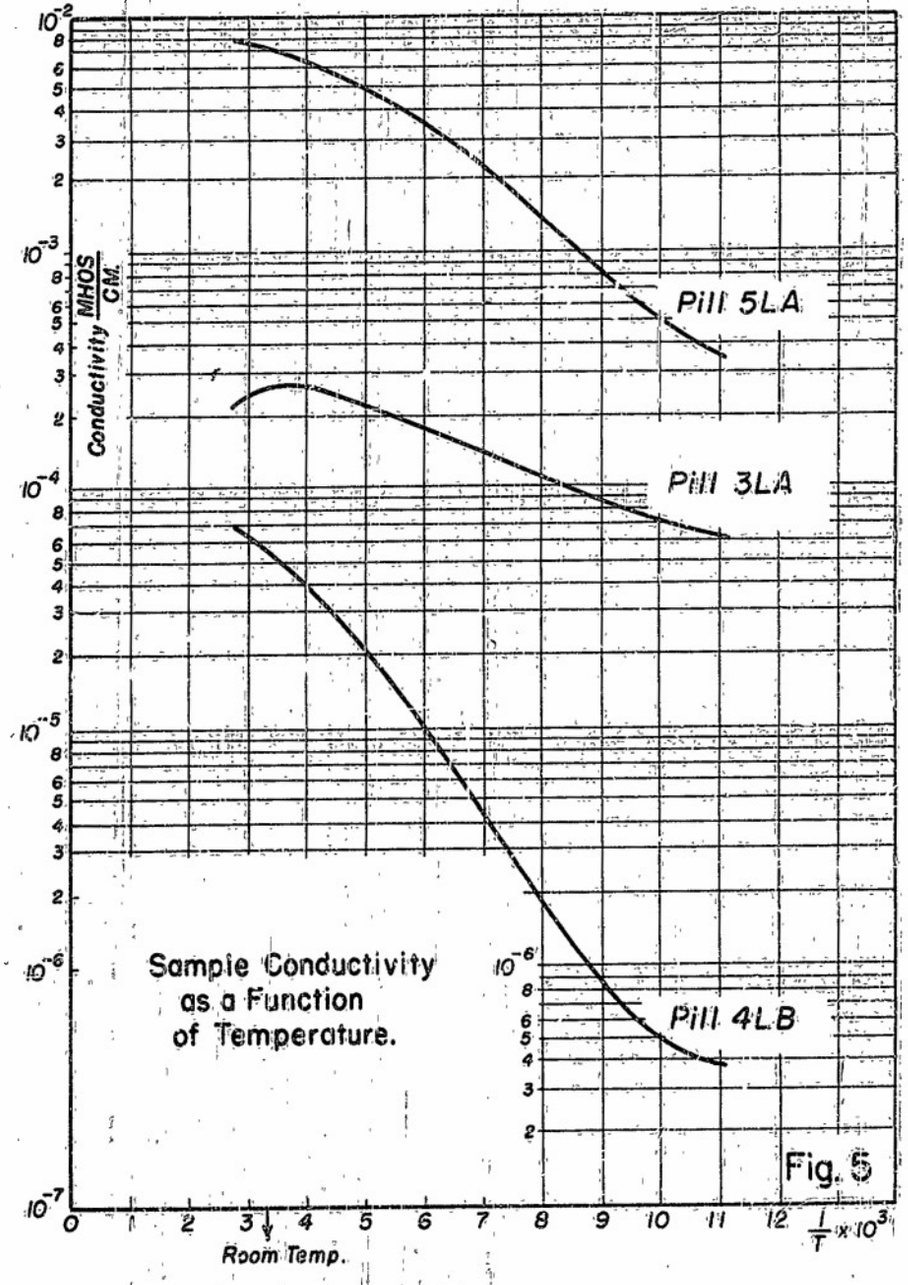

Fig. 5

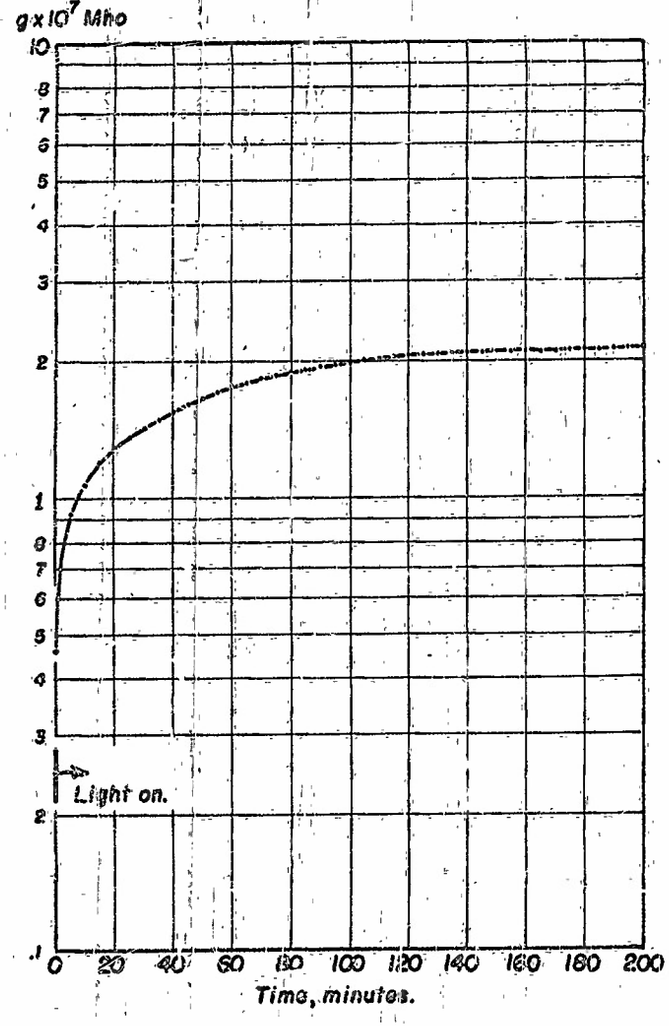

Time-Conductance of Zinc Oxide Pill 1A

Liquid Air Temp. White Light Illumination.

Fig. 8

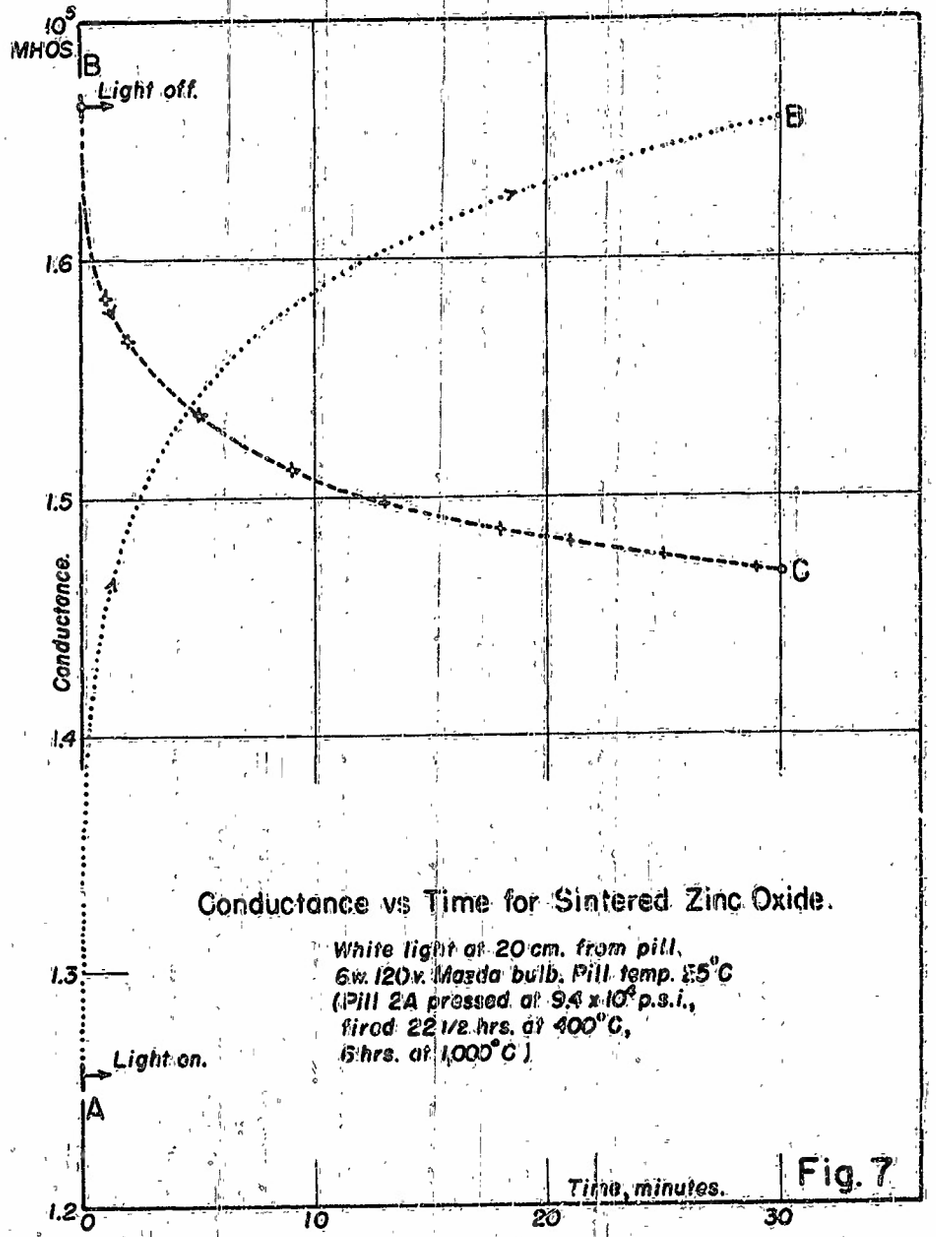

Conductance vs Time for Sintered Zinc Oxide.

White light at 20 cm. from pill.
6 w. 120 v. Mazda bulb. Pill temp. 35°C
(Pill 2A pressed at 9.4 x 10⁸ p.s.i.,
fired 2 2 1/2 hrs. at 400°C,
6 hrs. at 1,000°C.)

Fig. 7

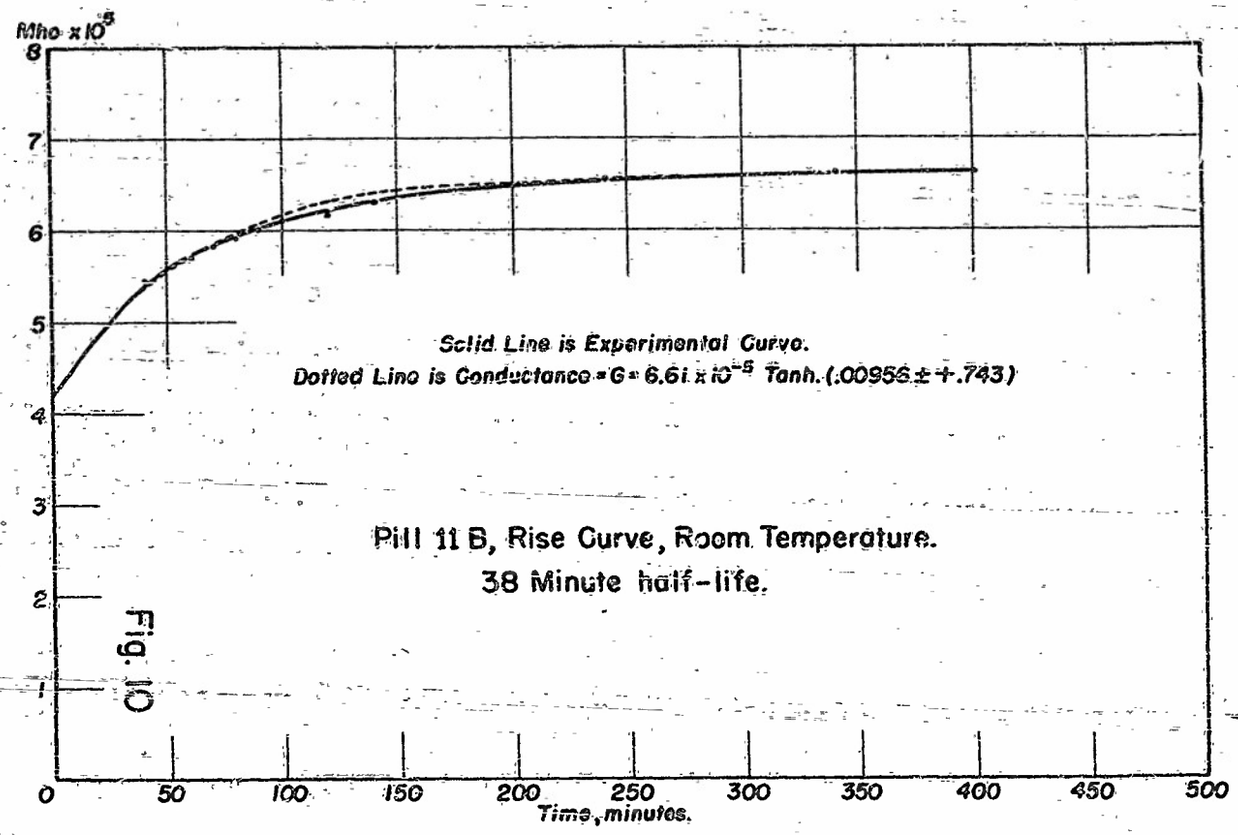
Mho x 10^-5
8
7
6
5
4
3
2
1
0
50
100
150
200
250
300
350
400
450
500
Time, minutes.
Solid Line is Experimental Curve.
Dotted Line is Conductance = G = 6.61 x 10^-5 Tanh. (.00956 ± .743)
Pill 11 B, Rise Curve, Room Temperature.
38 Minute half-life.

Fig. 10

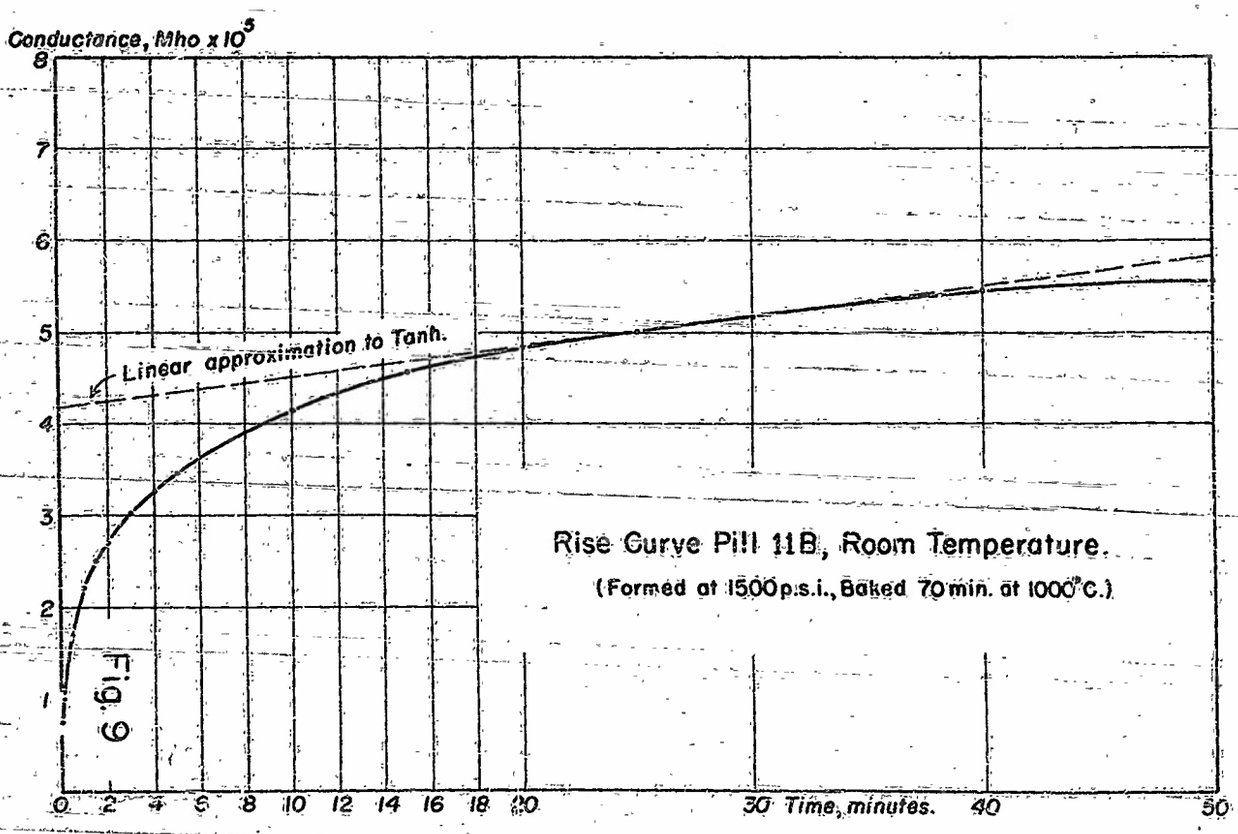
Conductance, Mho x 10^-5
8
7
6
5
4
3
2
1
Linear approximation to Tanh.
0
2
4
6
8
10
12
14
16
18
20
30
Time, minutes.
40
50
Rise Curve Pill 11B, Room Temperature.
(Formed at 1500 p.s.i., Baked 70 min. at 1000°C.)

Fig. 9

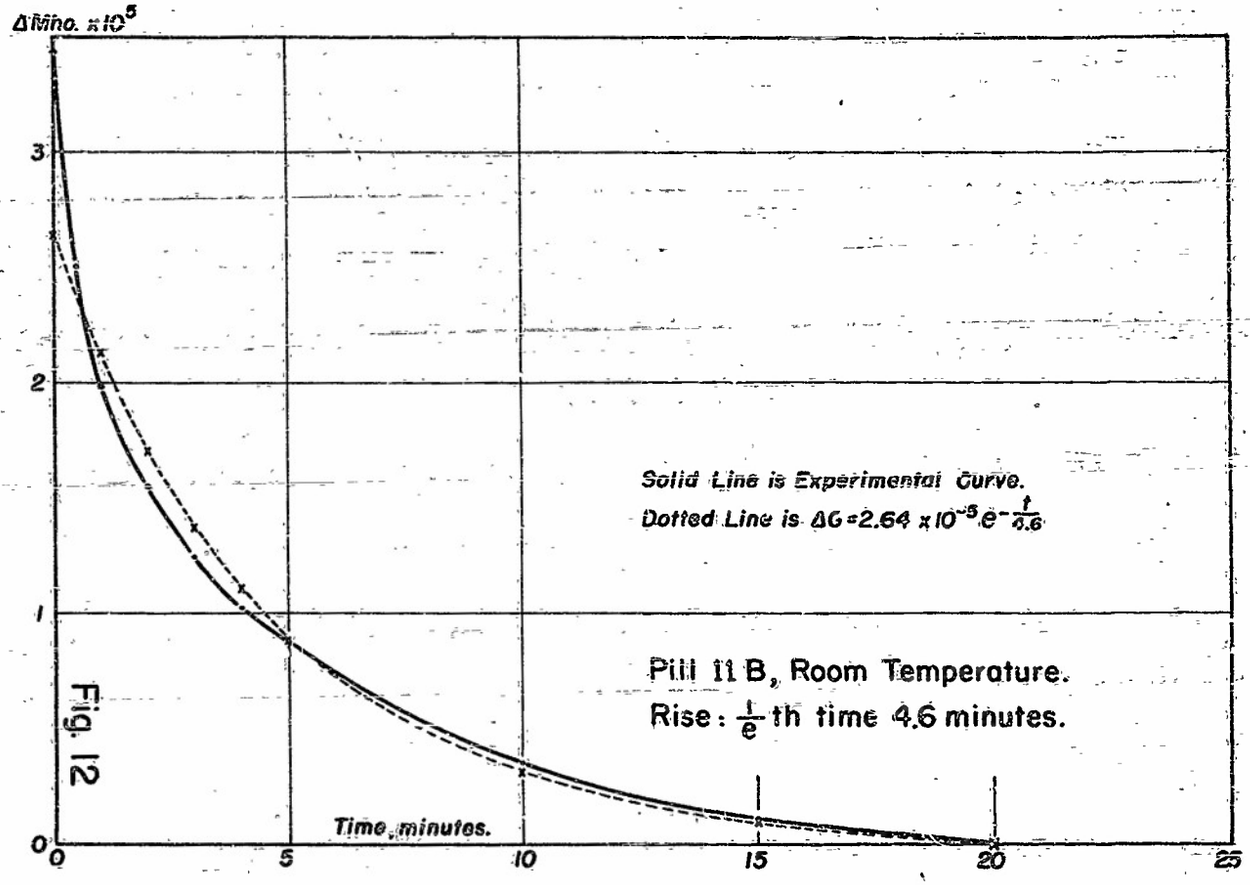
ΔMho. x10^5
3
2
1
0
0
5
10
15
20
25
Time, minutes.
Solid Line is Experimental Curve.
Dotted Line is ΔG=2.64 x10^-5 e^-t/5.6
Pill 11 B, Room Temperature.
Rise: 1/e th time 4.6 minutes.

Fig. 12

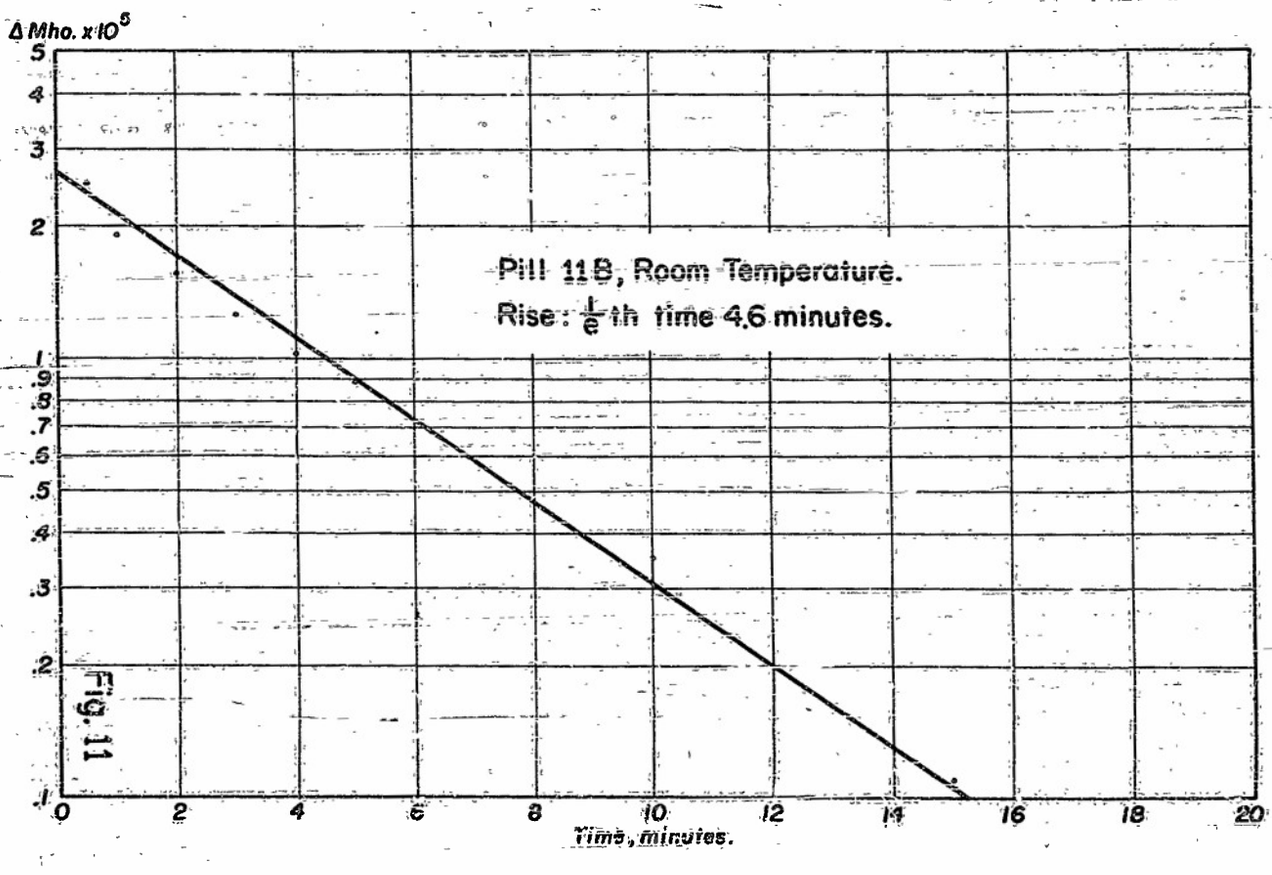
ΔMho. x10^5
5
4
3
2
1
.9
.8
.7
.6
.5
.4
.3
.2
.1
0
2
4
6
8
10
12
14
16
18
20
Time, minutes.
Pill 11B, Room Temperature.
Rise: 1/e th time 4.6 minutes.

Fig. 11

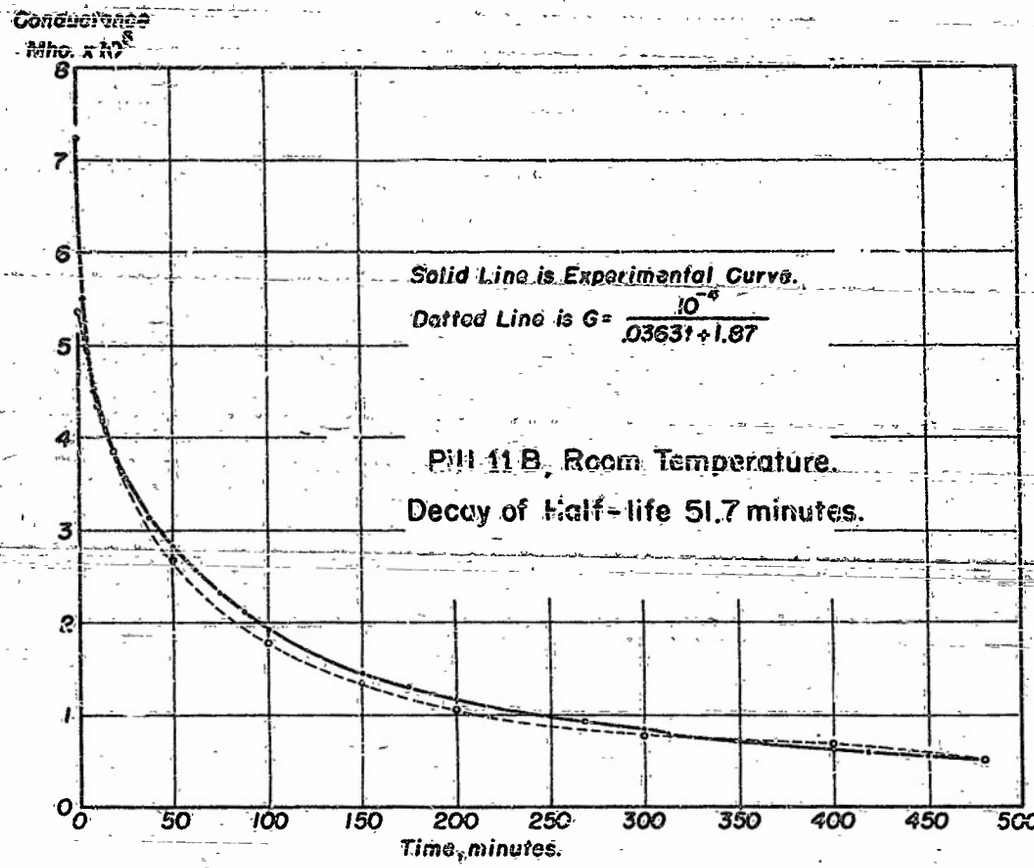
Conductance
Mho. x 10^6
8
7
6
5
4
3
2
1
0
0
50
100
150
200
250
300
350
400
450
500
Time, minutes.
Solid Line is Experimental Curve.
Dotted Line is G = 10^-6 / (.03631 + 1.87)
Pill 11 B, Room Temperature.
Decay of Half-life 51.7 minutes.

Fig. 14

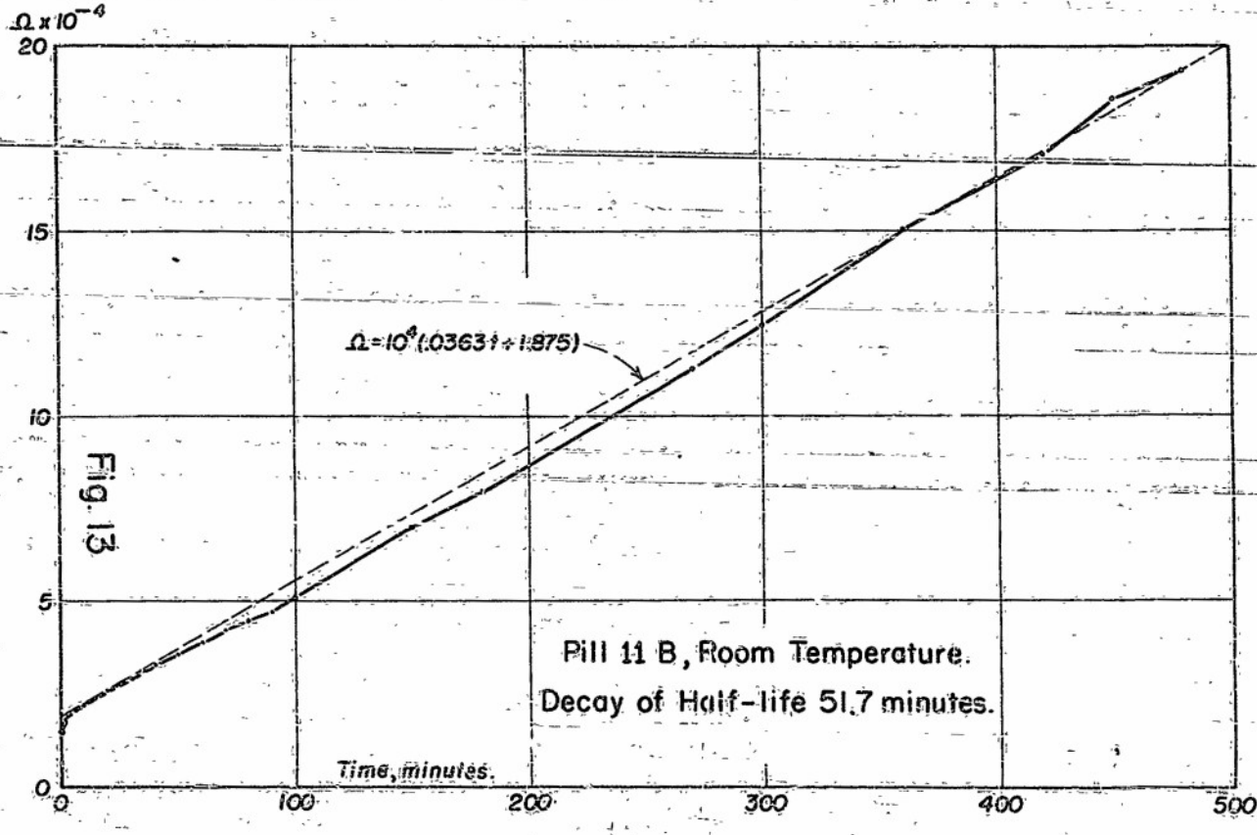
Ω x 10^-4
20
15
10
5
0
0
100
200
300
400
500
Time, minutes.
Ω = 10^4 (.03631 + 1.875)
Pill 11 B, Room Temperature.
Decay of Half-life 51.7 minutes.

Fig. 13

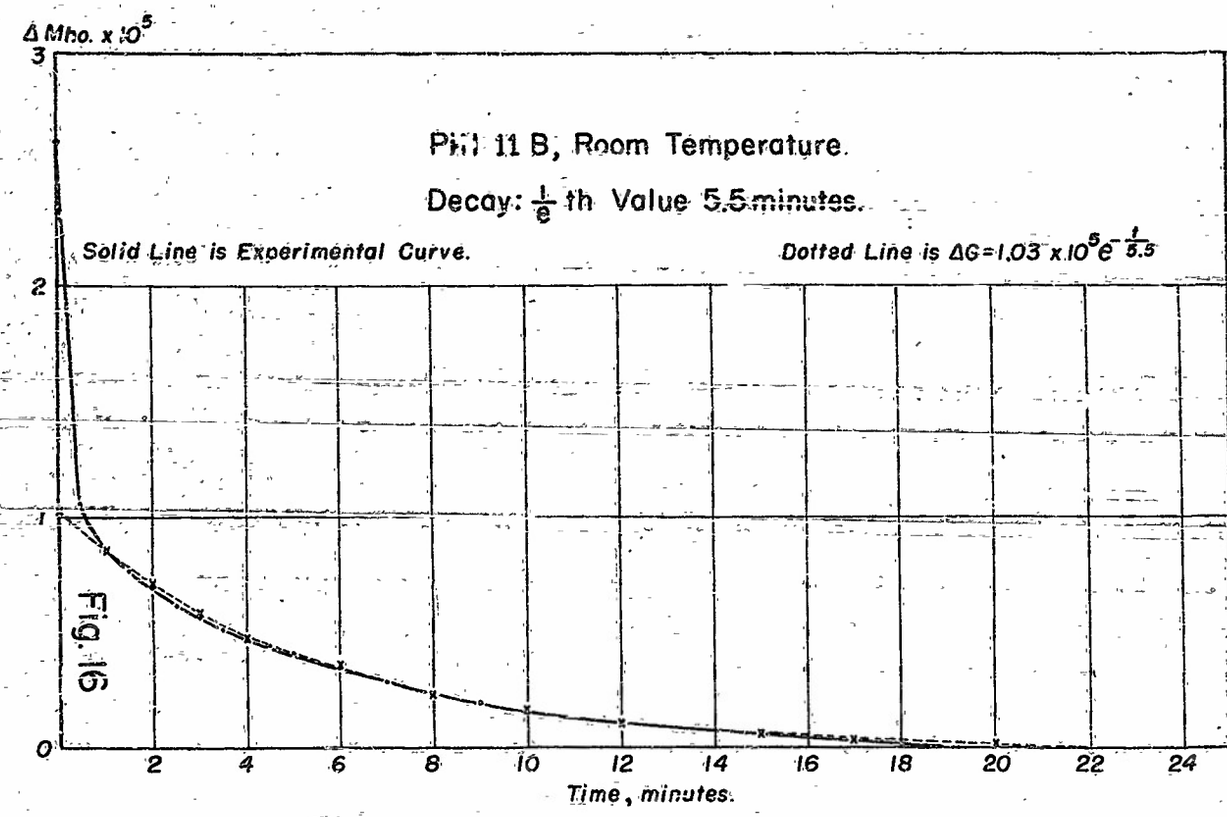
Δ Mho. x 10^5
Pill 11 B, Room Temperature.
Decay: 1/e th Value 5.5 minutes.
Solid Line is Experimental Curve.
Dotted Line is ΔG=1.03 x 10^5 e^-1/5.5
3
2
1
0
2
4
6
8
10
12
14
16
18
20
22
24
Time, minutes.

Fig. 16

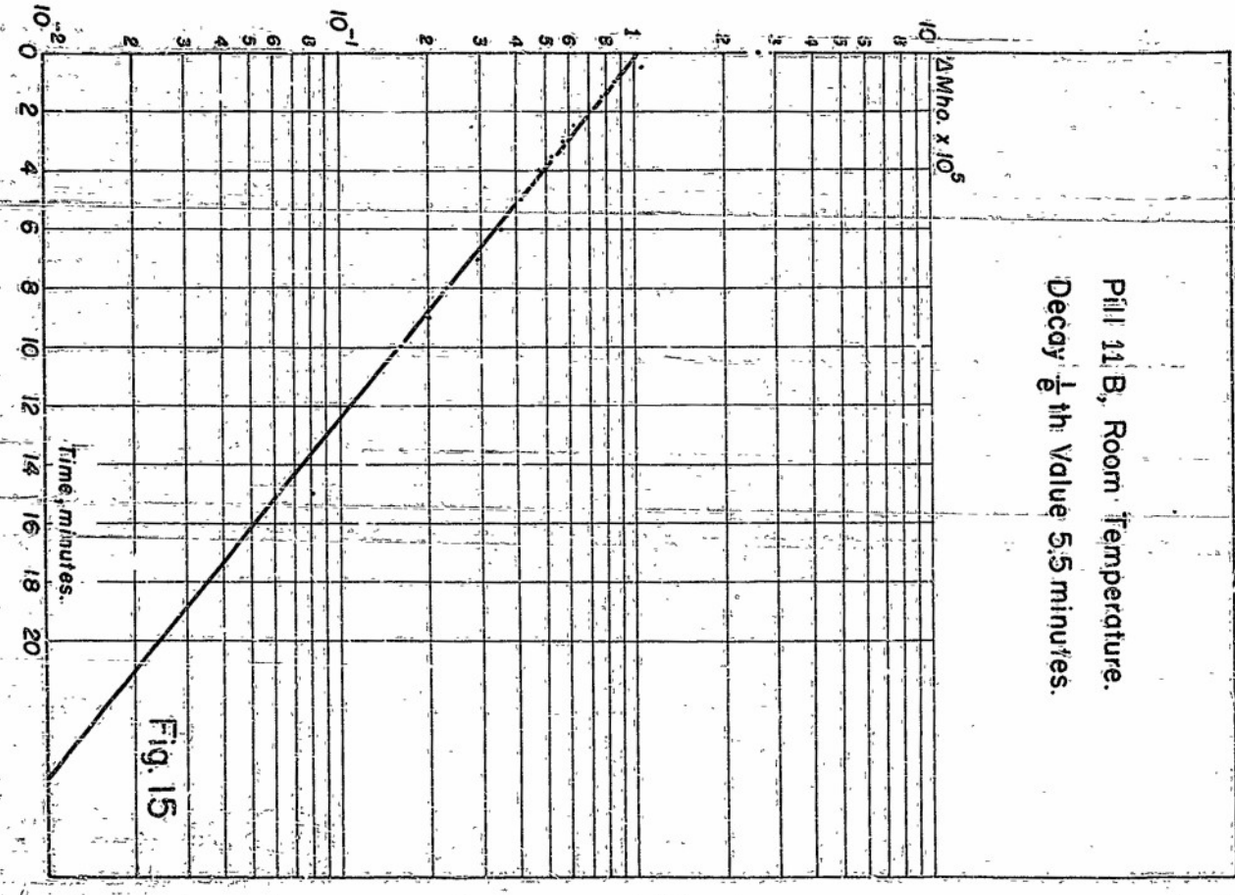
10^-2
10^-1
10
Δ Mho. x 10^5
Time, minutes.
0
2
4
6
8
10
12
14
16
18
20
Pill 11 B, Room Temperature.
Decay 1/e th Value 5.5 minutes.

Fig. 15

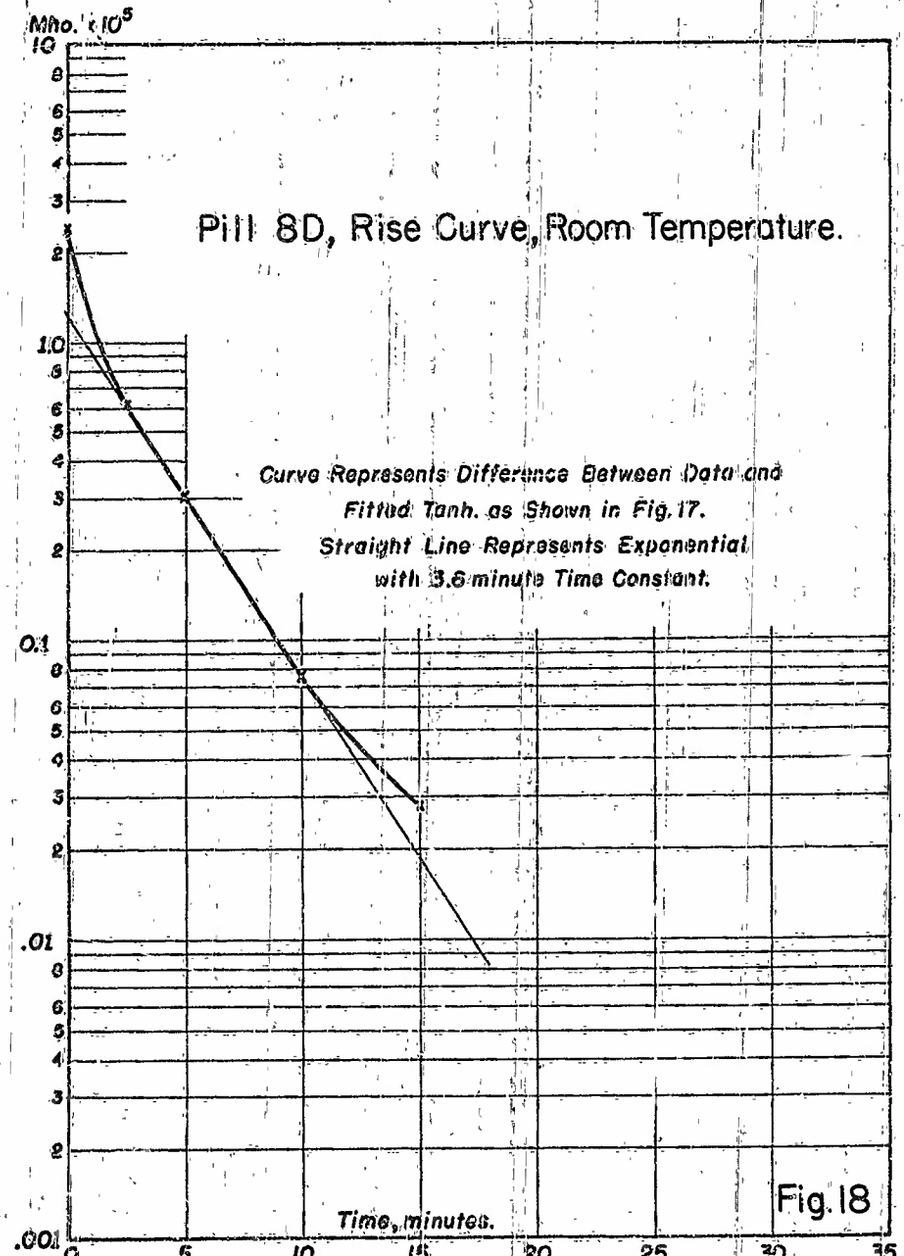
Mho. x 10^5
Pill 8D, Rise Curve, Room Temperature.
Curve Represents Difference Between Data and Fitted Tanh. as Shown in Fig. 17.
Straight Line Represents Exponential with 3.6 minute Time Constant.
Time, minutes.
0
5
10
15
20
25
30
35

Fig. 18

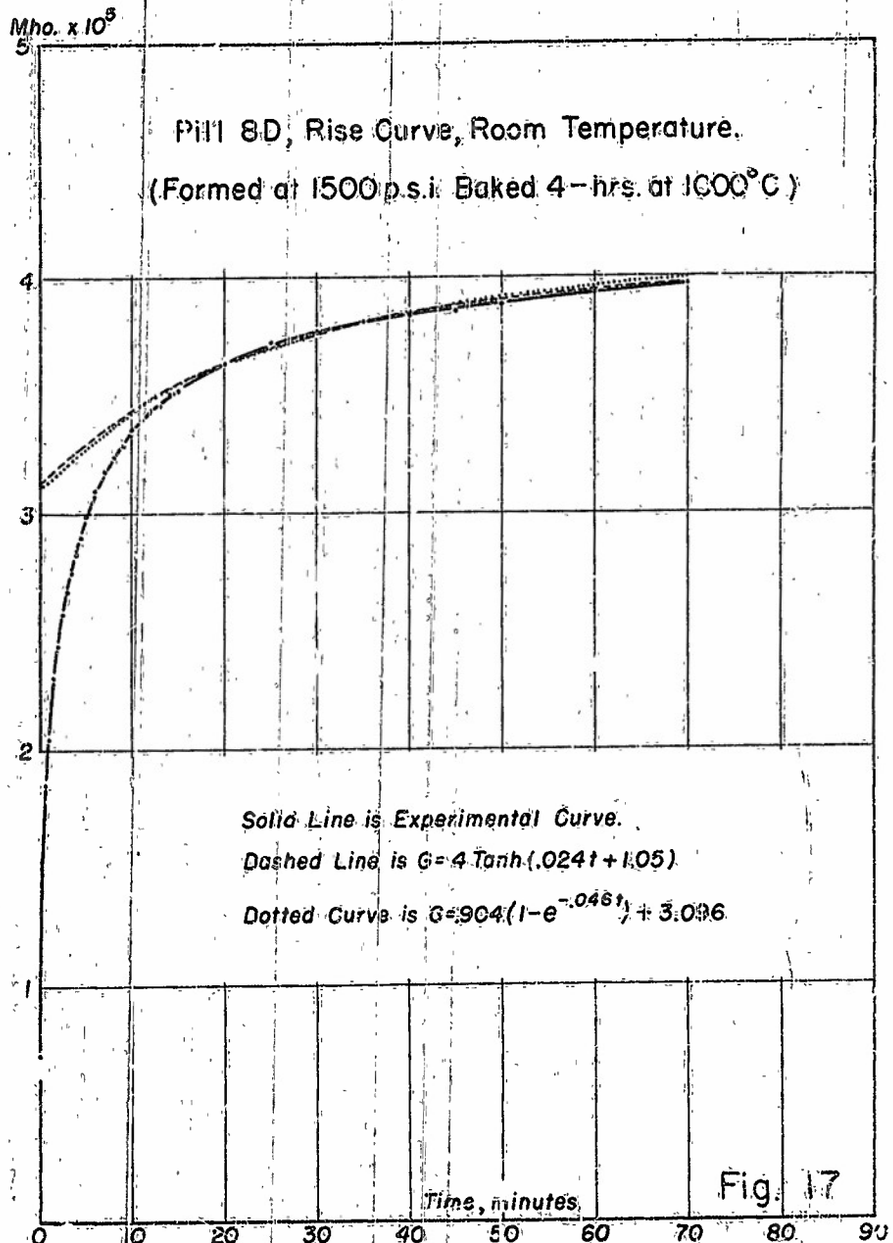
Mho. x 10^5
Pill 8D, Rise Curve, Room Temperature.
(Formed at 1500 p.s.i. Baked 4 – hrs. at 1000°C)
Solid Line is Experimental Curve.
Dashed Line is G = 4 Tanh (.024 t + 1.05)
Dotted Curve is G = .904 (1 – $e^{-.046t}$) + 3.096
Time, minutes.
0
20
30
40
50
60
70
80
90

Fig. 17

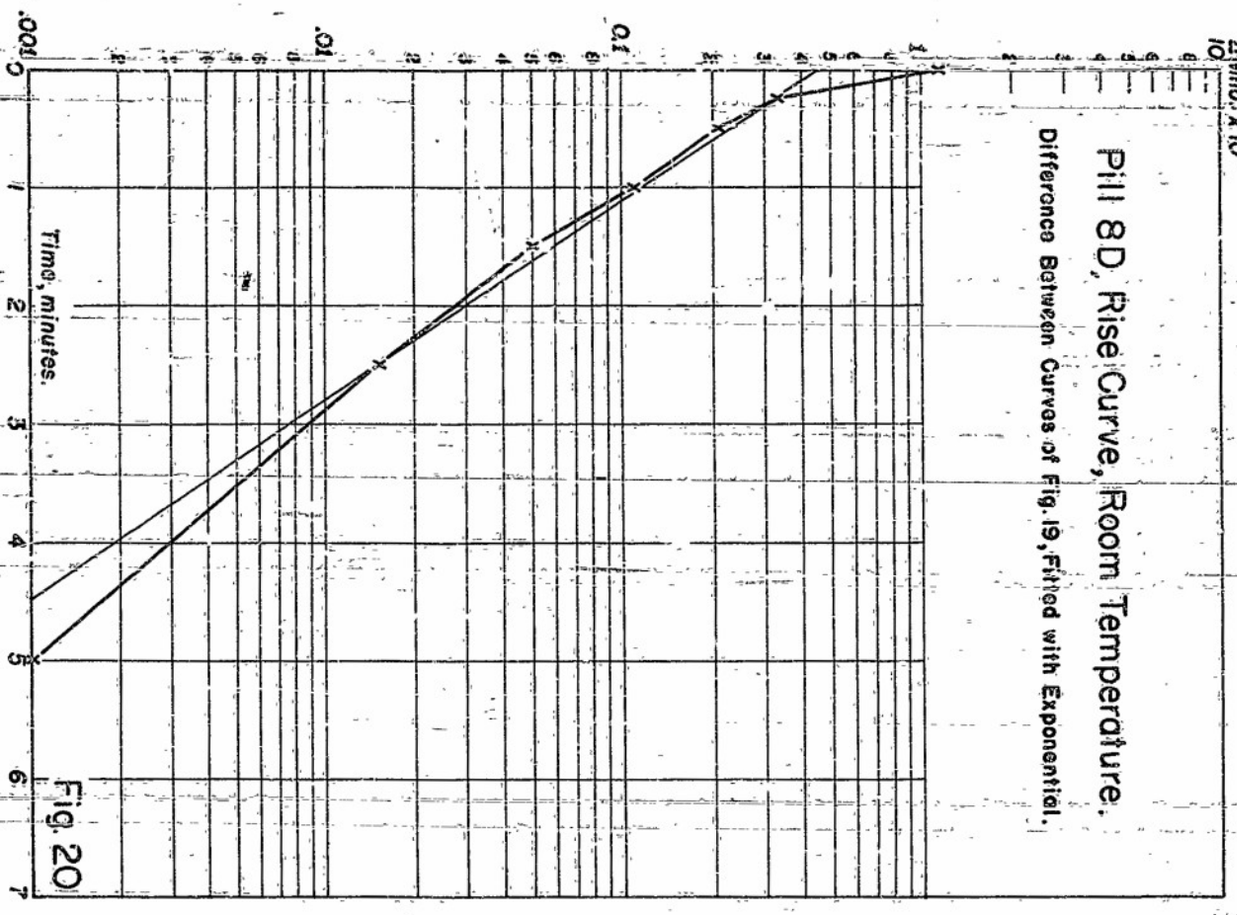
.001
.01
0.1
Δ Mho. x 10⁵
Time, minutes.
Pill 8D, Rise Curve, Room Temperature.
Difference Between Curves of Fig. 19, Fitted with Exponential.

Fig. 20

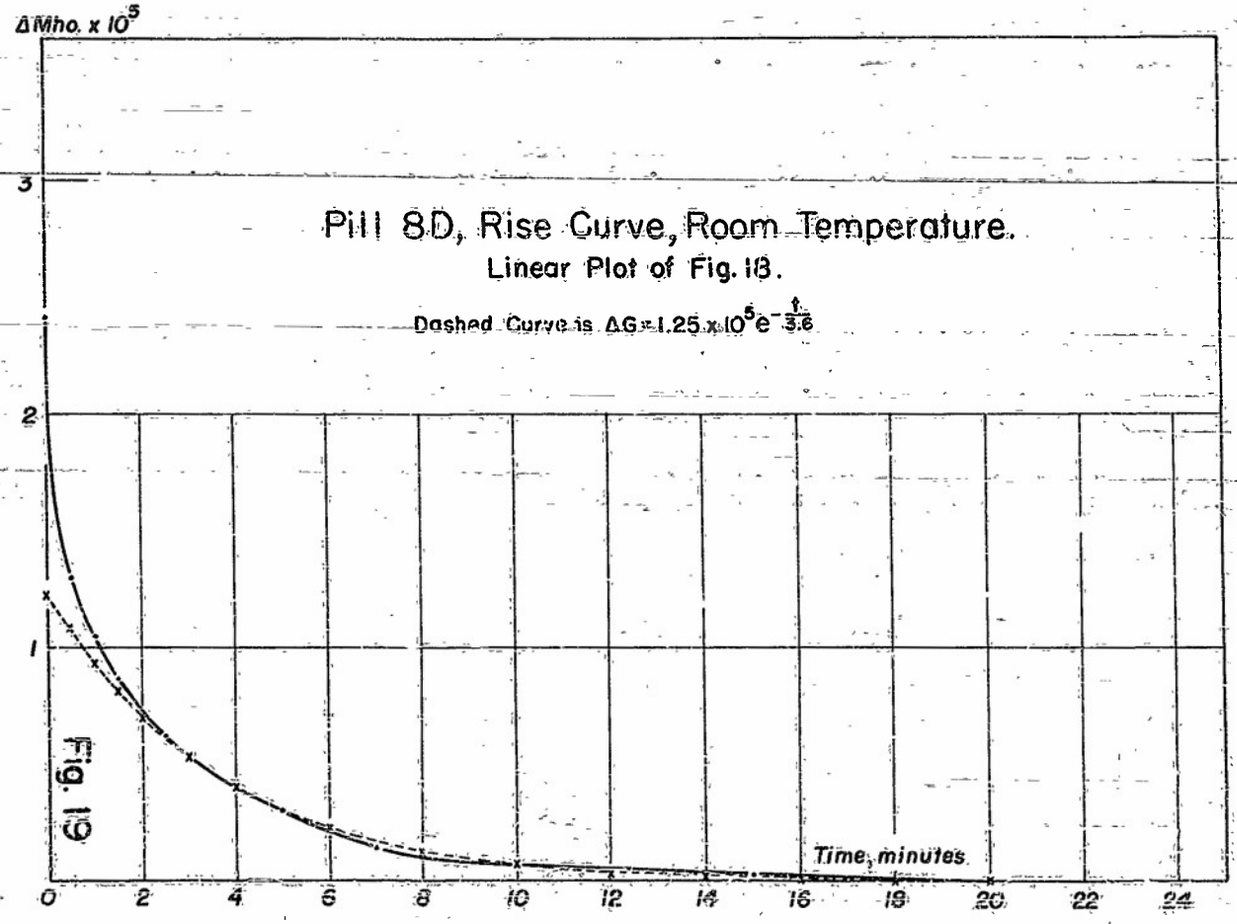
Δ Mho. x 10⁵
Pill 8D, Rise Curve, Room Temperature.
Linear Plot of Fig. 18.
Dashed Curve is ΔG = 1.25 x 10⁵ e^(-t/3.6)
Time, minutes

Fig. 19

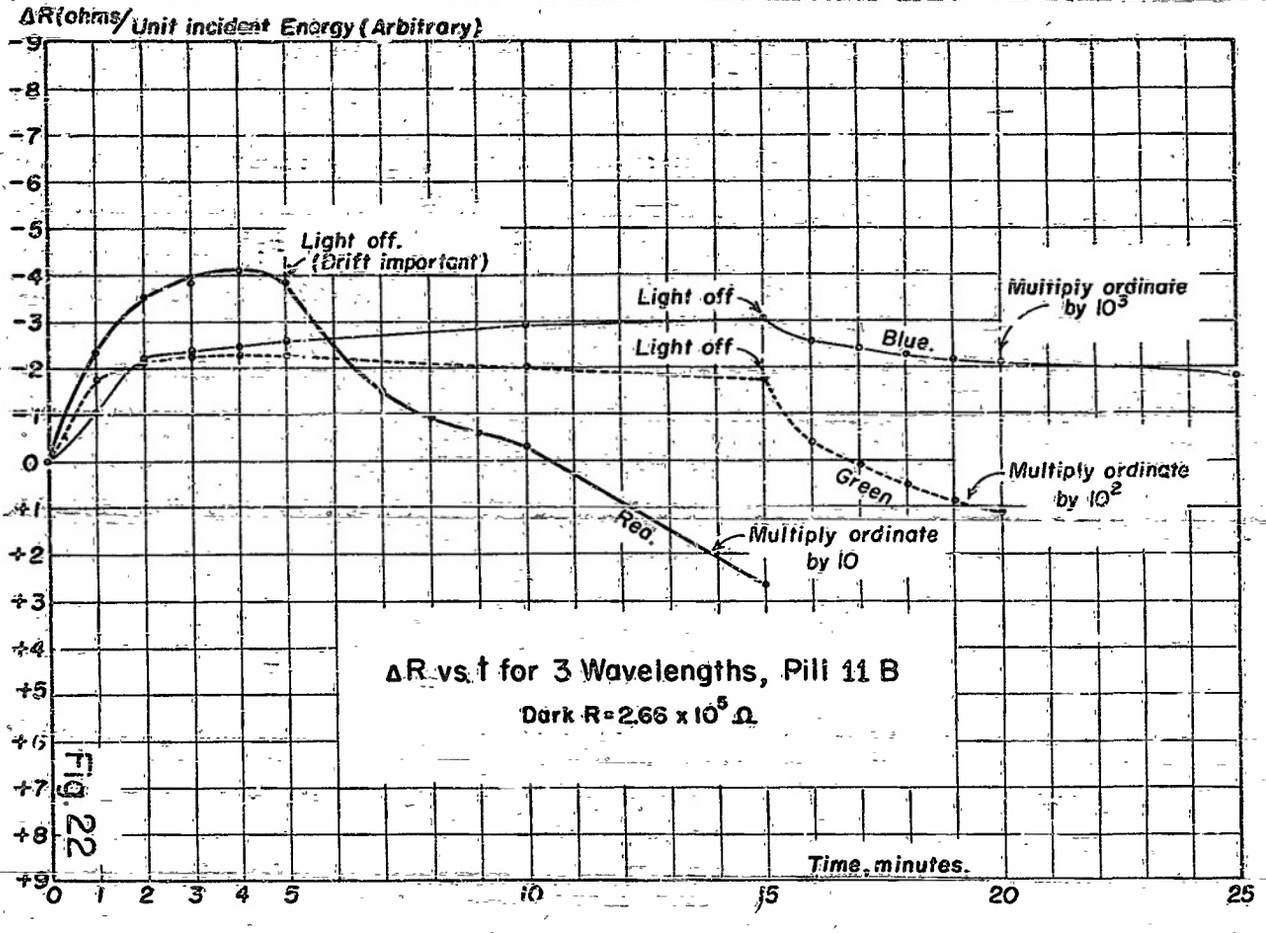
ΔR(ohms/Unit incident Energy (Arbitrary)
Light off.
(Drift important)
Light off
Light off
Blue.
Multiply ordinate by 10^3
Green
Multiply ordinate by 10^2
Red.
Multiply ordinate by 10
ΔR vs t for 3 Wavelengths, Pili 11 B
Dark R = 2.66 x 10^5 Ω
Time, minutes.

Fig. 22

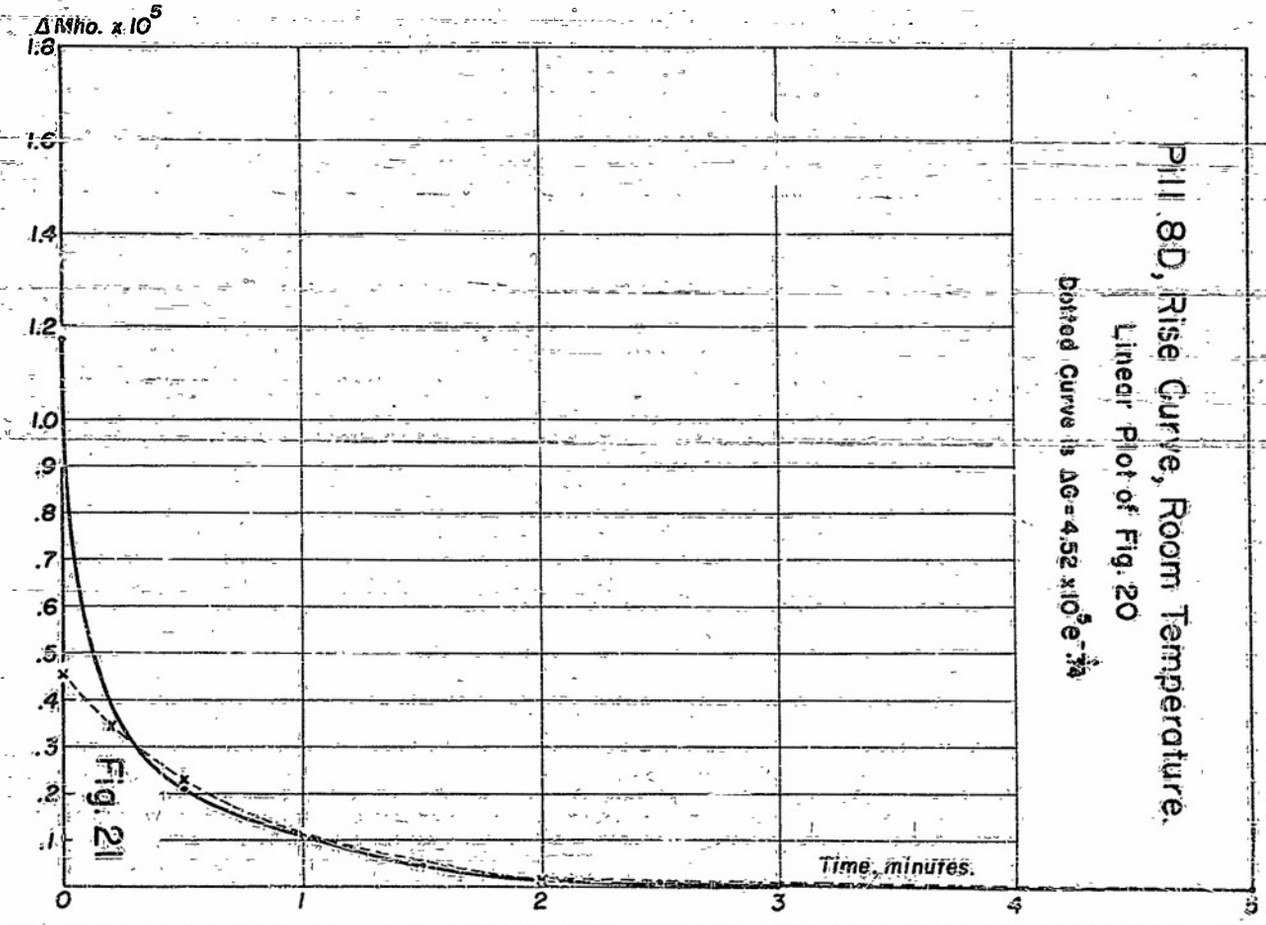
ΔMho. x 10^5
Time, minutes.
Pili 8D, Rise Curve, Room Temperature.
Linear Plot of Fig. 20
Dotted Curve is ΔG = 4.52 x 10^5 $e^{-t/4}$

Fig. 21

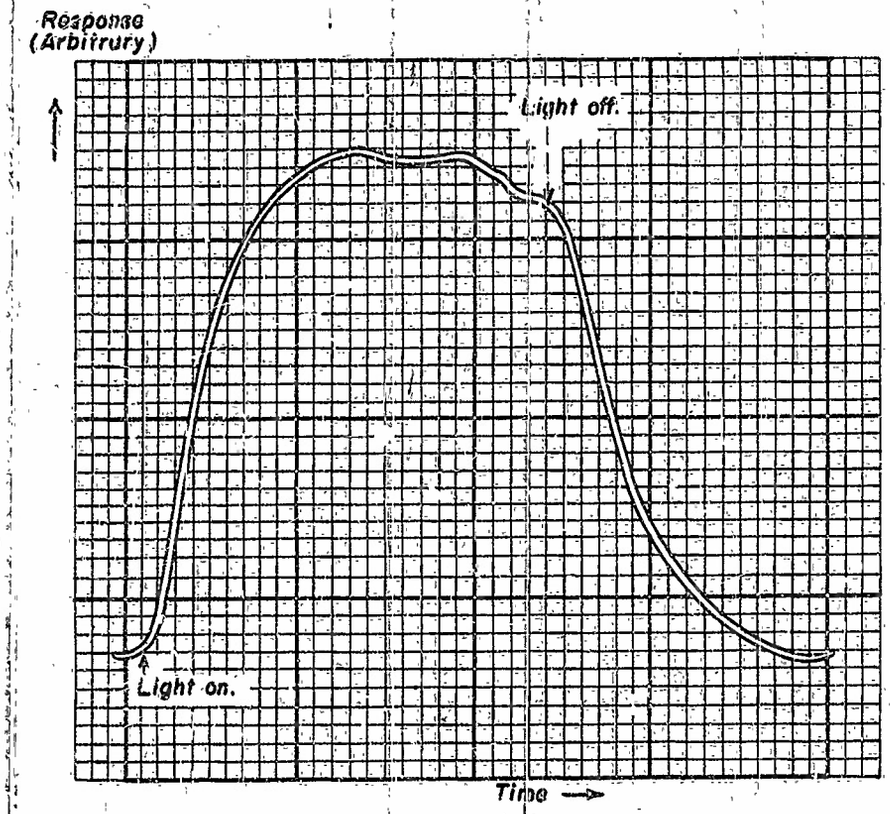

Tracing of Voltage Pulse with
2.5×10^{-2} sec. Flash Duration.

Fig. 24

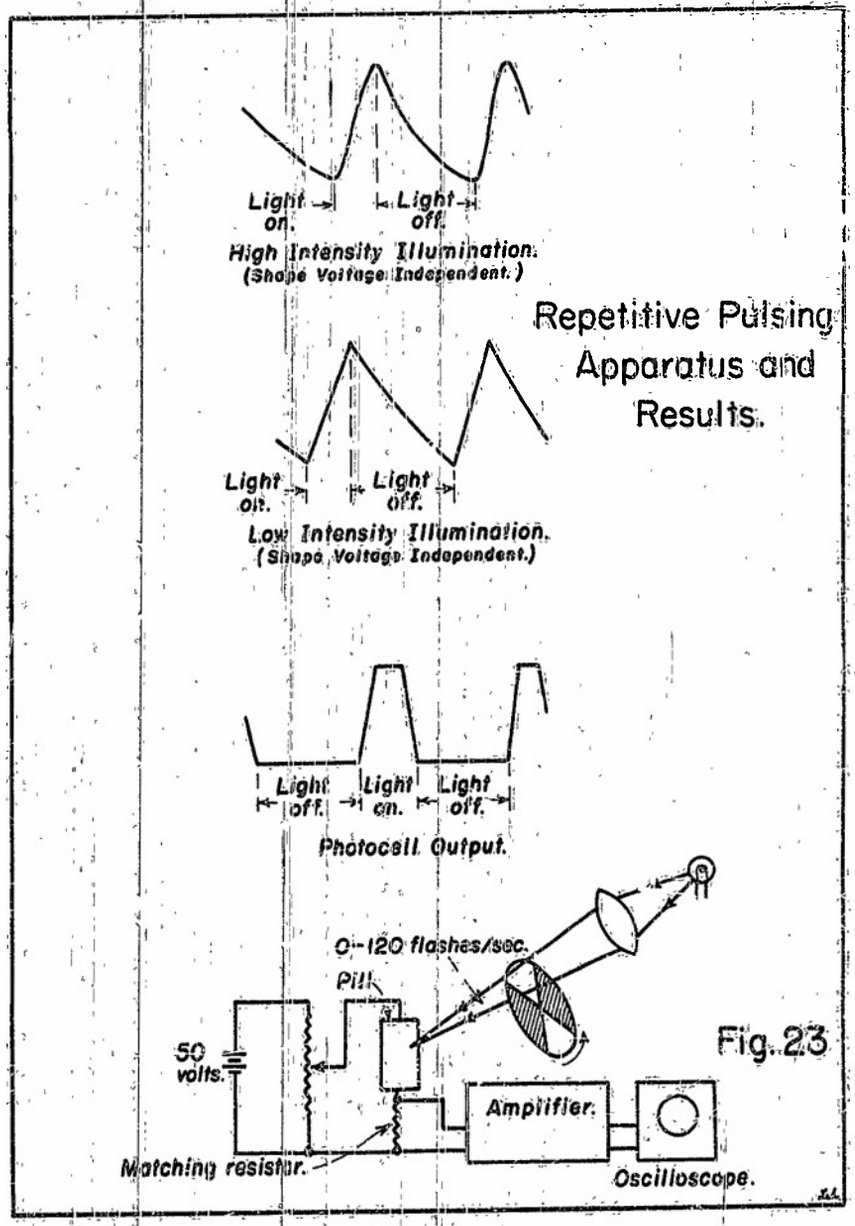

Repetitive Pulsing Apparatus and Results.

Fig. 23

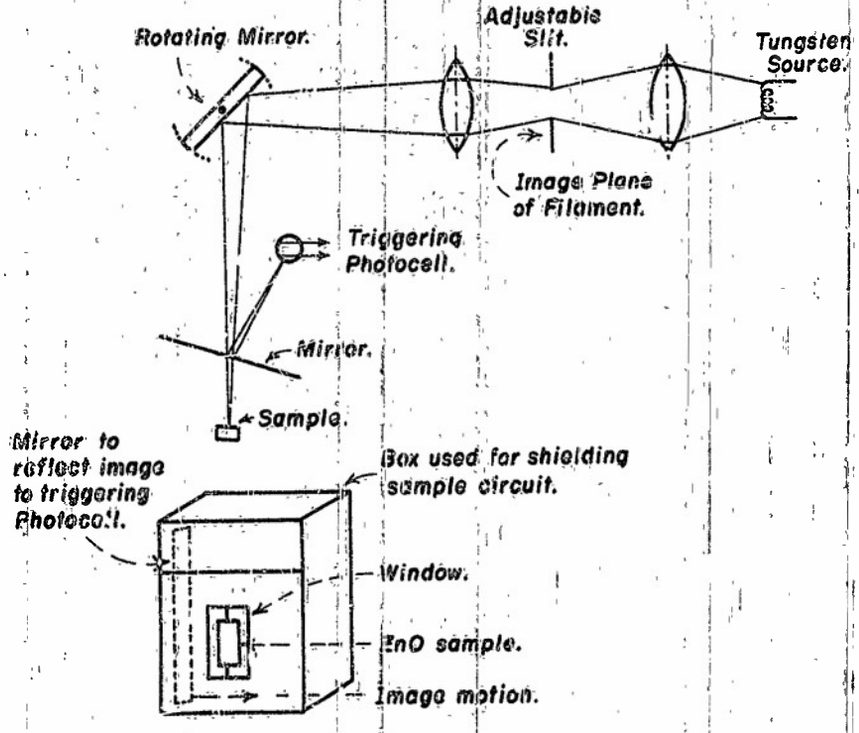

Separated Pulse Optical Arrangment.

Fig. 26

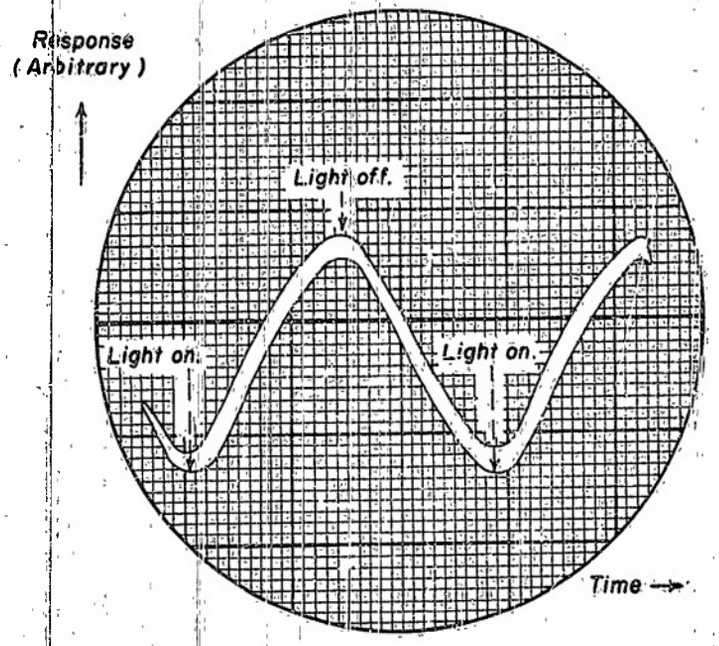

Tracing of Voltage Pulse with 1.7×10^{-3} sec. Flash Duration.

Fig. 25

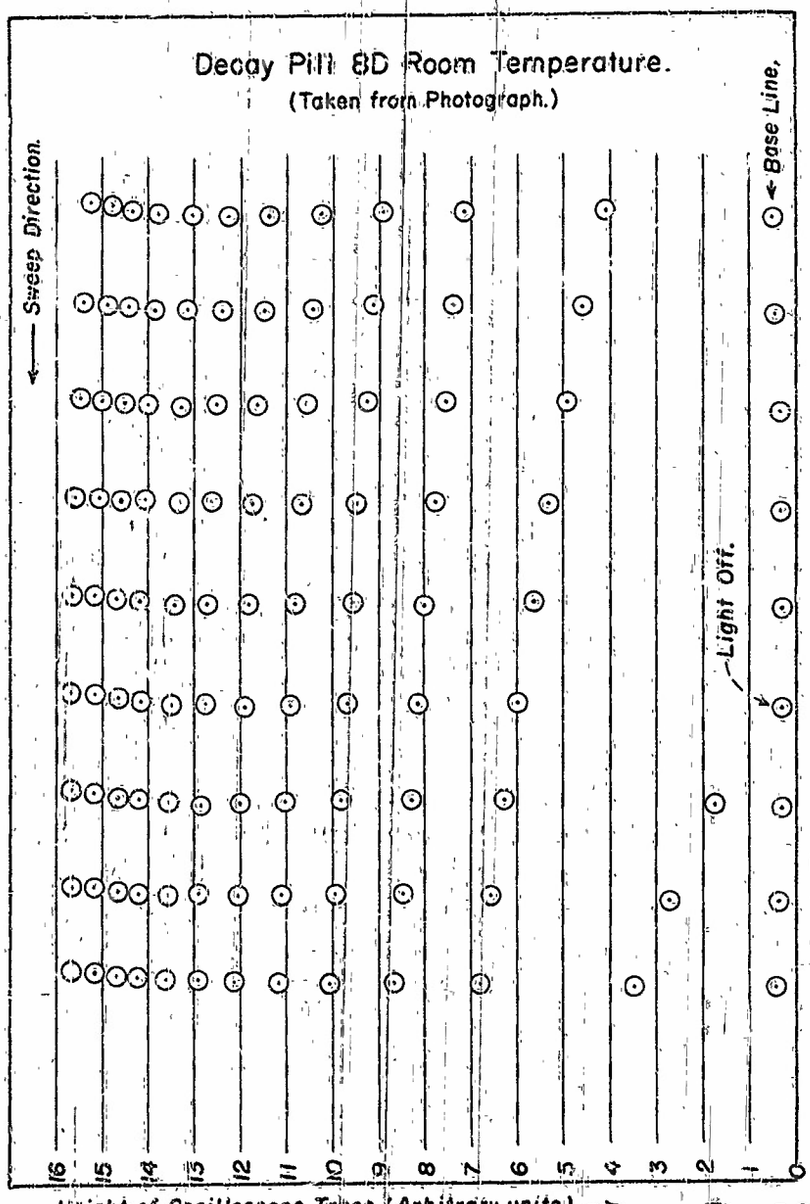

Fig. 28

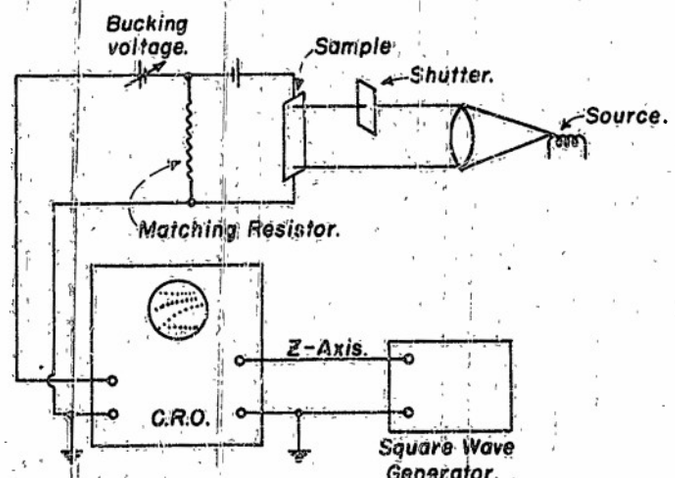

Apparatus for High Speed Rise and Decay.

Fig. 27

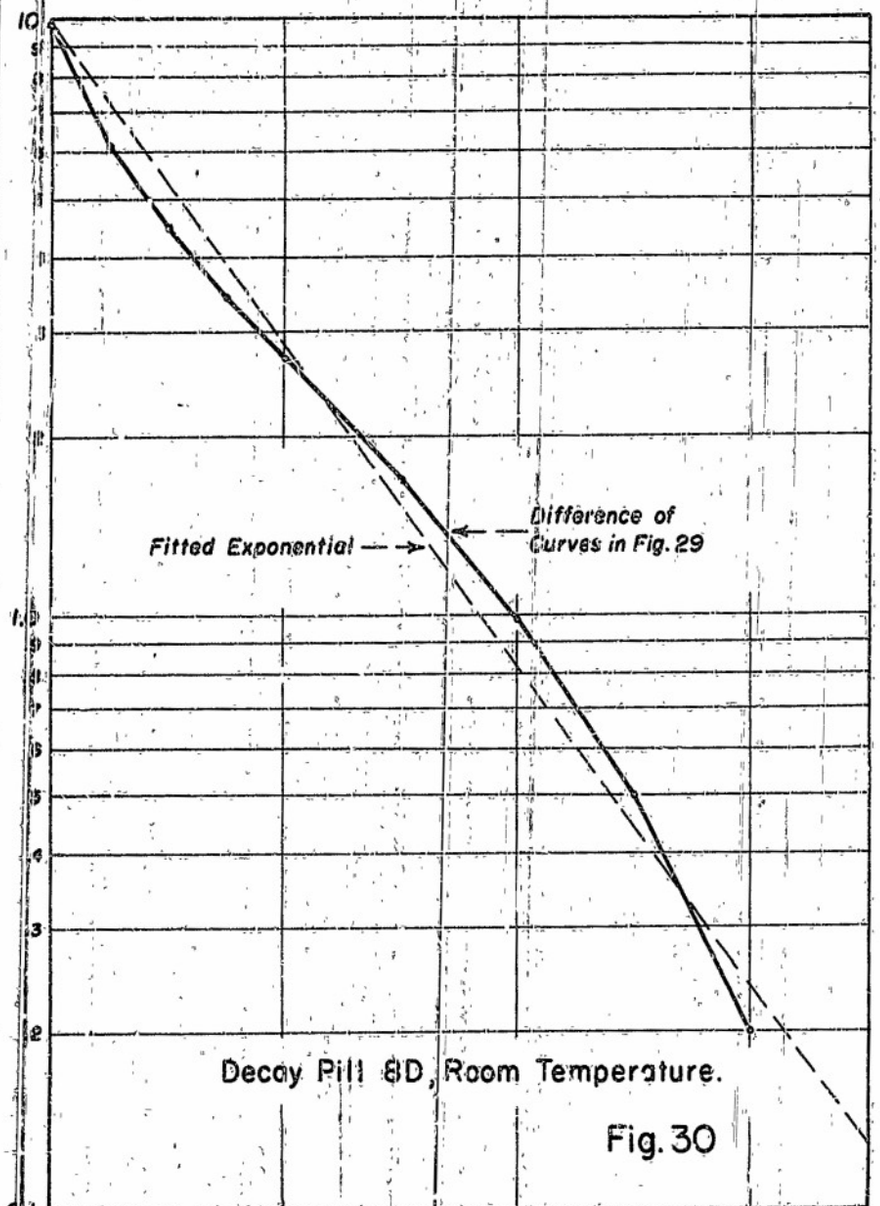
Fitted Exponential
Difference of Curves in Fig. 29
Decay Pill 8D, Room Temperature.
0
1
2
3 Seconds.

Fig. 30

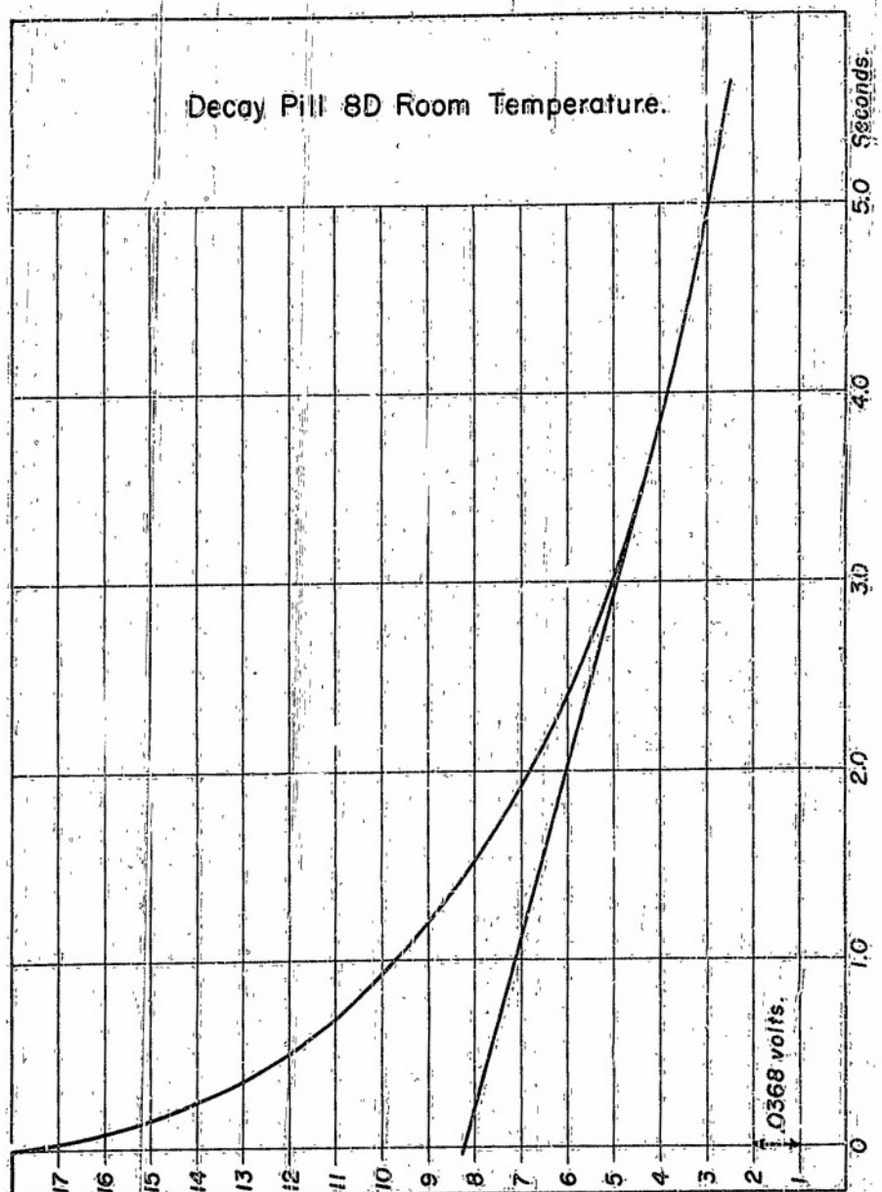
Decay Pill 8D Room Temperature.
Seconds.
.0368 volts.

Fig. 29

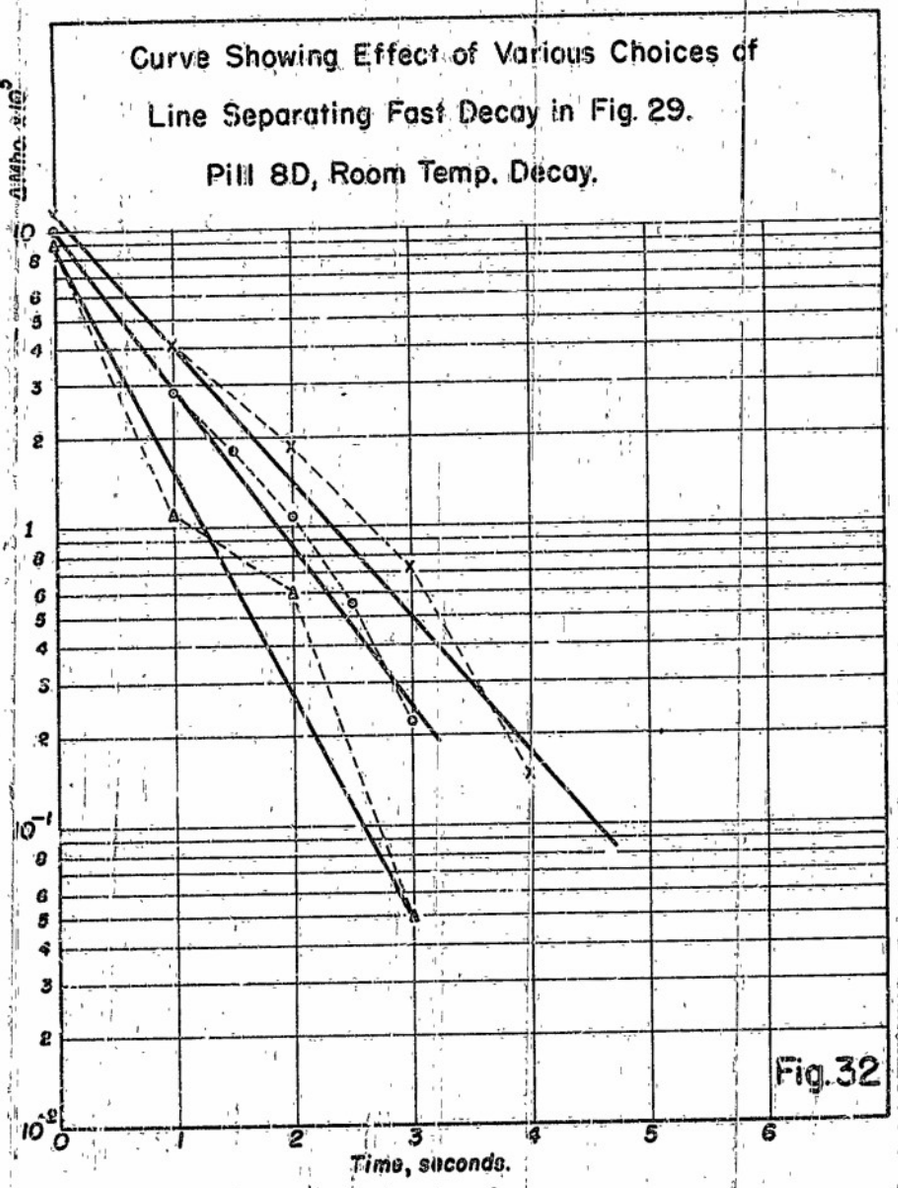
Curve Showing Effect of Various Choices of
Line Separating Fast Decay in Fig. 29.
Pill 8D, Room Temp. Decay.
Time, seconds.

Fig. 32

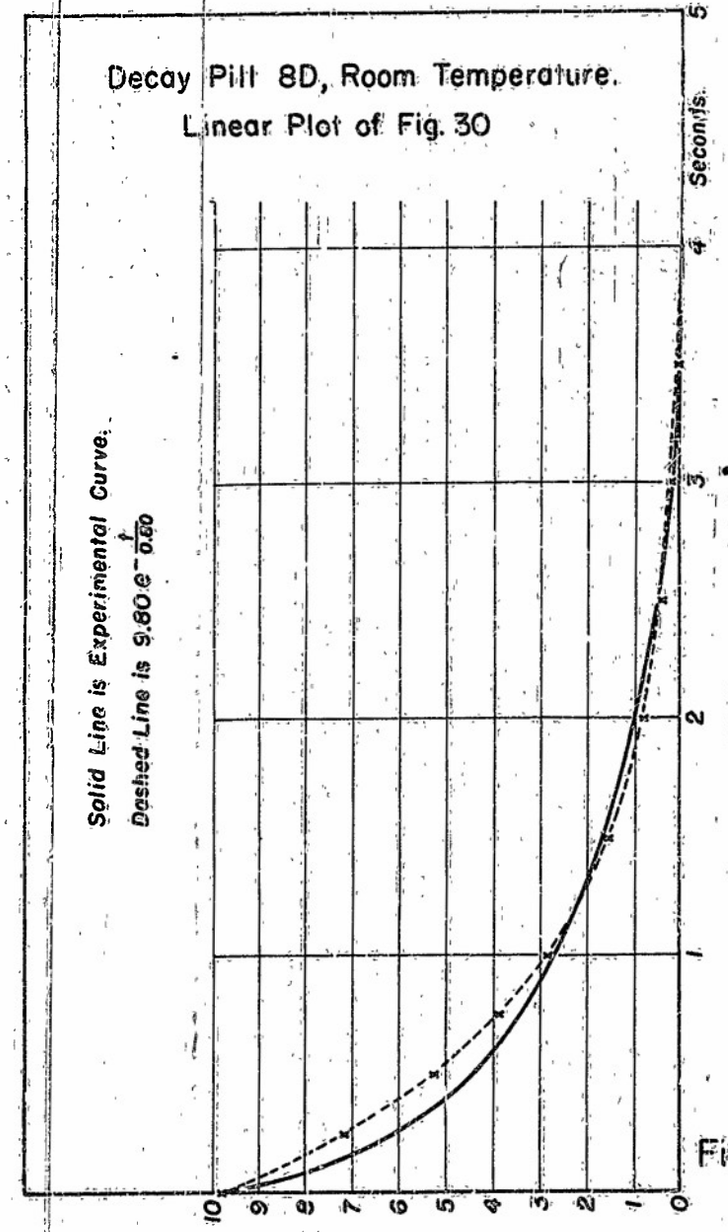
Decay Pill 8D, Room Temperature.
Linear Plot of Fig. 30
Solid Line is Experimental Curve.
Dashed Line is 9.80 e^-t/0.60
Seconds.

Fig. 31

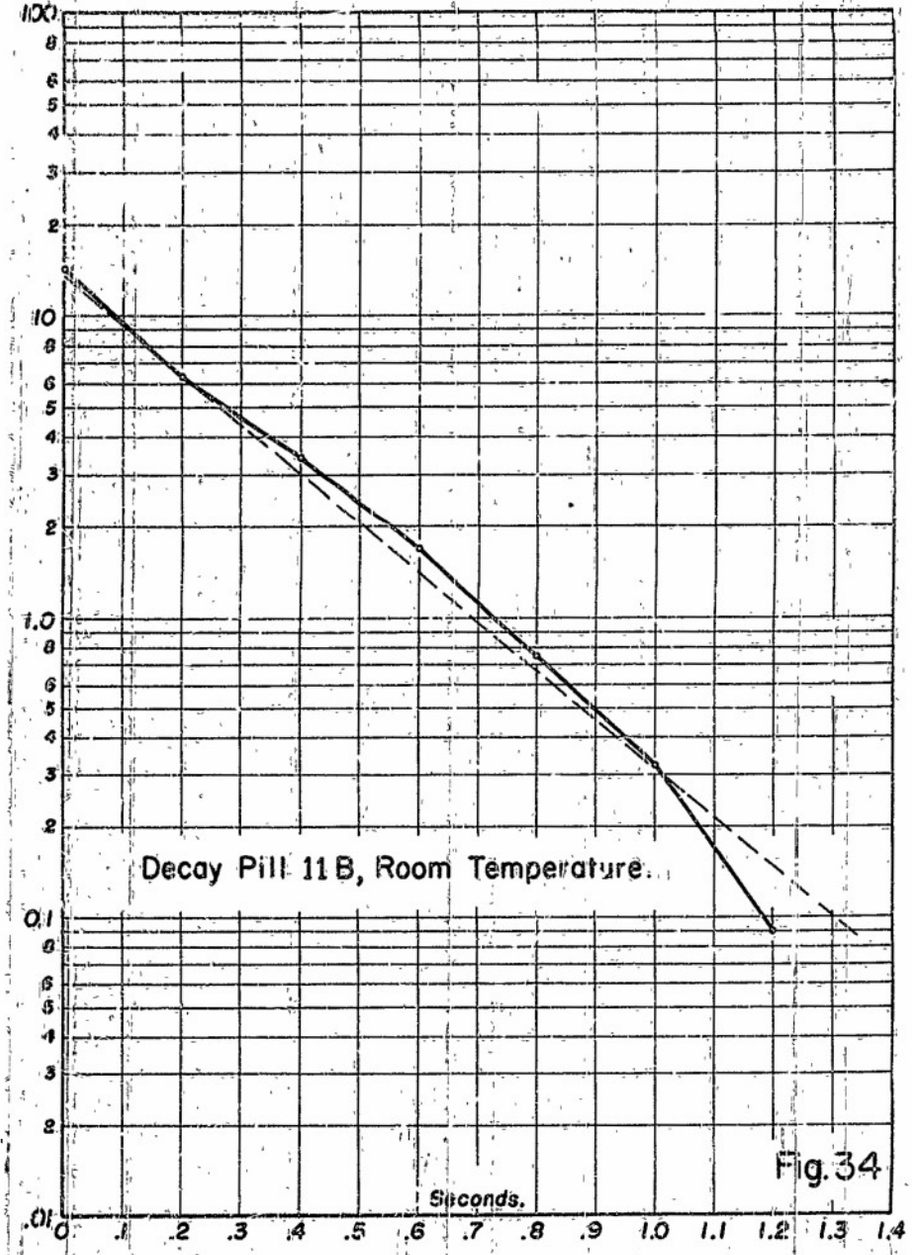
100
8
6
5
4
3
2
10
8
6
5
4
3
2
1.0
8
6
5
4
3
2
0.1
8
6
5
4
3
2
.01
Decay Pill 11 B, Room Temperature.
Seconds.
0 .1 .2 .3 .4 .5 .6 .7 .8 .9 1.0 1.1 1.2 1.3 1.4

Fig. 34

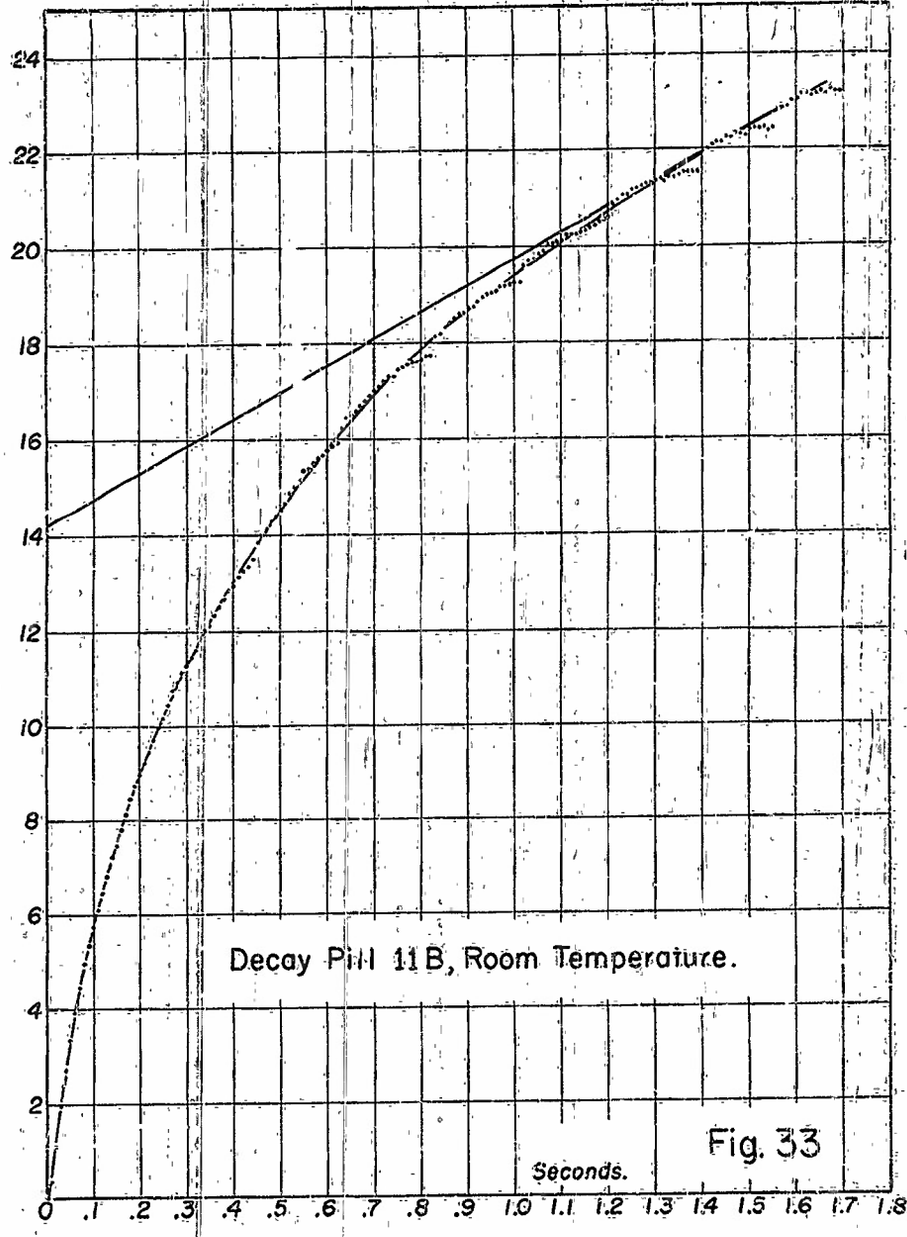
24
22
20
18
16
14
12
10
8
6
4
2
Decay Pill 11 B, Room Temperature.
Seconds.
0 .1 .2 .3 .4 .5 .6 .7 .8 .9 1.0 1.1 1.2 1.3 1.4 1.5 1.6 1.7 1.8

Fig. 33

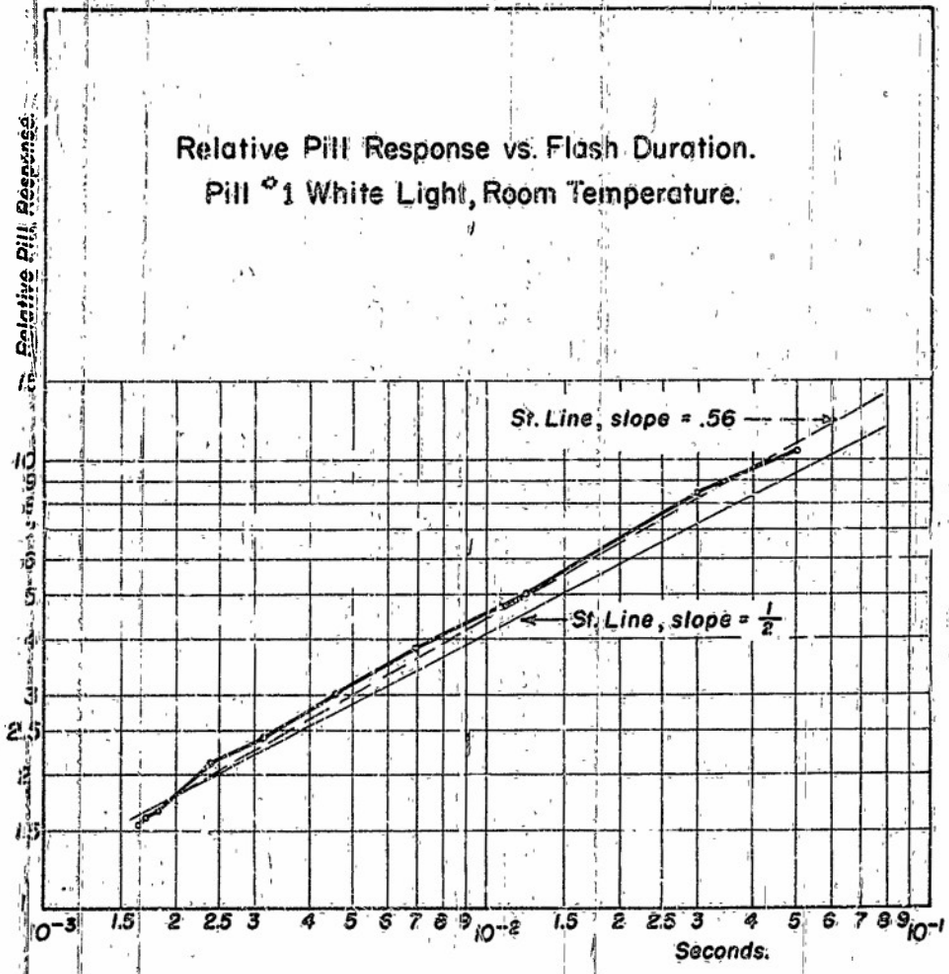
Relative Pill Response vs. Flash Duration.
Pill #1 White Light, Room Temperature.
Relative Pill Response
St. Line, slope = .56
St. Line, slope = 1/2
10⁻³ 1.5 2 2.5 3 4 5 6 7 8 9 10⁻² 1.5 2 2.5 3 4 5 6 7 8 9 10⁻¹
Seconds.

Fig. 36

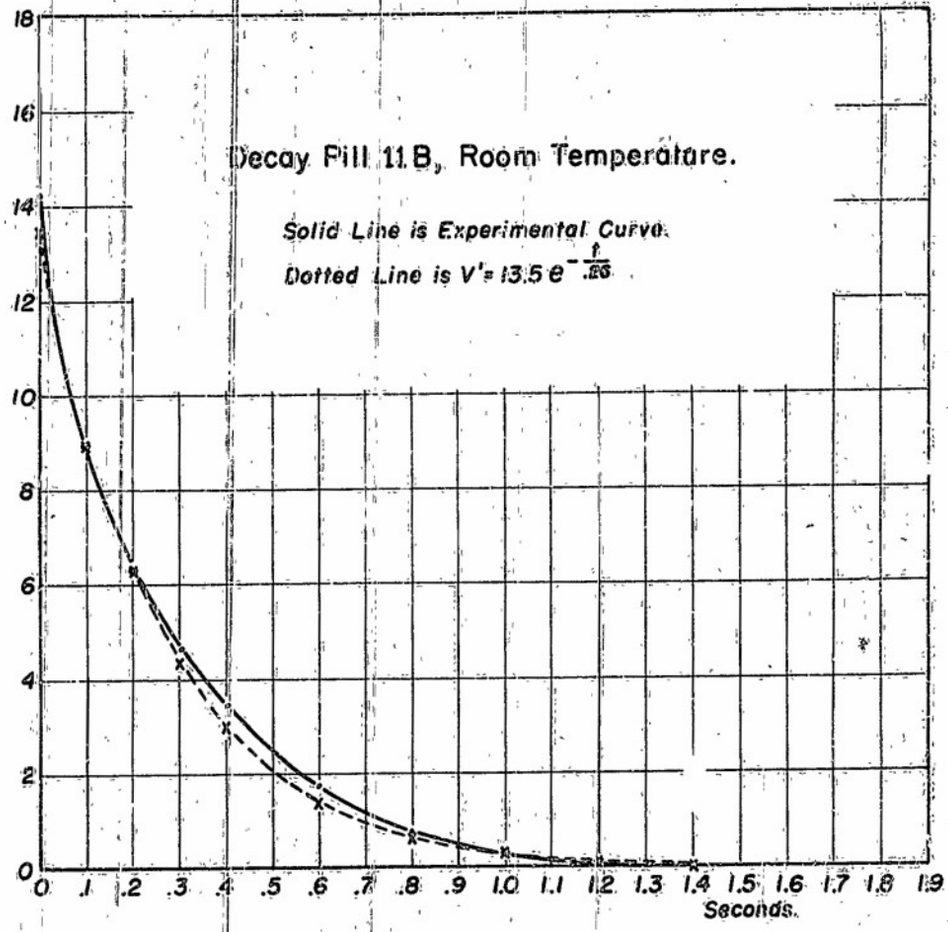
Decay Pill 11 B, Room Temperature.
Solid Line is Experimental Curve.
Dotted Line is V' = 13.5 e^(-t/.26)
0 .1 .2 .3 .4 .5 .6 .7 .8 .9 1.0 1.1 1.2 1.3 1.4 1.5 1.6 1.7 1.8 1.9
Seconds.

Fig. 35

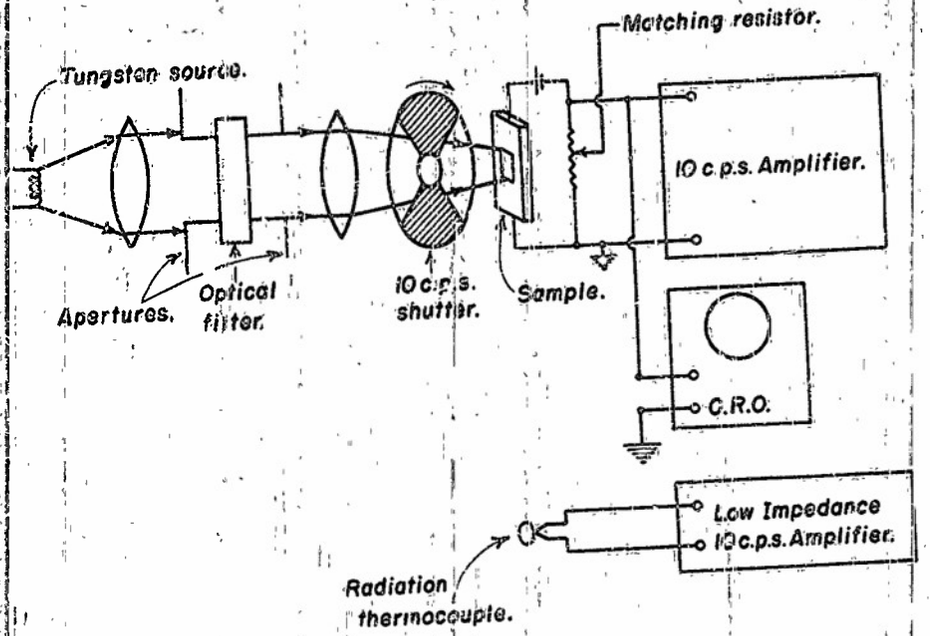

10 CYCLE MEASUREMENT APPARATUS.

Fig. 38

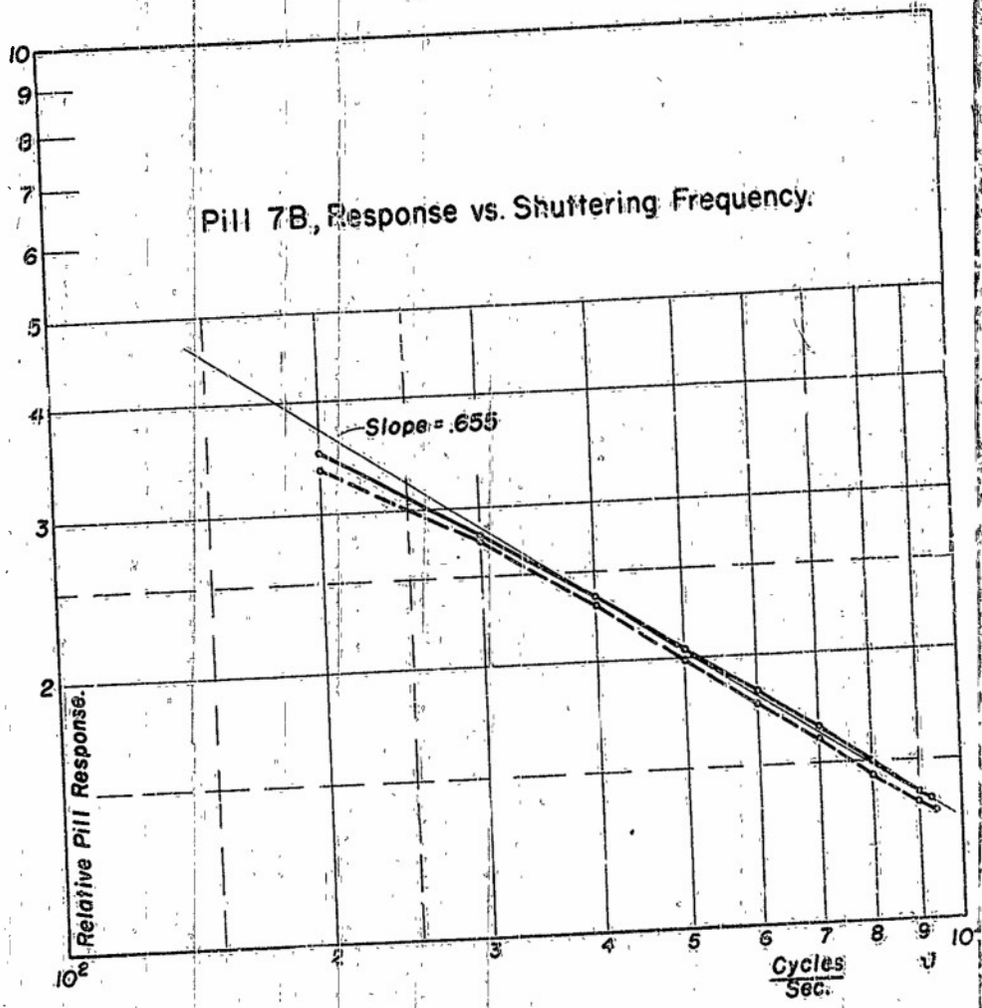

Fig. 37

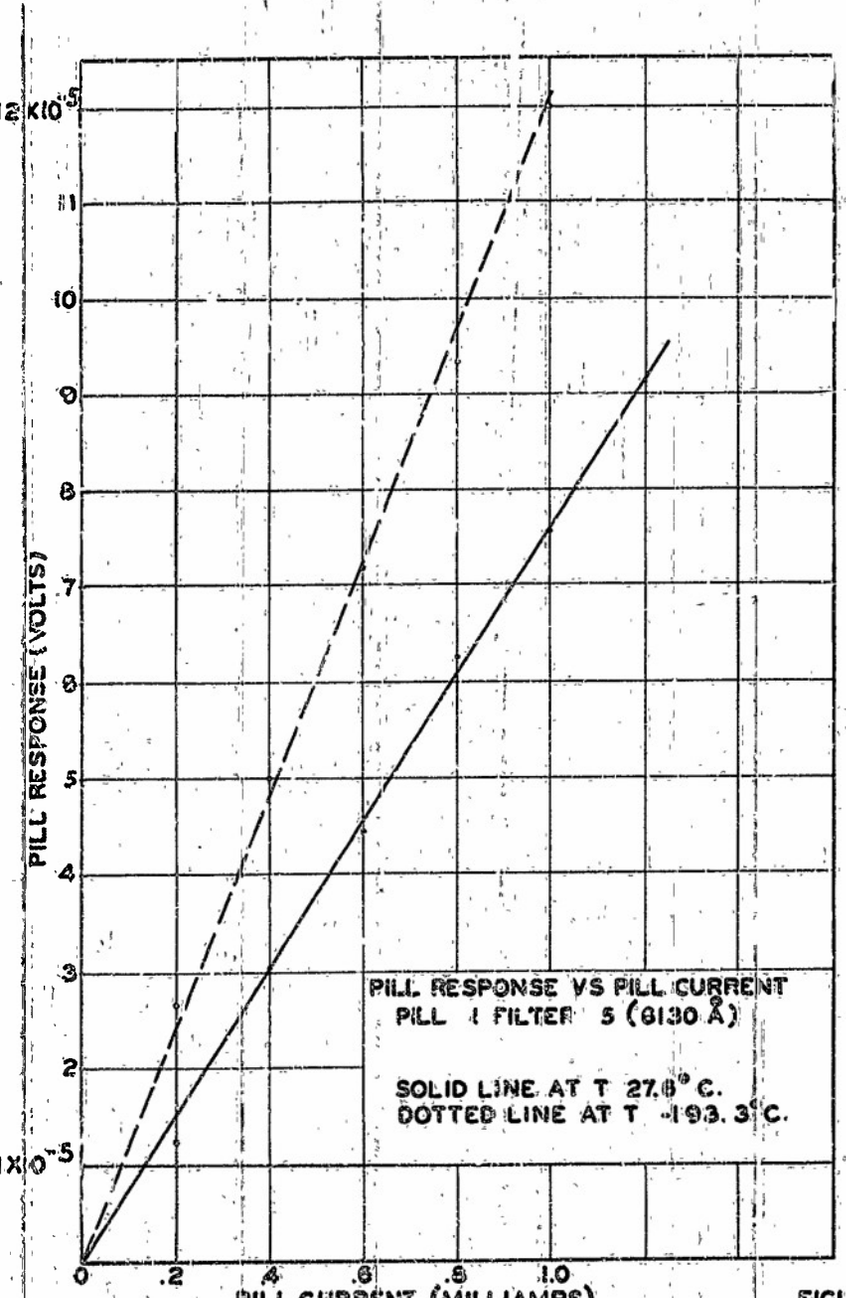

FIGURE 40

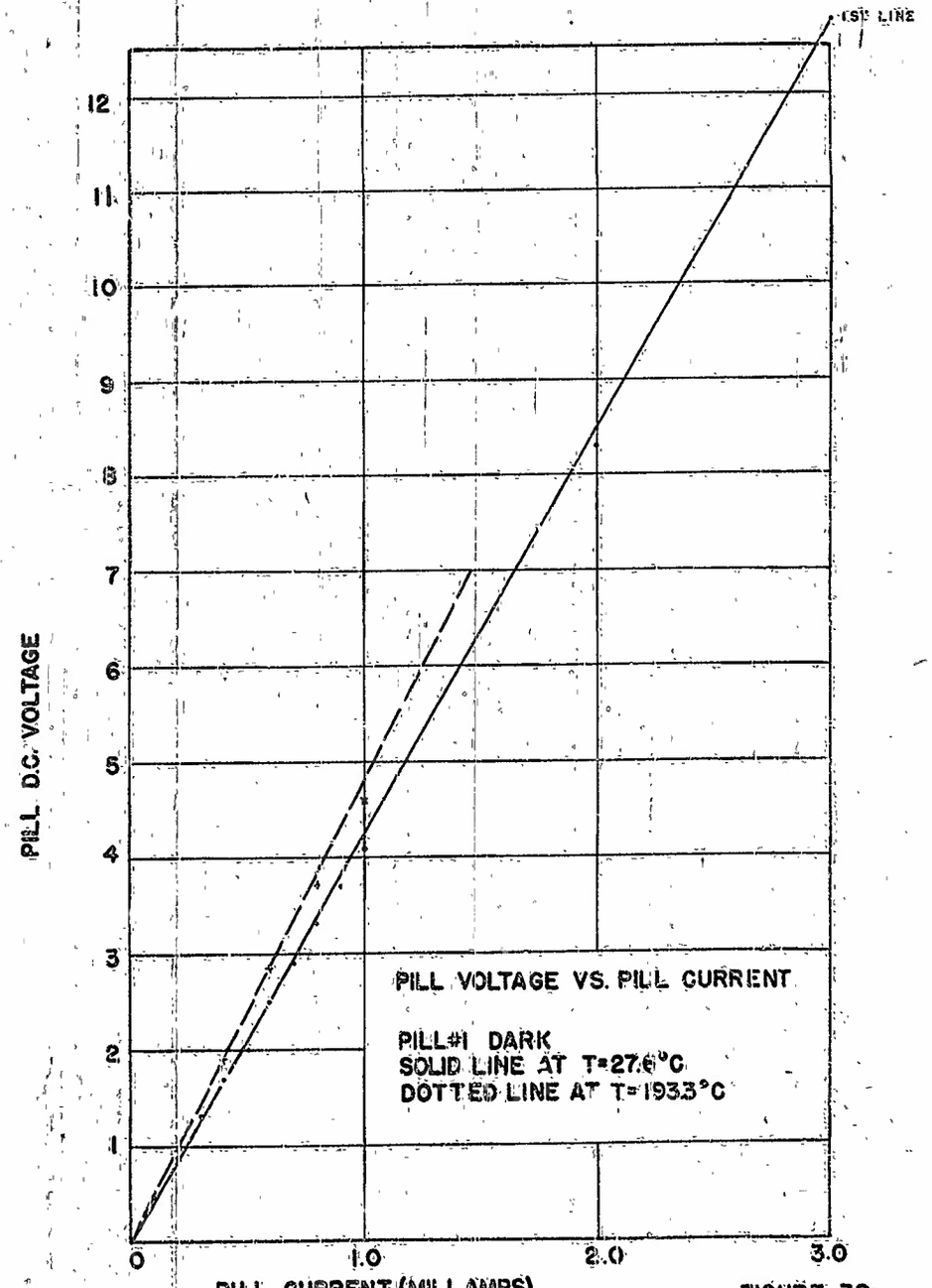

FIGURE 39

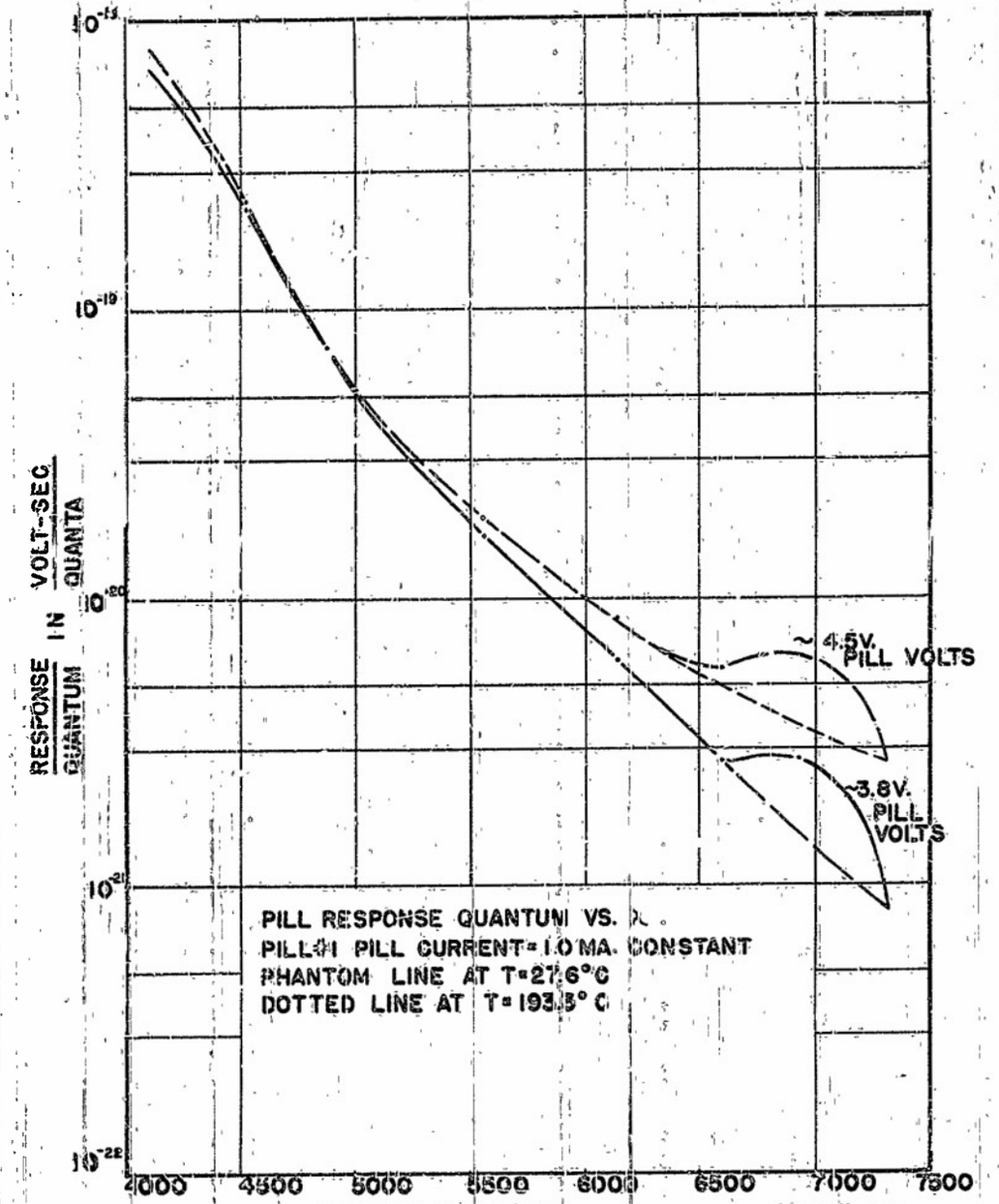

FIGURE 42

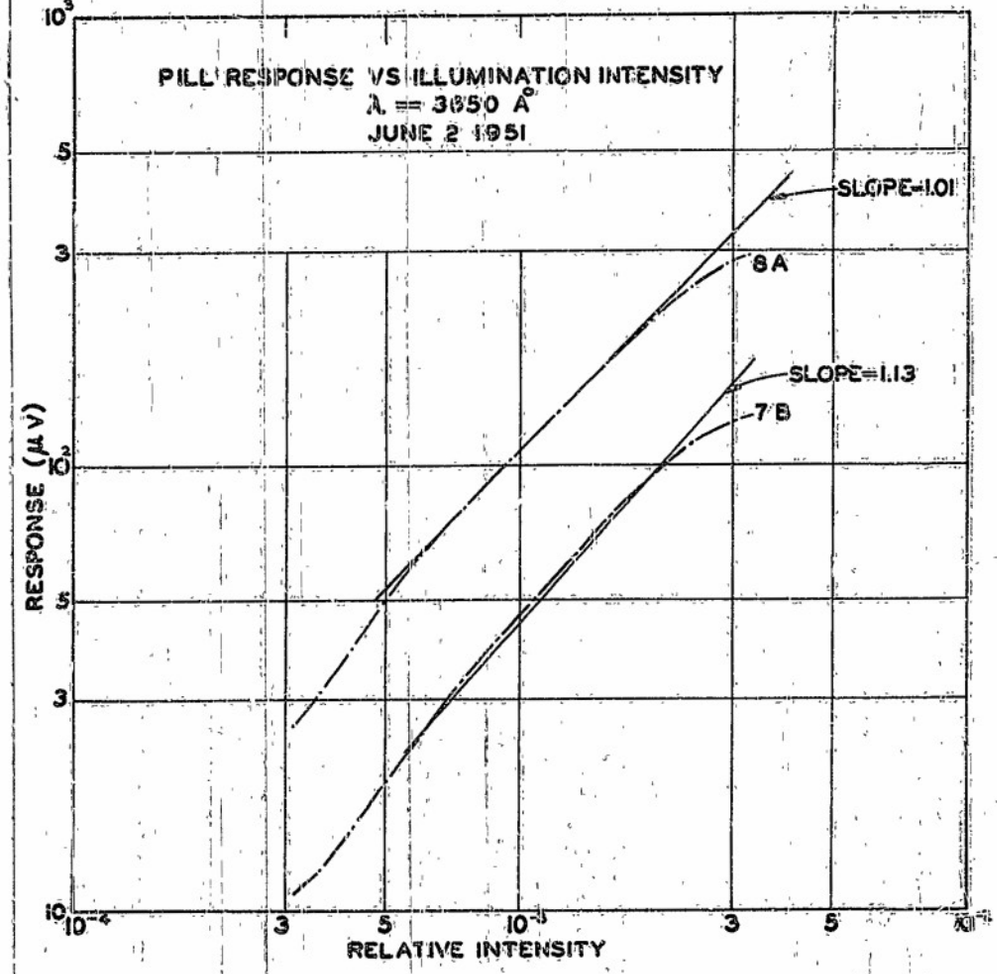

FIGURE 41

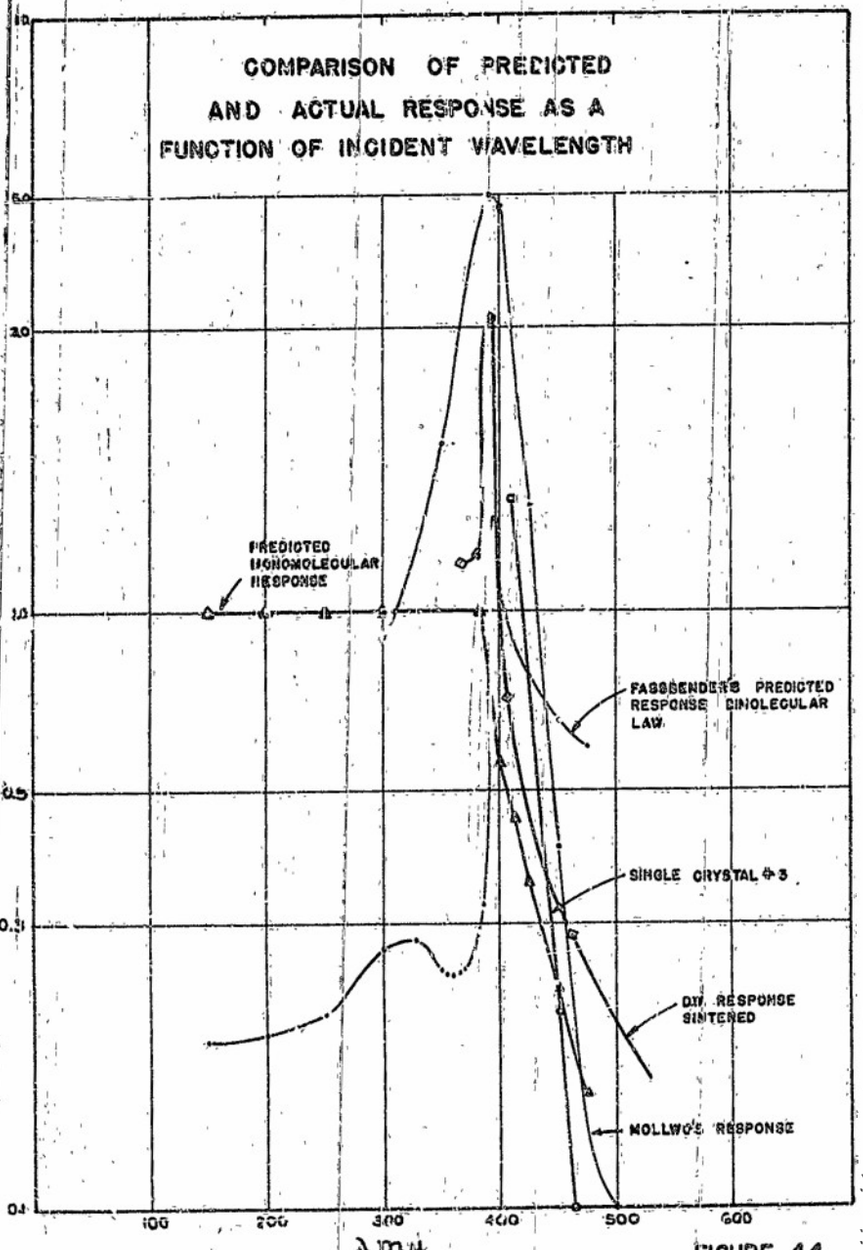

FIGURE 44

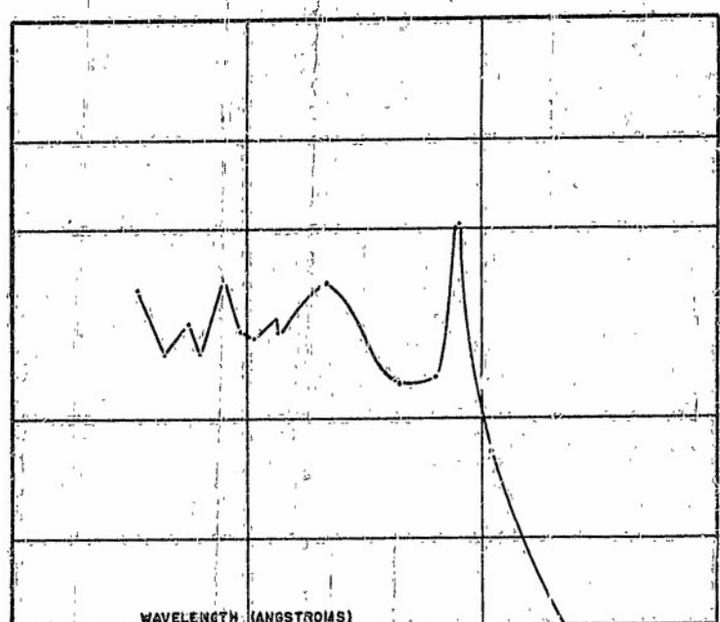

ZnO RESPONSE FOR ULTRA-VIOLET RANGE, EXPRESSED AS THE CHANGE IN PILL VOLTAGE PER INCIDENT PHOTON PER SEC.

PILL # 8 C

FIGURE 43

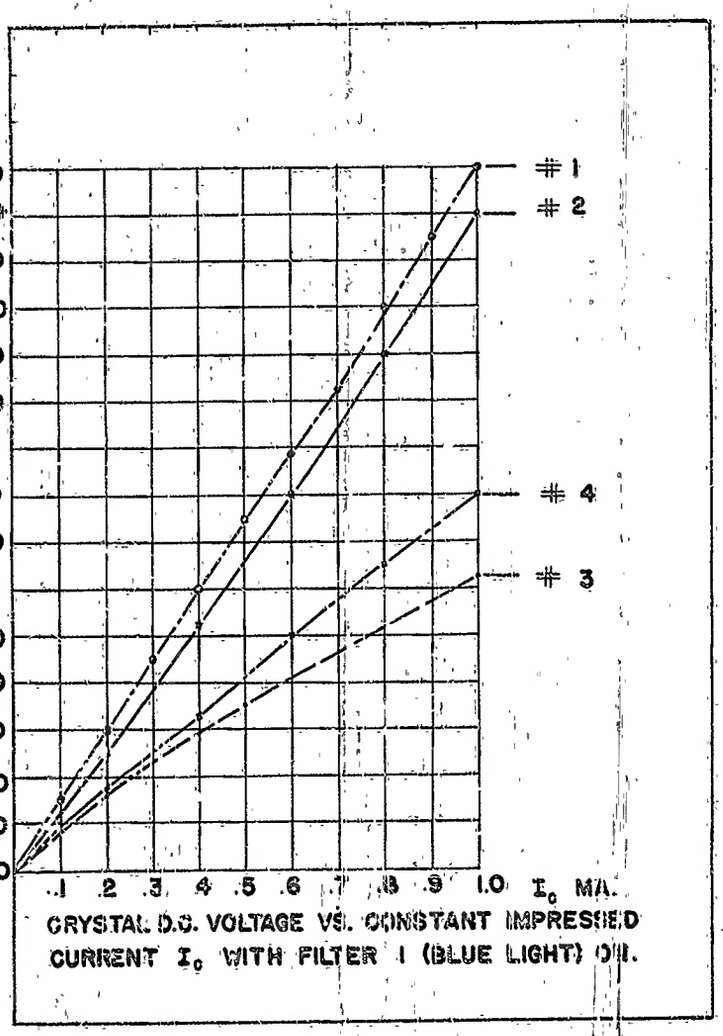

CRYSTAL D.C. VOLTAGE VS. CONSTANT IMPRESSED CURRENT I_0 WITH FILTER 1 (BLUE LIGHT) ON.

FIGURE 46

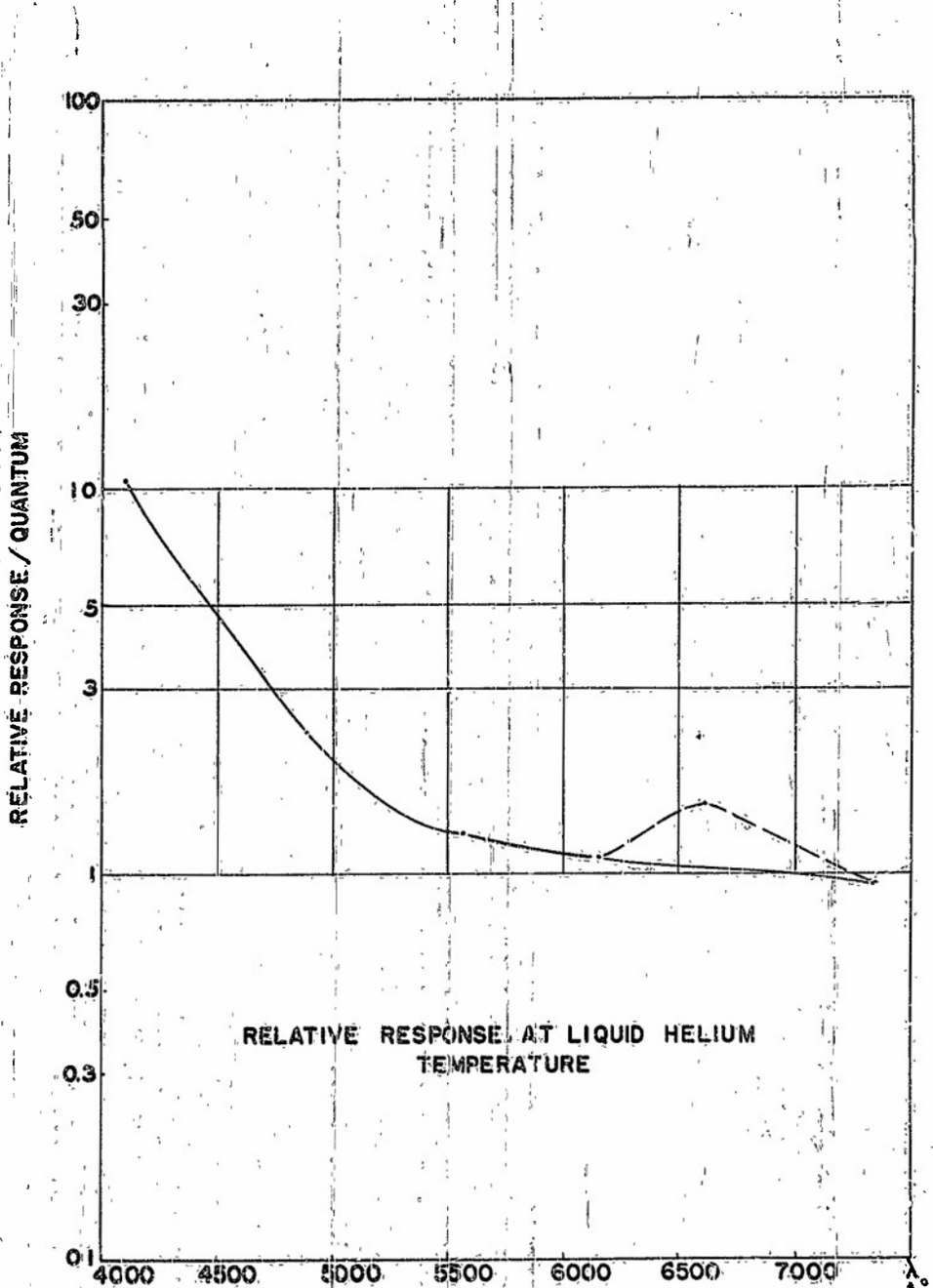

FIGURE 45

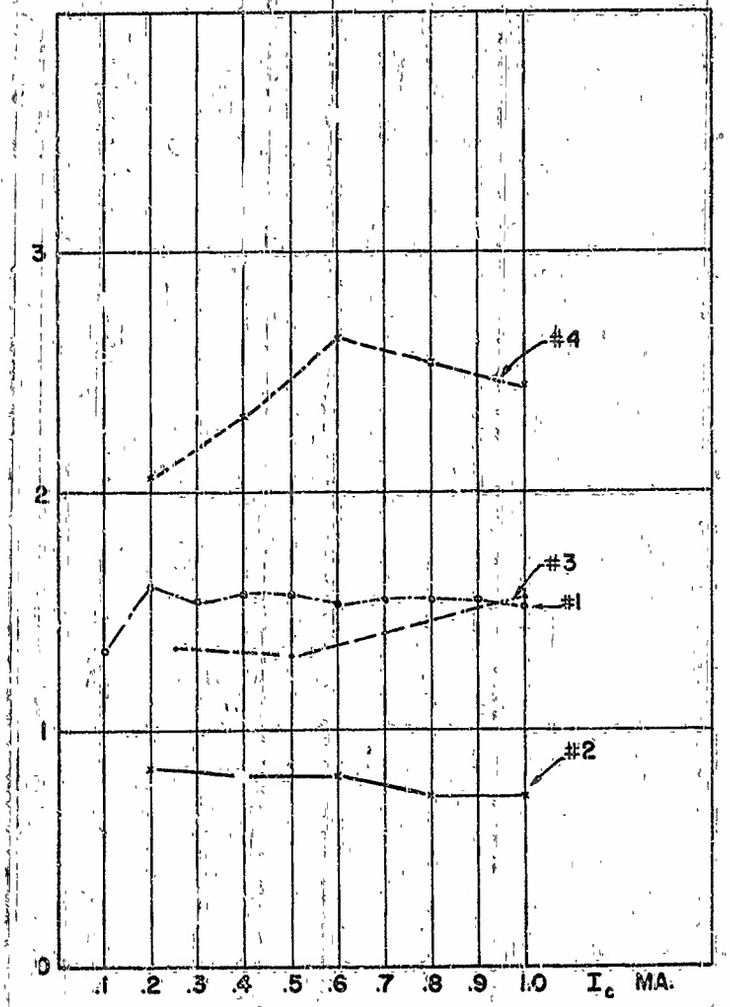

CRYSTAL RESPONSE VOLTAGE VS. I_c
FILTER #1

FIGURE 46

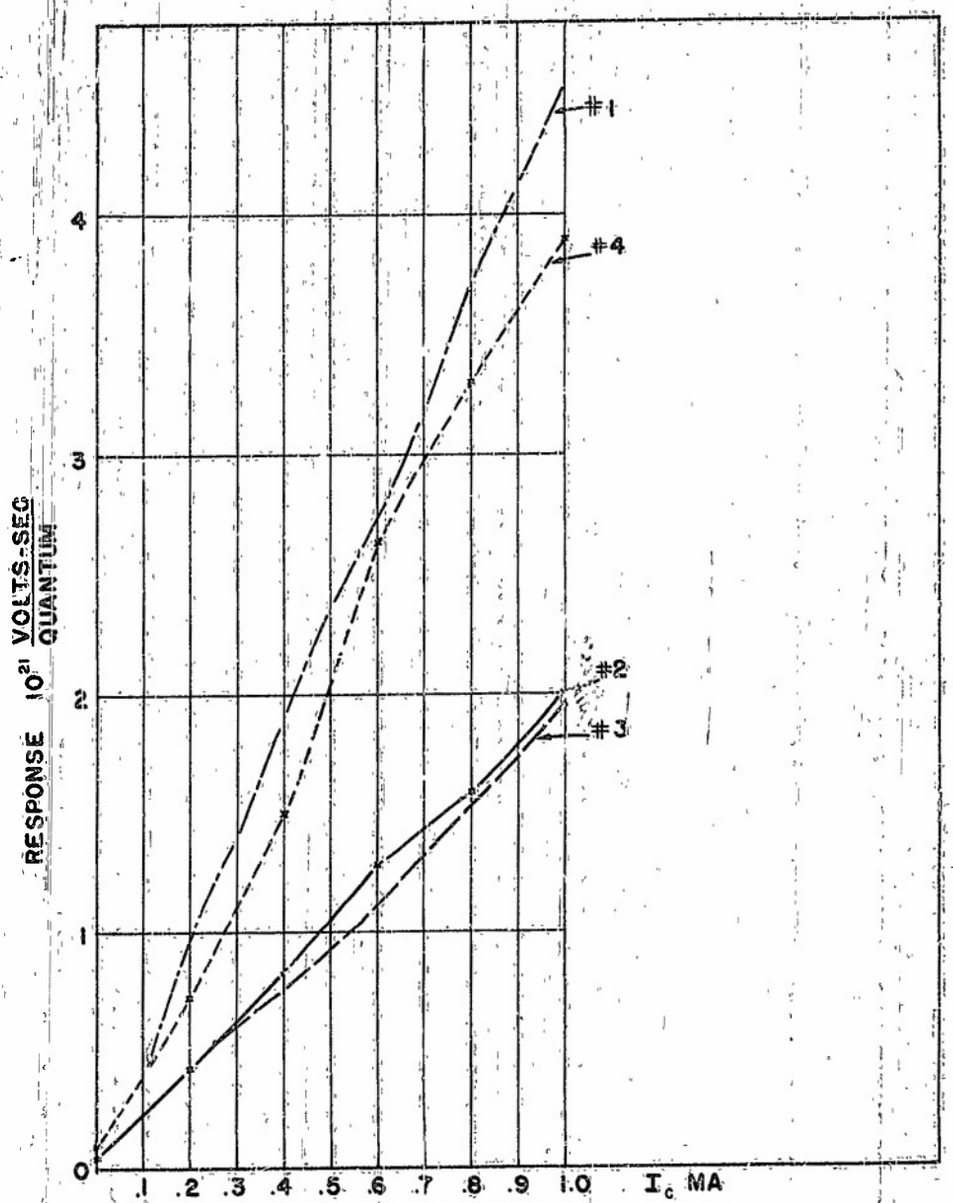

CRYSTAL RESPONSE VOLTAGE VS. I_c FILTER #1

FIGURE 47

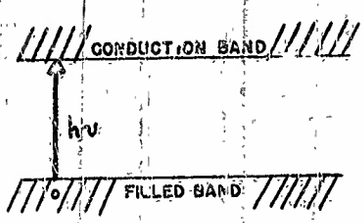

SIMPLE INTRINSIC BAND MODEL

FIGURE 50

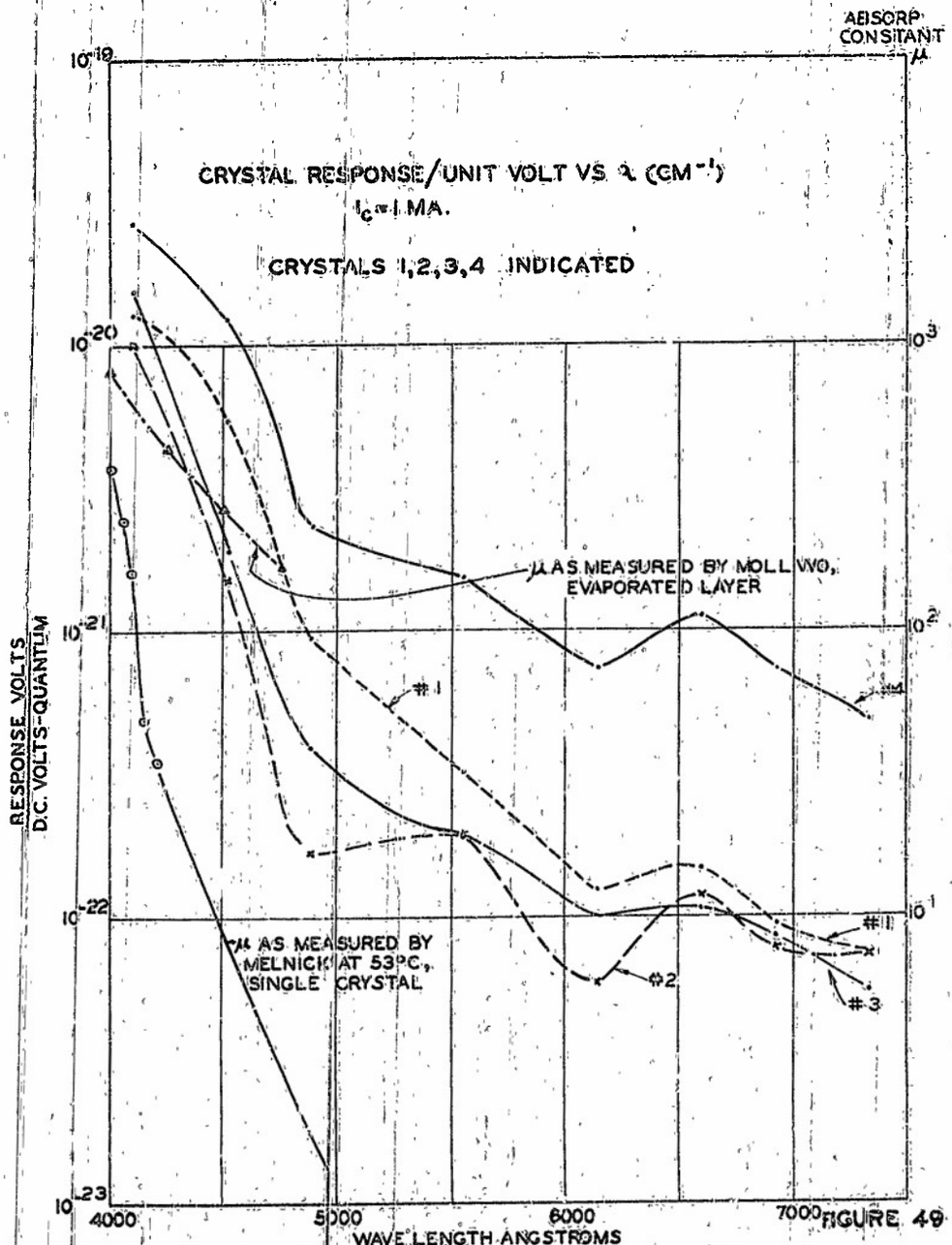

FIGURE 49

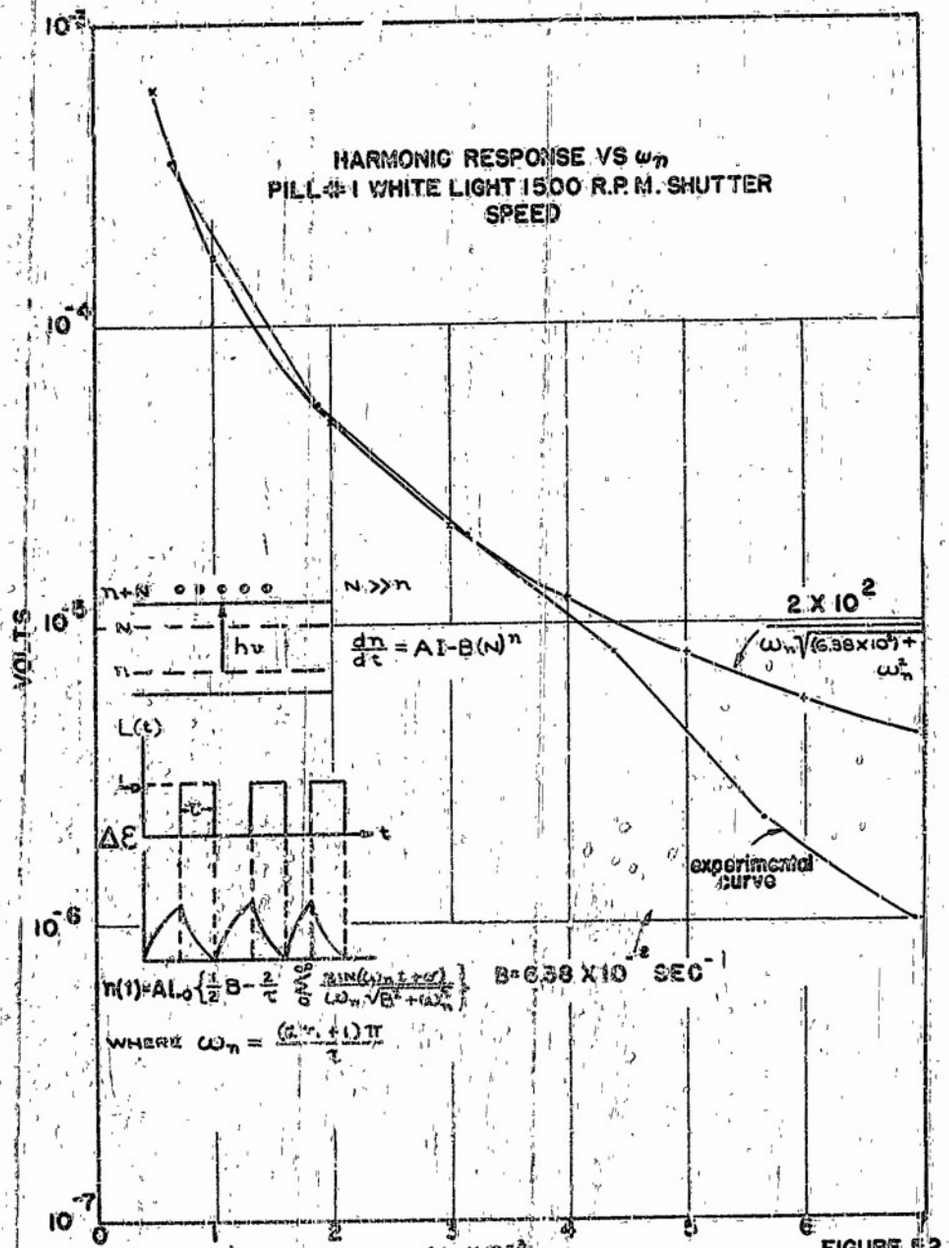

FIGURE 52

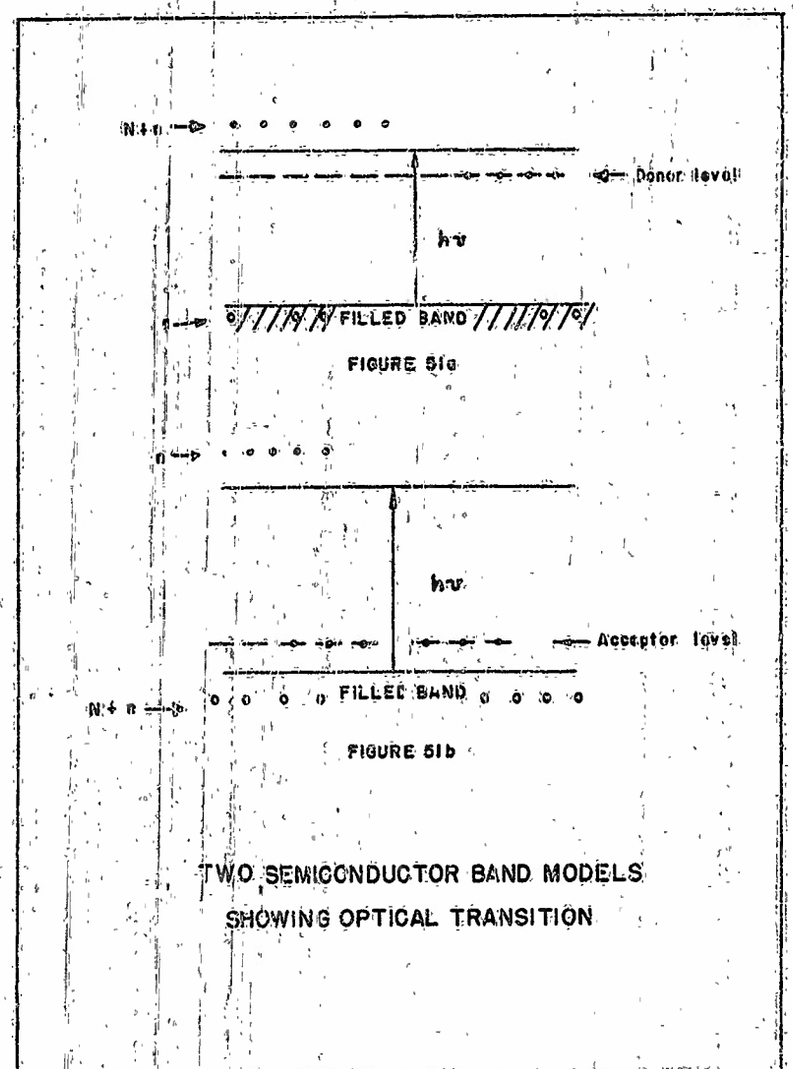

FIGURE 51a

FIGURE 51b

TWO SEMICONDUCTOR BAND MODELS SHOWING OPTICAL TRANSITION

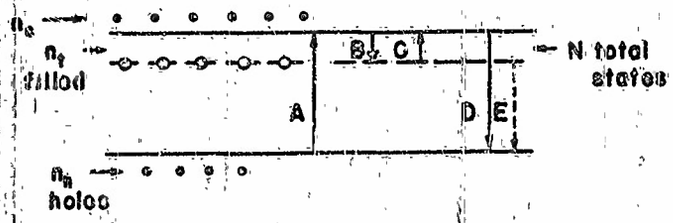

MODEL EMPLOYED IN INCREMENTAL CALCULATION

FIGURE 54

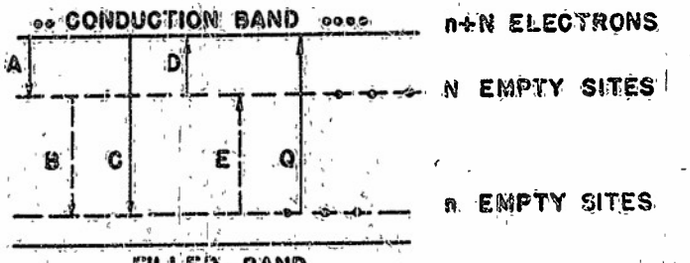

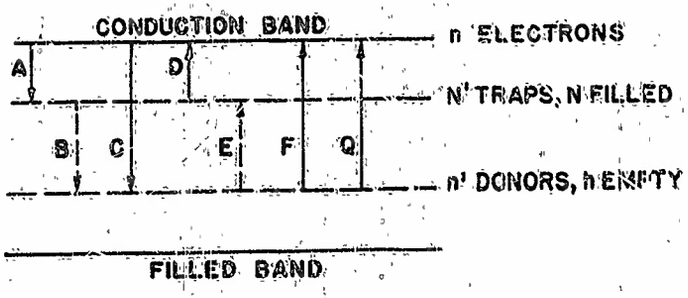

(F IS THERMAL; Q IS OPTICAL)

MODELS EMPLOYED IN DETERMINATION OF TRANSITION PROBABILITIES

FIG. 53

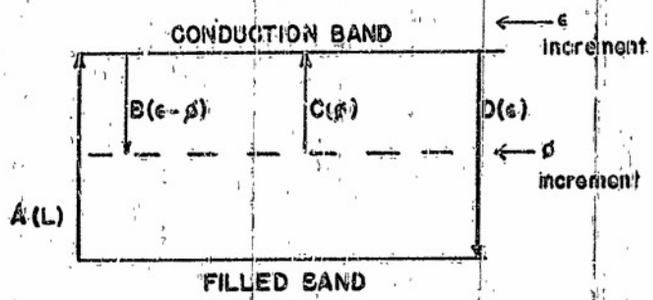

FUNCTIONAL DEPENDENCE OF TRANSITION RATES

FIGURE 56

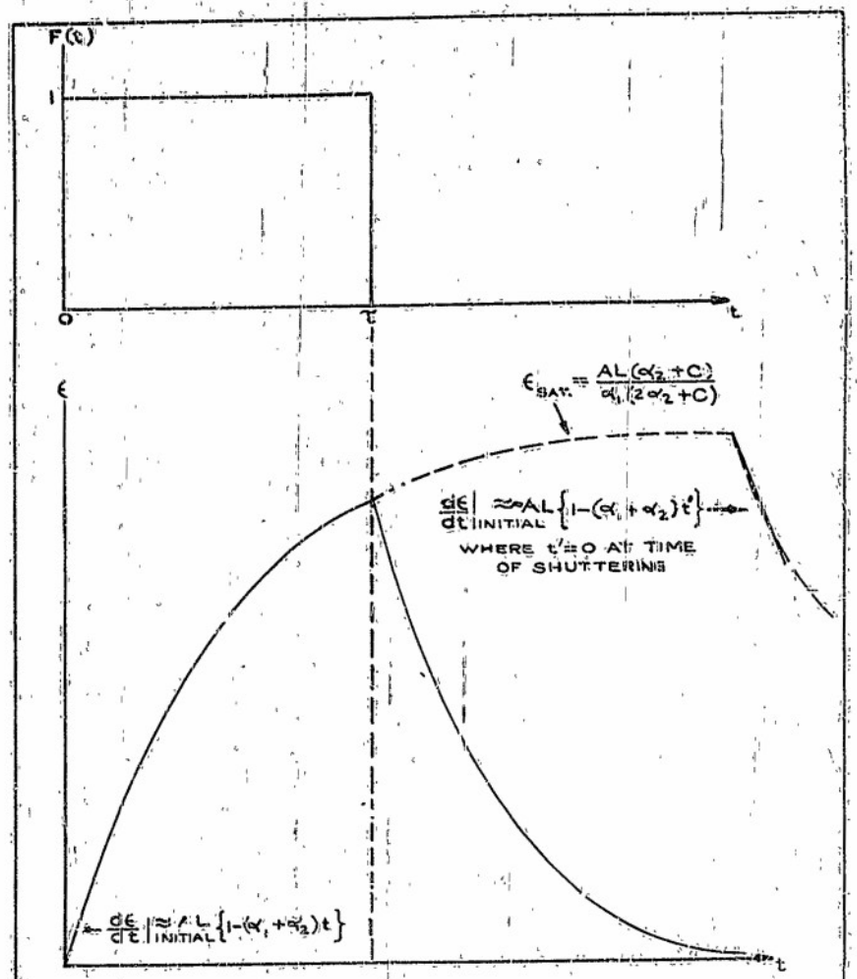

RESPONSE FOR RECTANGULAR LIGHT PULSE F(t)

FIGURE 55

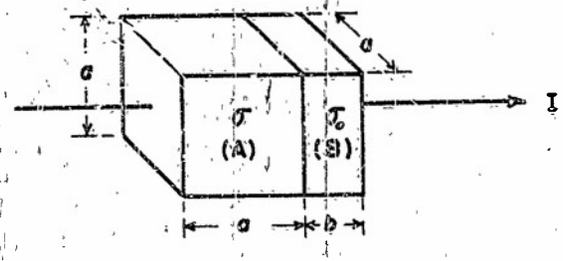

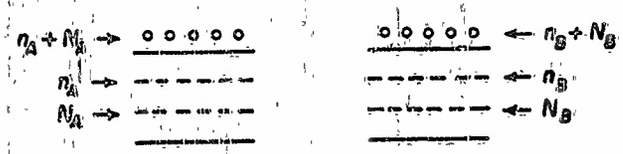

Fig. 58

Boundary Layer Cubic Block Model.

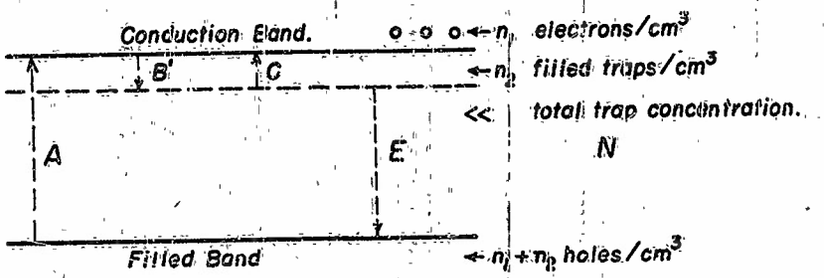

Fig. 57 a

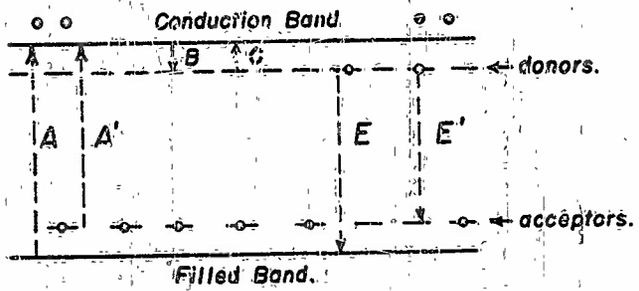

Fig. 57 b

Band Models Ernployed in Monomolecular–
–Bimolecular Calculation.

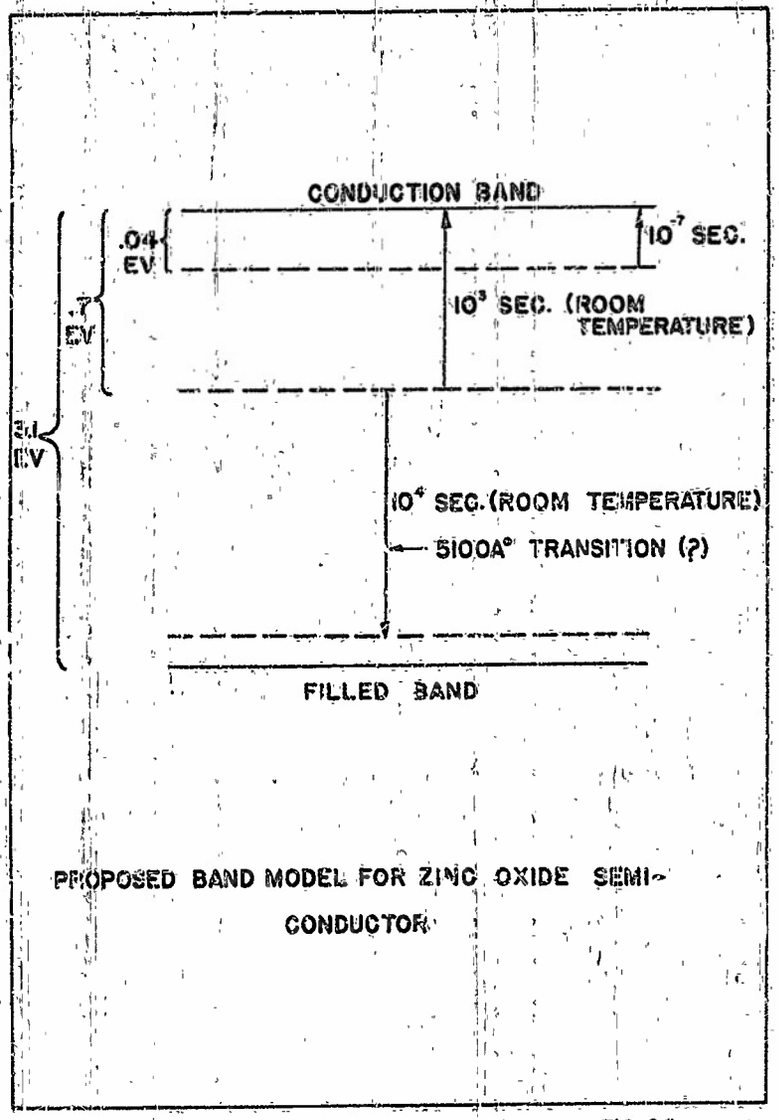

PROPOSED BAND MODEL FOR ZINC OXIDE SEMI-CONDUCTOR

FIG. 60

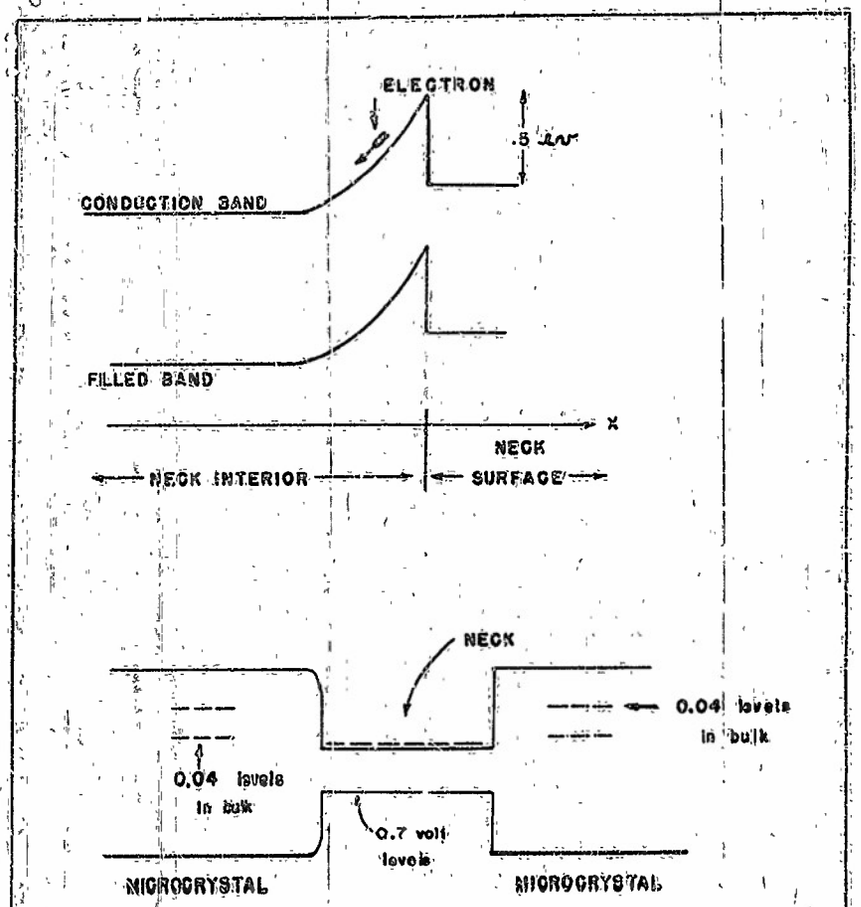

"NECK" MODEL OF CRYSTALLINE AGGREGATE

FIGURE 59

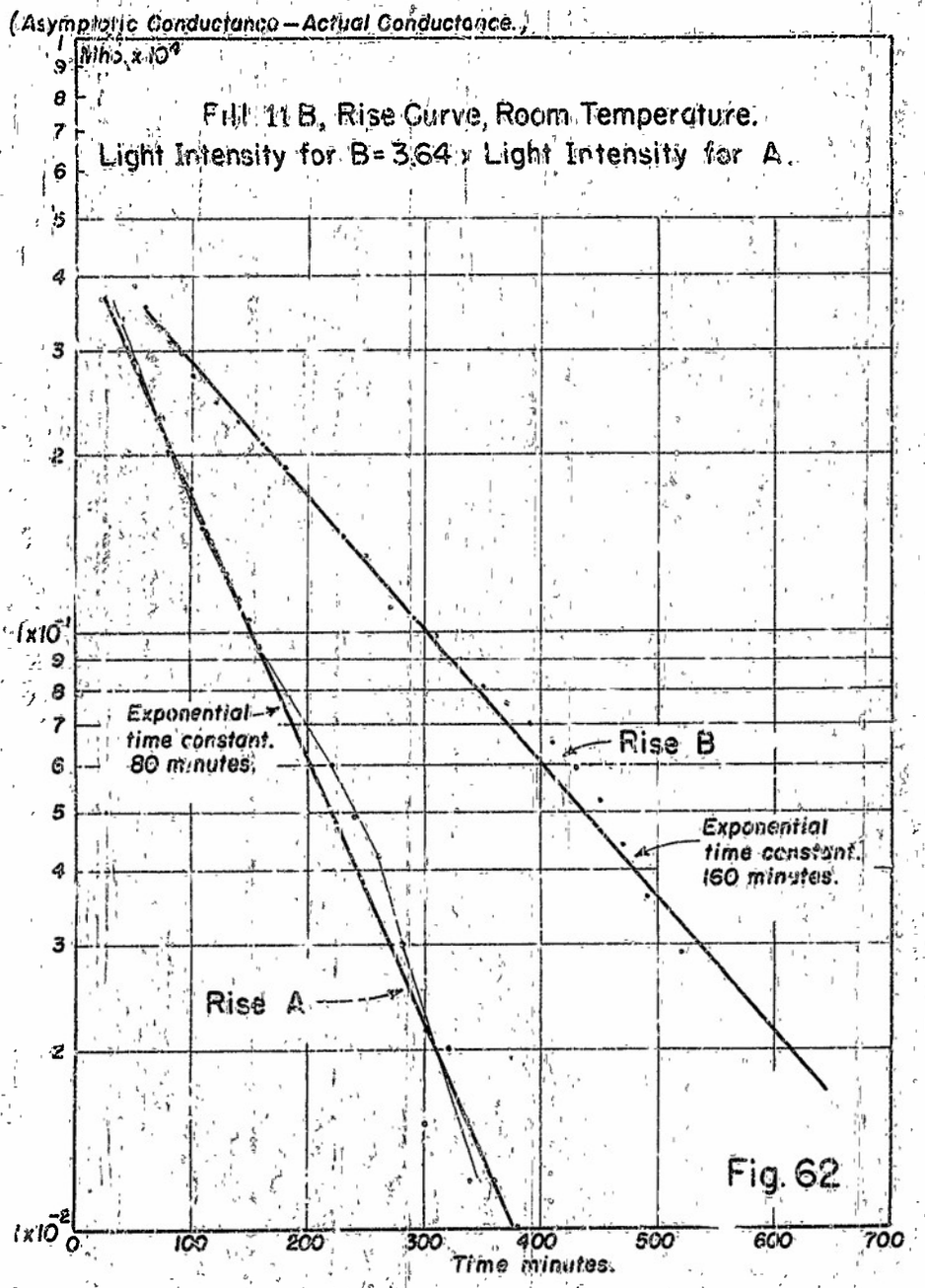
(Asymptotic Conductance – Actual Conductance.)
Mho. x 10⁻⁹
Pill 11 B, Rise Curve, Room Temperature.
Light Intensity for B = 3.64 x Light Intensity for A.
Exponential time constant. 80 minutes.
Rise B
Exponential time constant. 160 minutes.
Rise A
Time minutes.

Fig. 62

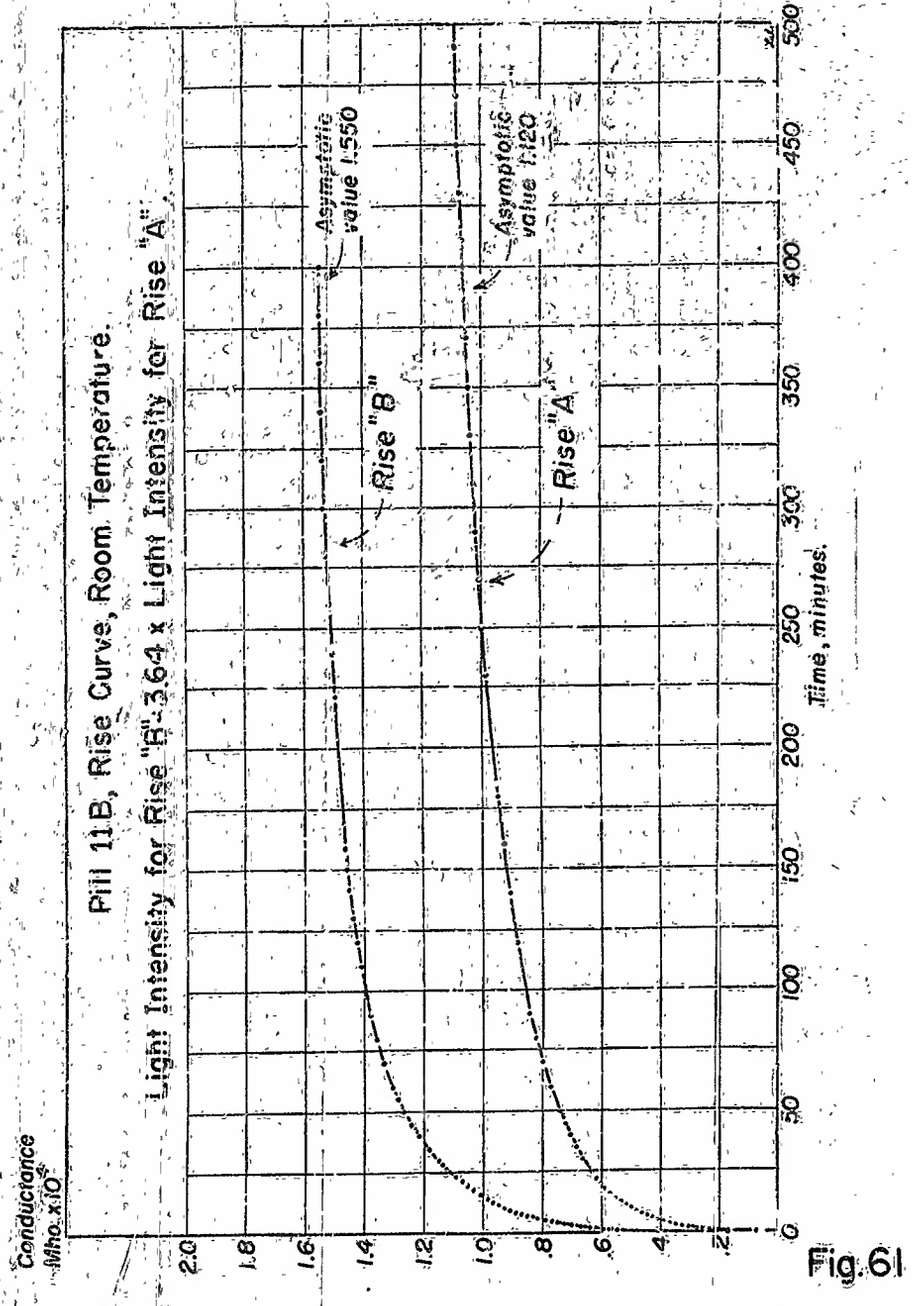
Pill 11 B, Rise Curve, Room Temperature.
Light Intensity for Rise "B" = 3.64 x Light Intensity for Rise "A".
Asymptotic value 1.550
Asymptotic value 1.120
Rise "B"
Rise "A"
Conductance Mho. x10⁻⁹
Time, minutes.

Fig. 61